Antibody Based Diagnostic and Therapeutic

Approach for Alzheimer's Disease

by

Huilai Tian

A Dissertation Presented in Partial Fulfillment
of the Requirements for the Degree
Doctor of Philosophy

Approved November 2014 by the
Graduate Supervisory Committee:

Michael Sierks, Chair
Lenore Dai
David Nielsen
Sarah Stabenfeldt
Stephen Helms Tillery

ARIZONA STATE UNIVERSITY

December 2014

ABSTRACT

Alzheimer's disease (AD) is the most common form of dementia leading to cognitive dysfunction and memory loss as well as emotional and behavioral disorders. It is the 6th leading cause of death in United States, and the only one among top 10 death causes that cannot be prevented, cured or slowed. An estimated 5.4 million Americans live with AD, and this number is expected to triple by year 2050 as the baby boomers age. The cost of care for AD in the US is about $200 billion each year. Unfortunately, in addition to the lack of an effective treatment or AD, there is also a lack of an effective diagnosis, particularly an early diagnosis which would enable treatment to begin before significant neuronal damage has occurred.

Increasing evidence implicates soluble oligomeric forms of beta-amyloid and tau in the onset and progression of AD. While many studies have focused on beta-amyloid, soluble oligomeric tau species may also play an important role in AD pathogenesis. Antibodies that selectively identify and target specific oligomeric tau variants would be valuable tools for both diagnostic and therapeutic applications and also to study the etiology of AD and other neurodegenerative diseases.

Recombinant human tau (rhTau) in monomeric, dimeric, trimeric and fibrillar forms were synthesized and purified to perform LDH assay on human neuroblastoma cells, so that trimeric but not monomeric or dimeric rhTau was identified as extracellularly neurotoxic to neuronal cells. A novel biopanning protocol was designed based on phage display technique and atomic force microscopy (AFM), and used to isolate single chain antibody variable domain fragments (scFvs) that selectively recognize the toxic tau oligomers. These scFvs selectively bind tau variants in brain tissue of human

AD patients and AD-related tau transgenic rodent models and have potential value as early diagnostic biomarkers for AD and as potential therapeutics to selectively target toxic tau aggregates.

ACKNOWLEDGEMENTS

I would like to thank my research advisor, Dr. Michael R. Sierks from department of chemical engineering (SEMTE) at ASU for giving me the opportunity to work on this project and for his continuous guidance and support. I am appreciative for the help from the current and former group members, especially Dr. Sharareh Emadi, Dr. Srinath Kasturirangan and Dr. Shanta Boddapati. I would also give my sincere thanks to Dr. James Moe and Dr. Eliot Davidowitz from Oligomerix Inc. in New York for the long-term collaboration and the partial funding for the project. I appreciate the generous gift of human or animal brain samples from Dr. Thomas Beach and Dr. Paul Coleman from Banner/Sun Health Research Institute, Dr. Travis Dunkley from TGen, Dr. Fiona Crawford from Roskamp Institute, Sarasota, FL, Dr. Sarah Stabenfeldt from Arizona State University, Dr. Birgit Hutter-Paier from JSW Life Sciences GmbH, Austria. I'm grateful for AFM bioscope access from Keck's lab in life science and Dr. Debra Page Baluch in Arizona State University Life Science Department. I also thank National Institute of Health(NIH)-National Institute of Aging(NIA), Arizona Alzheimer's Consortium and Department of Defense for funding this project.

TABLE OF CONTENTS

Page

LIST OF TABLES viii

LIST OF FIGURES ix

CHAPTER

1 INTRODUCTION.....1

1.1 Background and Introduction.....1

1.2 References.....4

2 ALZHEIMER'S DISEASE (AD) AND TAU TARGETED

THERAPEUTIC STRATEGIES….....5

2.1 Alzheimer's Disease.....5

2.2 Tau's Role in AD and Treatment Targeting Tau.....8

2.3 Antibody Based Therapeutics for Alzheimer's Disease.....10

2.4 Research Objectives and Hypotheses.....11

2.5 Introduction to Related Techniques.....12

2.5.1 Phage Display Library Construction and Functions.....12

2.5.2 Atomic Force Microscope and Its Application

in Tau Size Analysis and Biopanning.....13

CHAPTER Page

2.5.3 Particle Size Distribution Analysis Based on AFM Imaging.....17

2.5.4 scFv Expression and Purification.....18

2.5.5 Material and Methods.....19

2.6 Figures and Tables.....23

2.7 References.....31

3 TRIMERIC TAU IS TOXIC TO HUMAN NEURONAL CELLS AT LOW NANOMOLAR CONCENTRATIONS.....36

3.1 Abstract.....36

3.2Introduction.....37

3.3Material and Methods.....41

3.4 Results.....43

3.5 Discussion.....45

3.6 Acknowledgements.....48

3.7 Figures and Tables 49

3.8 References.....56

CHAPTER Page

4 ISOLATION AND CHARACTERIZATION OF SINGLE CHAIN VARIABLE FRAGMENTS SELECTIVE FOR NEUROTOXIC TAU OLIGOMERS….....61

4.1 Abstract.....61

4.2 Introduction.....62

4.3 Material and Methods.....65

4.4 Results and Discussion.....72

4.5 Summary.....76

4.6 Acknowledgements.....78

4.7 Figures and Tables 80

4.8 References.....90

5 THE ROLE OF TAU OLIGOMER IN TRAUMATIC BRAIN INJURY PROGRESSION IN RODENT MODELS.....97

5.1 Abstract.....97

5.2 Introduction.....98

5.3 Material and Methods.....100

5.4 Results and Discussion.....104

5.5 Summary.....106

CHAPTER Page

5.6 Acknowledgements.....109

5.7 Figures and Tables 110

5.8 References.....116

6 PROPOSED FUTURE WORK.....118

6.1 Introduction.....118

6.2 Material and Methods.....120

6.3 Preliminary Results and Future Work Plan.....123

6.3.1 Preliminary Diagnosis of AD Using AFM and Size Distribution..123

6.3.2 Detection of Tau Oligomers in Tissue Implies Early Diagnostic Potential.....124

6.3.3 scFvs Display Their Therapeutic Potential in Toxicity and Aggregation Test.....125

6.4 Figures and Tables 126

6.5 References.....128

REFERENCES.....130

LIST OF TABLES

Table Page

4.1 DNA Sequences of the N-terminal Region and the First Heavy Chain Framework Region (HCFR1) of Recovered scFvs after Panning compared to Known scFvs.....88

4.2 Designed Primers for Correction of Missing Base Pair. 89

LIST OF FIGURES

Figure Page

2.1 Schematic Basis of Alzheimer's Disease Pathogenesis.....23

2.2 Schematic of Tau Structure, Function and Possible Location.....24

2.3 Schematic Monoclonal scFv Display Phage Particle with Phagmid DNA (Magnified) Encoding scFv and the Terminal Protein III. 25

2.4 Schematic of AFM Working Principle. 26

2.5 AFM Image of Tau 441 Fibril, Bacteriophage of F9T Clone and Tau Oligomers with Various Sizes and Location Either on one End of the Phage or Scattered on the Background. 27

2.6 AFM Can Distinguish Different Size and Morphology of A-Synuclein from Small Globular Protein Monomer, Grainy Oligomer, Rod-Like Protofibril and Long Thick Fibril. 28

2.7 Schematic Principle of 6-His Tag Ligated Protein Purification Through Nickel Charged Affinity Column. 29

2.8 scFv Expression and Its Distribution in Culture Supernatant, Periplasm and Cell Lysate. 30

3.1 Tau Protein Structural Features in Linear Diagram. 49

3.2 Schematic of Non-Reactive Monomer, Reactive Monomer and Reactive Oligomer..50

Figure Page

3.3 Recombinant Human Tau (rhTau) Monomeric and Oligomeric Species Production and Purification.....51

3.4 Plots of Height Distribution of Monomeric, Dimeric and Trimeric Fractions of rhTau 1N4R (A) and Tau 2N4R (B). 52

3.5 Neurotoxicity of Extracellular 15.5nm Monomeric, Dimeric and Trimeric Forms of 1N4R and 2N4R Tau Variants toward (A) Non-Differentiated Human Neuroblastoma Cells (SH-SY5Y) and (B) Retinoic-Acid-Differentiated SH-SY5Y Cells were Measured after 48 Hour Incubation Using an LDH Assay.....53

3.6 Time and Concentration Dependence of Neurotoxicity Induced by Trimeric rhTau (1N4R and 2N4R) toward Neuroblastoma Cells Measured by LDH Assay. 54

3.7 Comparison of rhTau-Induced Neurotoxicity toward Non-Differentiated SH-SY5Y Cells and Retinoic Acid (RA)-Differentiated SH-SY5Y Cells. 55

4.1 The Novel Biopanning Process Combines Subtractive Panning and Positive Panning from Phagemid scFv Library and the Single Cloning Screening Using AFM. 80

4.2 Single Clones Against Trimeric rhTau Selection, Expression and Purification....81, 82

4.3 Particle Size Analysis of Oligomeric Tau Bound to scFv-Displayed Phage from rhTau 2N4R Mixed Aggregates.....83

4.4 Selective Reactivity of F9T, D11C and H2A scFvs with 9-Month 3×TG-AD Mouse Brain Tissue. 84

Figure Page

4.5 Capture ELISA for Detection of Oligomeric Tau.....85

4.6 Oligomeric Tau Levels in Different Age 3×TG-AD Mice Brain Extracts….....86

4.7 Oligomeric Tau Levels in Post-Mortem Human Brain Samples as a Function of Braak Stage.....87

5.1 F9T and AT8 can Identify Different Forms of Tau In SH-SY5Y-TMHT441 Neuroblastoma Cells Using Immunofluorescence Techniques. 110

5.2 Small Tau Targeting scFvs Screening Using Capture ELISA with SHSY5Y-TMHT441 Lysate as Analyte.....111

5.3 Affinity Analysis of Small Tau Targeting scFvs to SHSY5Y-TMHT441 and Wild-Type SHSY5Y Lysate Portion Captured by F9T scFv.....112

5.4 Mutant Human Tau Knockin Mouse(Tau406+/TauKO) at Different Ages Have a Varying Oligomeric Tau amount compared to Negative Control(Tau406-/TauKO) 113

5.5 F9T scFv Detects Abnormal Tau Lesion in Hippocampal Sections of Wild Type Mice after Single or Repetitive Traumatic Brain Injuries.....114

5.6 Plots of Affinity Difference of F9T to TBI Mice in Different Brain Regions and Different Time after TBI Treatment.....115

6.1 Human Brain Derived Tau Analyzed By AFM on the Particle Size Distribution.....126

Figure Page

6.2 Tau Oligomers Observed by F9T and D11C scFv in SHSY5Y-TMHT441 Expressing Mutant Human Tau. 127

Chapter 1

Introduction

1.1 Background and Introduction

Alzheimer's disease (AD) is the most common form of dementia resulting in the progressive neuronal and cognitive loss. About 5.4 million Americans suffer from AD and this number is expected to triple by 2050. It costs United States $200 billion annually including medication and care provision that doesn't include the unpaid care valued $210 billion given by more than 15 million Americans. AD is now the sixth leading cause of death in US and unfortunately is the only disease among the top ten death causes that cannot be prevented, cured or even slowed[1]. The current therapeutic approaches such as acetylcholinesterase inhibitor only treat symptom and not the underlying causes of the disease that remain elusive. AD is neuropathologically characterized by the presence of extracellular senile plaques containing aggregates of amyloid beta (Aβ) and intracellular neurofibrillary tangles (NFTs) containing aggregates of tau[2-3]. Increasing evidence correlates protein misfolding and aggregation of Aβ and tau with the pathogenesis of AD[4]. Normal tau plays an important role in assembling neuron microtubule and stabilizing its structure and physiological function while hyperphosphorylated tau oligomers and aggregates are diffuse from microtubule and likely responsible for synapse loss[5]. Therefore selectively targeting AD related forms of tau such as hyperphosphorylated and oligomeric forms of tau represents a promising diagnostic and therapeutic approach. One way to generate reagents against specific protein variants is to

pan for selected binding activities from surface display antibody libraries such as phage display library[6-8].

Single chain variable fragment (scFv) against tau oligomers is such a reagent. scFv is a fusion of one pair of heavy and light chain variable domains of immunoglobulin G (IgG)[9]. The lack of constant regions will greatly reduces the possibility of inflammation in scFv recipients in clinical tests[10]. The smaller molecular weight of around 29 kD facilitates scFv permeating blood-brain-barrier[11-12] before it's compromised in the later stage of AD. ScFv only has one antigen-binding site specific to a single epitope on the antigen and its specificity is readily increased by affinity mature. To fulfill scFv screening, recovering and reproducing, we used Sheets phagemid library which is a human phage-displayed scFv library with complexity of 6.7×10^9 [9]. A phage clone from this phagemid clone is a filamentous M13-derived bacteriophage with a molecule of scFv expressed on its surface and linked with a g3p. It is easy to be identified with atomic force microscope (AFM) and infectious to common E. coli strains to facilitate genetic modification.

We developed and performed a novel biopanning technique that combines the binding variety of phagemid scFv library and imaging capability of AFM[6-8] to obtain groups of scFvs that have specific tau target. One group of scFv clones is specific to trimeric tau which showed in lactate dehydrogenase (LDH) tests as the most toxic of all available tau species in our lab. After DNA sequence modification, F9T keeps specificity to oligomeric tau and displays efficient soluble scFv expression and purification. In preliminary human brain tests, F9T demonstrates the potential of discriminate AD from

ND on human middle temporal gyrus (MTG) tissue and human cerebrospinal fluid, both of which are affluent with abnormal tau in AD. Another group of scFv clones targets all types of small molecular tau such as monomer, dimer, oligomers regardless of their phosphorylated conditions.

1.2 References

1. 2012 Alzheimer's disease facts and figures. Alzheimers Dement, 2012. **8**(2): p. 131-68.

2. Goedert, M., et al., Tau proteins of Alzheimer paired helical filaments: abnormal phosphorylation of all six brain isoforms. Neuron, 1992. **8**(1): p. 159-68.

3. Spillantini, M.G., et al., Topographical relationship between beta-amyloid and tau protein epitopes in tangle-bearing cells in Alzheimer disease. Proc Natl Acad Sci U S A, 1990. **87**(10): p. 3952-6.

4. Hardy, J. and D.J. Selkoe, The amyloid hypothesis of Alzheimer's disease: progress and problems on the road to therapeutics. Science, 2002. **297**(5580): p. 353-6.

5. Mandelkow, E.M. and E. Mandelkow, Tau in Alzheimer's disease. Trends Cell Biol, 1998. **8**(11): p. 425-7.

6. Emadi, S., et al., Isolation of a human single chain antibody fragment against oligomeric alpha-synuclein that inhibits aggregation and prevents alpha-synuclein-induced toxicity. J Mol Biol, 2007. **368**(4): p. 1132-44.

7. Liu, R., et al., Single chain variable fragments against beta-amyloid (Abeta) can inhibit Abeta aggregation and prevent abeta-induced neurotoxicity. Biochemistry, 2004. **43**(22): p. 6959-67.

8. Zameer, A., et al., Single chain Fv antibodies against the 25-35 Abeta fragment inhibit aggregation and toxicity of Abeta42. Biochemistry, 2006. **45**(38): p. 11532-9.

9. Sheets, M.D., et al., Efficient construction of a large nonimmune phage antibody library: the production of high-affinity human single-chain antibodies to protein antigens. Proc Natl Acad Sci U S A, 1998. **95**(11): p. 6157-62.

10. Check, E., Nerve inflammation halts trial for Alzheimer's drug. Nature, 2002. **415**(6871): p. 462.

11. Pardridge, W.M., Alzheimer's disease drug development and the problem of the blood-brain barrier. Alzheimers Dement, 2009. **5**(5): p. 427-32.

12. Pardridge, W.M. and R.J. Boado, Pharmacokinetics and safety in rhesus monkeys of a monoclonal antibody-GDNF fusion protein for targeted blood-brain barrier delivery. Pharm Res, 2009. **26**(10): p. 2227-36.

Chapter 2

Alzheimer's disease (AD) and tau targeted therapeutic strategies

2.1 Alzheimer's disease

Alzheimer's disease is a progressive neurodegenerative disease. Patients suffering from AD experience memory loss and decrease in cognitive function. The long term medical care for AD patients not only costs US billions of dollars yearly, but also causes great emotional stress for their families. An estimated 36 million people worldwide live with AD, of which nearly 1/7 live in US. The number of people suffering from AD in the US is expected to triple by 2050 as the baby boomers age [1]. Unfortunately, there are still no effective treatments to prevent, hinder or reverse AD. Therefore, it is extremely crucial to develop reliable diagnostic approaches and effectual therapeutic strategies against AD.

Apart from the symptoms of dementia such as cognition loss and mental and behavioral problems, AD patients display a series of noticeable anatomical alterations including brain volume and weight decrease, cerebral gyrus atrophy, neuron loss in specific brain regions such as hippocampus and entorhinal cortex, and a progressive cortical thickness decrease which can be traced by MRI in multiple regions of AD brain, which associates with cognition decline and predicts the development from mild cognitive impairment (MCI) to AD[2-3]. Aberrant neural networking activities have also been observed in patients with AD [4]. Synapse and dendrite loss correlates better with cognitive loss than neuron loss does[5], therefore increasing acetylcholine levels by either acetylcholinesterase inhibitor or direct dosage of this neurotransmitter is an effective way

of temporarily ameliorating AD symptoms [6]. The use of acetylcholinesterase inhibitors is thus an approved clinical treatment for AD.

Scientists have been investigating AD etiology for more than a century. While many aspects of the disease are still unknown due to the multiple complex interactions, some key factors contributing to the disease are known. Genetic factors include mutations in the amyloid precursor protein (APP), presenilin-1 (PS-1) and presenilin-2 (PS-2) genes causing early-onset automosonal dominant Alzheimer's, however these mutations account for less than 1% of all AD cases[7-8]. Apolipoprotein E4, on the other hand, is semi-dominant inheritance for most of the familial and sporadic AD cases, and individuals with two copies of apoE4 alleles are more likely to develop AD, implicating ApoE4 as the most significant risk factor for AD[9].

In addition to genetic factors, aberrantly folded and aggregated proteins have also been implicated in AD. The two distinct hallmarks of AD are the presence of extracellular senile plaques composed mainly of fibrillar aggregates of amyloid beta (Aβ) and intracellular neurofibrillary tangles (NFT) enriched with aggregates of abnormally hyperphosphorylated tau[10-11]. While these features were first found postmortem over a hundred years ago, they can now be traced in living patients using advanced radiological imaging techniques such as PET scanning[12]. Accumulating evidence suggest that an increase in Aβ levels contributes causally to AD development. Aβ regulates neuronal and synaptic activities and accumulation of Aβ in the brain causes a combination of aberrant network activity and synaptic depression[5]. Of particular interest, the aggregation state of Aβ is critically important as neither Aβ monomer nor insoluble Aβ fibrils found in

amyloid plaques is as pathogenic or toxic as soluble nonfibrillar Aβ assemblies such as dimer, trimer and other oligomer forms. Although it remains controversial which Aβ assemblies are the most toxic and how the Aβ assembly forms into insoluble aggregates and cause neuronal synaptic dysfunction, Aβ oligomers have been shown to have toxic interactions with several cell-surface molecules including the tyrosine kinase receptor (tkR) and the receptor for advanced glycation end product. Aβ oligomers may change the distribution and activity of neurotransmitter receptors and related signaling molecules, disrupt intracellular calcium homeostasis, and impair axonal transport and mitochondrial functions[12].

Similar to the toxic role of oligomeric species of Aβ, oligomeric forms of tau are more toxic than monomeric or fibrillar tau aggregates[13-14]. Despite the toxic role of oligomeric Aβ and tau in AD, the presence of fibrillar Aβ aggregates and tau NFTs is used to corroborate AD in living patients, partly because we lack reliable tests to quantify soluble Aβ and tau oligomeric species in human brain tissue. Development of such tests is important because they may enable a better correlation of cognitive impairment with levels of selected toxic oligomers, provide a means of monitoring the effect of drugs on lowering the levels of related toxic oligomers in AD afflicted brain sections during clinical trials, and provide an earlier diagnosis of AD. While several reagents have been developed to target different oligomeric Aβ species, very few have been developed to target oligomeric tau.

2.2 Tau's role in AD and treatment targeting tau

Tau is a microtubule-associated protein (MAP) which was first identified as a crucial factor in assembly and stabilization of microtubule in the mid 1970s[15-16] and later in signaling pathways[17]. Despite of the multiple roles of tau in neuronal physiology, hyperphosphorylated tau is a major component of the insoluble filamentous neurofibillary tangles (NFTs) of Alzheimer's disease. All neurodegenerative diseases with abnormal tau inclusions are termed as tauopathies, including AD, progressive supranuclear palsy (PSP), frontotemporal lobar degeneration with tau inclusions (FTLD-tau) such as Pick's disease and genetic forms of Parkinson's disease[18]. The complete in vivo function and the role in pathogenesis of tau remain elusive. Some of the cellular functions of tau such as microtubule stabilization overlap with the function of other MAPs since tau knockout mice display no functional impairment or shortened longevity[19]. While the presence of abnormal tau aggregates in Alzheimer's suggests the association with pathology, this does not prove a cause-effect relationship.

The human tau gene is encoded on chromosome 17q21 with at least 16 exons[20]. By alternative splicing on exon 2, 3 and 10 of tau mRNA, tau is known to exist in six isoforms in human brain[21]. Many tau gene mutation sites have been related to tauopathies including AD. Tau also undergoes multiple posttranslational modifications such as phosphorylation of serine and threonine residues that can regulate tau function. Evidence suggests that 4R tau is more prone to be hyperphosphorylated than 3R tau[22], which makes 4R tau a favorable target to treat AD. Tau found in paired helical filaments (PHF) autopsied AD brain tissue has 3 to 4 times higher phosphorylation levels compared to normal tau[23-24].

Since tau hyperphosphorylation is related to AD pathology, reagents have been developed to inhibit tau phosphorylation including inhibitors of kinases such as GSK-3β and cdk5[25]. A major drawback to kinase inhibitors is that they disrupt the normal functions of kinases. For example, the reduction of GSK-3β impairs NMDAR-mediated long-term depression[26] and memory consolidation[27]. Tau aggregation inhibitors are also being developed along with other amyloidosis inhibitor to reverse the formation of NFT. Many drugs that inhibit tau aggregation may have the similar benefits towards multiple pathological targets including Aβ and α-synuclein[28]. While promising, it is far from certain that the insoluble aggregated tau is actually toxic and responsible for tau-dependent neuron loss and neurodegeneration. One unexpected effect of tau aggregation inhibitor may be to enhance the formation of soluble tau oligomers[29] which are potentially neurotoxic[13, 30] and can form during the early stages of tau aggregation in AD[31]. This potential side effects strongly underline the importance of treatments targeting toxic tau oligomers instead of filamentous aggregates. Reagents that are able to selectively inhibit tau-tau interactions, or oligomer formation and not just inhibit fibrillar aggregation are needed. Assuming ongoing experiments confirm that reduction of overall tau levels is safe and beneficial for ameliorating the cognition of patients, tau can be either directly targeted by reagents or be reduced indirectly by targeting molecules that regulate the expression or clearance of tau. Either way, reagents such as antibodies or antibody fragments that can selectively bind individual protein morphologies can be very useful.

2.3 Antibody based therapeutics for Alzheimer's disease

Active and passive immunization with full length antibodies against different regions and forms of Aβ have demonstrated great potential in clearing Aβ and reversing AD related cognition impairment in animal models although clinical trials in humans have been less encouraging and have led to side effects including inflammation[32] and micro-hemorrhaging. Single chain variable fragments (scFv) which contain only the antibody binding domain are a promising route to overcome inflammation issues. ScFvs are composed of variable regions of full size antibodies to form one specific binding site which retains the binding specificity of the full antibody. Since the scFvs lack the antibody constant region responsible for the inflammatory response, scFvs can have selective advantages over active immunization strategies for a range of in vivo applications[33]. ScFvs have already shown promise as interventional reagents targeting pathogenic features in cancer[34]. ScFv genes can be engineered into the genome or plasmid of bacteria, yeast or even plant systems for efficient expression[35]. A typical scFv molecular weight is around 29kDa which is only about 1/6 of the full immunoglobulin size. This is a potential advantage for facilitating penetration of blood brain barrier (BBB) that guards the brain from large non-lipid-soluble interstitial particles[36]. Due to their small size, low level of kidney uptake and efficient blood clearance, scFvs are increasingly used as an in vivo carrier of radionuclei and drugs as well[37]. ScFvs can be readily affinity matured to obtain higher binding specificity and affinity to its target[38]. In summary, scFv based therapeutic strategies represents a promising way of understanding pathogenesis of diseases including Alzheimer's and treating AD by interacting with amyloid misfolded forms and featured aggregates.

2.4 Research objectives and hypotheses

Alzheimer's disease is a progressive neurodegenerative disease resulting in memory loss and cognitive impairment. AD is characterized by the presence of two hallmark pathological features, Aβ senile plaques[39] and tau neurofibrillary tangles[10]. While the amyloid cascade hypothesis which states that accumulation of Aβ is a primary factor in the onset of AD has strongly influenced the direction of AD therapeutic development for over a decade[5, 40-42], because tau now has also been shown to play a critical role in AD [43-46] therapeutics targeting tau are drawing increasing interest. Normal monomeric tau functions in healthy neurons as a microtubule-associated protein[15-16]. When it becomes hyperphosphorylated tau does not bind microtubules and is more prone to misfolding and aggregation[18, 47]. While current reagents can detect total tau and certain hyperphosphorylated tau levels, it is not clear that these forms are the most relevant tau forms correlated with AD. Therefore, reagents that can selectively target additional tau isoforms, in particular neurotoxic tau forms are critically important. The long term goal of our lab is to develop recombinant antibody fragment that can be an effective and safe part of diagnostic, preventive and therapeutic approaches to neurodegenerative diseases such as Alzheimer's. To achieve this goal, we have been using single chain variable fragment (scFv) to target pathological AD species. We have already developed scFvs against various forms of Aβ[48-51], its precursor APP[38, 52] and against the protein α-synuclein[53-54] implicated in Parkinson's disease. We have shown that targeting oligomeric Aβ or α-synuclein can effectively reduce cytotoxicity and have promise both as therapeutic and diagnostic reagents. We have developed a novel biopanning process that combines the binding diversity of a phage display scFv

library with the powerful imaging capabilities of atomic force microscopy (AFM) for the purpose of monitoring antigen-antibody interaction[55]. This novel biopanning protocol enables us to isolate scFvs to antigen targets using nanogram amounts of target or less, even down to a single molecule.

2.5 Introduction to related techniques

2.5.1 Phage display library construction and functions

The traditional monoclonal antibody development including immunization of animal[56] and hybridomas technology encountered a bottleneck of unwanted immune response elicited by the immunized animal monoclonal antibodies, restriction to a group of particular natural antibody isotypes, poor immunogenicity of certain targets and general issues associated with the full length antibody expression[33, 57]. On the contrary, phage display technique provides a powerful tool of screening monoclonal single chain variable fragment (scFv) from a scFv library against a wide array of antigen targets. The scFv library was designed and created from natural human antibody repertoires[58-59] therefore the resulting scFvs should be safe for human applications.

The phage display library used in this study is based on genetic engineering of coat proteins of filamentous bacteriophages of Escherichia coli such as M13[59]. During phage propagation, the phage is elongated by the polymerization of major geneVIII and in the end capped by the terminal geneIII protein. By genetic fusion of geneIII with a particular peptide sequence (such as single chain variable fragment), we can expect this peptide expressed and displayed on the end of the phage along with geneIII protein. There are two ways of implementing this genetic fusion. One is by direct engineering of

the phage genome. The other is to incorporate scFv sequence into a geneIII-expressing plasmid combined with a helper phage system. The phage library used for screening scFv against AD-associated proteins is constructed by the latter method. It is human scFv repertoire phagemid library in TG1 bacteria. To express scFv phage, it requires VCSM13 helper phage. Typically, it produces and secretes scFv into the E.coli periplasm where scFv remains at a high level.

2.5.2 Atomic force microscope (AFM) and its application in tau size analysis and biopanning

Atomic force microscope (AFM) is a relatively new and perhaps the most versatile member of a microscope family named scanning probe microscopes (SPM). Different from the conventional optic microscopes well-known to most people, SPM generates images by ‘touching’ and ‘feeling’ instead of ‘looking at’ samples. It’s similar to reading Braille or a blindfolded man touching an object and forming in the mind an image of its shape and size. SPM sense the structure of a surface by scanning it with a nano-scaled sharp probe and measuring some form of interaction between the surface and the probe. In AFM, the interaction detected is the vertical (z direction) displacement of probe due to intermolecular force change between probe and sample. The most common detection method is laser beam deflection. As shown in the schematic diagram in Figure 2.4, the probe-sample interaction is preset at a certain value. A laser beam is adjusted on the tip end of the probe and reflected onto a photo detector, which usually is a photodiode. As the probe raster scans along the sample in one dimension (x direction), the sample surface feature will change the probe-sample interaction causing an extension or deflection on the tip. This tip extension or deflection will be magnified by the displacement and intensity

of laser beam received by photo diode. A vivid analogy would be that of a naughty pupil sitting in the back of a classroom trying to dazzle the teacher by reflecting the sunlight through his watch face. The tiny movement of the watch can cause a large change of the light path and thus position the light spot to the teacher's face. The change of laser position and intensity is captured by a photo diode. It transforms the received signal into electrical signal that triggers the feedback loop to notify the piezoelectric scanner to make adjustments to the sample vertical position in order to keep the preset value for probe-sample interaction. This series of scanner adjustment is recorded along the raster scan. After one line is scanned, the probe starts an adjacent line scan until the whole appointed area is scanned.

The AFM image is obtained using height mode which is analogous to a contour map. The particle height range is scale by color gradient in which darkest brown represents the baseline level and white as z values of 10 nm or higher. The particle horizontal size is represented by the pixels on the image. We use freshly cleaved mica as our sample carrier for its special layered structure that appears flat in angstrom-scale under AFM image. Monomeric tau size is about 43 kDa for 1N4R and 46 kDa for 2N4R, while scFv size is around 29 kDa. When imaged by AFM, these tau particles appear as white dots of various sizes on a brown background. The fibril and the phage are filamentous objects with a noticeable width difference.

The mica is naturally negative charged thus can retain any protein that contains a positive group and repel any negatively charged particles such as bacteriophage. Its surface can be chemically treated for the special purposes such as holding certain objects.

In our case, we use natural mica during biopanning process in order to ensure that phage retain on the mica surface only due to the paratope-epitope interaction not due to static electric force.

To prepare a sample for imaging, a 10µl aliquot of tau dissolved in 50mM Tris buffer was deposited on freshly cleaved mica and incubated at room temperature for 10 minutes. Additional DI water was applied as necessary to moisturize the mica surface to prevent the salt in the buffer from crystallizing on the mica surface. To avoid contamination, the whole sample preparation process is recommended to be performed in a dust-free air-circulated biosafety cabinet. After the incubation, the mica was rinsed thoroughly with autoclaved filtered DI water and dried with pressured nitrogen air flow. Any new sample should be imaged in a series of dilutions to have a general idea of its density condition on AFM image. The proper sample concentration for AFM imaging depends on the purpose of the imaging and antigen availability. As stated previously, M13 phage cannot stay on untreated mica surface due to the negative surface charge while its display scFv can bind to its specific target immobilized on the mica. To check the morphology of phage, a 10 µl aliquot of the Sheets library phage in phosphate buffer saline (PBS) was deposited on a piece of tau-coated mica and washed after 10 minutes with 0.1% Tween20/DI water to remove all non-specific binding or phage trapped by large salt particles. Afterwards, the mica was rinsed with DI water to remove the residual unbound phage and Tween. The mica was then dried with pressured nitrogen flow.

AFM is particularly useful for differentiating biomolecules according to their shapes and sizes. Figure 2.5 is a typical AFM image demonstrating the morphological

features of tau monomer, oligomers, fibrils and scFv displayed bacteria phage. Tau monomer and low degree oligomers can be deemed as nanoscaled spherical particles that appear like fine salt or sand on AFM while tau fibrils and tangles are thick filamentous objects on AFM. One can also differentiate amyloid fibril from a M13 family phage by their distinctive width difference as shown in Figure 2.5. It requires software for image process and analysis to further distinguish scFv or scFv binding antigen from antigen by size distribution analysis addressed later in this section. Additionally, the scFv cannot be recovered and replicate itself. On the other hand, the scFv-display phage can be identified by AFM easily. Because a phage clone displays a reactive scFv on its end, the antigen-antibody complex is located on the tip of the filamentous phage captured by AFM as shown in Figure 2.5 the filamentous object spot by a blue arrow. Besides, the spot phage can be collected by AFM probe and replicated following normal phage production. Therefore, scFv displayed phage is a desirable replacement for soluble scFv during panning process for AFM to detect antigen-antibody interaction.

We can also use AFM to monitor the polymerization and aggregation process of amyloid because of this powerful capability. We performed the thioflavin T (ThT) fluorescence assay to monitor beta amyloid (Aβ) aggregation. ThT is a type of fluorescent dye that combines with protein beta sheet in direct proportion to its molecular weight. The fluorescent intensity of the complex is detected and compared with calibration chart for Aβ oligomer or aggregates molecular weight and thus the aggregation degree is known. Despite of its precision, ThT fluorescence assay is time-consuming and restricted to β-sheet structured protein. Contrarily, AFM can image and identify easily all types of protein morphologies as shown in Figure 2.5 and Figure 2.6.

Generally, we investigate amyloid oligomerization and aggregation by incubate in room temperature or 37°C multiple aliquots of amyloid monomers in proper buffer and set the starting day as day 0. On each of the following days of interest, one aliquot of amyloid is transferred from the incubator into the freezer. After completing the aggregation time frame, all aliquot of amyloid at different stages of oligomerization and aggregation are deposited on multiple pieces of mica for AFM image. Figure 2.6 shows the AFM images of different morphologies of α-synuclein from globular monomer, larger grainy oligomer, rod-like protofibril and filamentous fibrils. The AFM image results showing Aβ ascending size and apparent fibril elongation is in line with the aggregation process.

2.5.3 Particle size distribution analysis based on AFM imaging

AFM technique is a powerful tool for imaging protein molecules (e.g. amyloid, antibody fragment and bacteriophage) for their quaternary structure in air or liquid with great precision. To image tau, we used two rhTau stocks available in our lab, 1N4R and 2N4R tau isoforms. They have been separated from the oligomer mixture and purified into monomer, dimer, trimer. On AFM images, tau molecules absolute size, its isoforms size difference and oligomer size difference are not perceivable by naked eyes but can be detected and analyzed with AFM image process and analysis softwares including SPIP, Gwyddion and Nanoscope.

First the height of a series of oligomeric degree tau morphologies is measured to generate a calibration chart. One cannot avoid noise on AFM image of even the most purified sample because it is dissolved in Tris buffer that contains salt and the preparation in a low dust level environment doesn’t guarantee dust free. Therefore it is reasonable to

calculate the middle size range of the majority of particles. In this way, we not only eliminate background noises, but exclude small particles like salt and large grain like dust as well. In order to obtain the mean value of the molecular size of new stock of sample, one can prepare it on mica as described and take AFM images of 20 μm^2 and zoom in to take representative images of 5 μm^2 or 2 μm^2 where the protein coating appears uniform without outstanding large objects. The software detects all the particles, records the particles' heights as their molecular sizes and sorts them in ascending order. We can sum up total counts of particles of continuous interval sizes and calculate the percentage counts of each size range. Table 3.1 is a representative size distribution analysis result of various tau morphologies. We can see it is in accordance with the valid assumption that tau 2N4R of the higher molecular weight is larger than tau 1N4R at the same polymerization degree and that the higher degree oligmer is larger than the lower ones and the monomer. With this calibration chart, we can perform the similar AFM imaging and analysis on any tau samples either purified or mixed oligomers in order to corroborate its polymerization degree or indentify a specific particle in interest.

2.5.4 scFv expression and purification

The phage displaying scFv on its surface can readily infect bacteria facilitating their recovery and amplification. Together with the phage shell protein genome, the phage injects the bacteria with the scFv encoded plasmid. Soluble scFv expression is induced and regulated by *lac* operon from an E.Coli strain HB2151. The bacteria with plasmid encoding scFv proliferate rapidly in 2xYT media with glucose. At this stage, a high density of bacteria is desirable while scFv expression is suppressed. It is analogous to purchase machines for a factory in the first step. After the glucose in media is depleted,

isopropylthiogalactoside(IPTG) is added to induce the *lac* operon to start scFv expression. This is when the machines in the factory start to make products. The location and the concentration of scFv depend on the incubation temperature and duration. The scFv expressed in inclusion body is inactive and vulnerable to lysozyme. The soluble scFv, on the contrary, is excreted into periplasm in most cases. For certain clones or the longer incubation, considerable proportion of scFv will pass through the outer membrane into the culture media. All portions of bacteria, culture supernatant, periplasm and lysate, should be collected and concentrated for newly screened clones to investigate scFv yield and location by SDS-PAGE and western blot.

The expressed scFv is fusion with N-terminal hexahistidine (6×His) tag for purification purpose. The concentrated portion is run through a nickel-charged beads affinity column that interacts with 6×His tag with micromolar affinity. On the other hand, non-specific proteins go through the column with flow-through or stringent wash. The scFv protein bound on the nickel column is displaced by competitive ligand of imidazole and eluted off for dialysis. The purified scFv is the reagent for tissue affinity test, neurotoxicity test and aggregation inhibition effects.

2.5.5 Material and Methods

Soluble scFv expression and confirmation- The complete corrected scFv gene are confirmed and then cleaved and ligated into pIT2 which tails on scFv N-terminal with c-myc tag, 6×His tag and with the Amber stop codon. Amber codon is mute in TG1 E.coli strain facilitating phage expression, while activated in HB2151 E.coli strain enabling soluble scFv expression. The clone HB2151 transfected with scFv encoded pIT2 vector

grow in 37 ºC shaker overnight in 2xYT media with 100 µg/ml Ampicillin and 2% glucose. On the following day, overnight culture is used in 1/100 volume ratio to inoculate a large scale media of 2xYT with 100 µg/ml Ampicillin and 0.1% glucose. Glucose can greatly enhance the proliferation rate of bacteria and suppress scFv expression at this stage. The culture is incubated in 37 ºC grow until its optical density at 600 nm (OD_{600}) goes beyond 0.8, which means the glucose in the media is depleted thus the suppression to the *lac* operon is off. The scFv expression is triggered by the inducer isopropylthiogalactoside (IPTG) of 1 mM and kept in 30ºC shaker overnight.

On the third day, the bacteria are spun down at 8000g for 30min. The supernatant is collected and concentrated on ice through 10 kDa molecular weight cut-off membrane (Millipore) using tangential flow filter (TFF). The periplasm in which the excreted scFv usually lies is extracted from the bacteria pellet. The pellet is first completely dissolved in TSE buffer (30mM Tris-HCl pH 8, 20% sucrose, 1 mM EDTA) of 1/20 culture volume and incubated on ice for 20 min. The mixture is then centrifuged without brake for 30 min 5000g and divided with caution supernatant and pellet which are dissolved separately in equal volume of PBS. Another 20 min ice incubation and 10,000g 20 min centrifuge with brake is performed. The ‘supernatant’ portions collected from both parts are combined as the periplasm of the culture. The remaining cell pellet is incubated on ice for 1.5h in 1 ml/mg lysis buffer containing lysozyme and protease inhibitor PMSF at the volume of 5 ml per 1 g pellet. The bacteria mixture is vortex for thorough lysis and centrifuged to separate lysate and cell debris. At this point of time, three major portions are obtained and their protein constituents are by MW on sodium dodecyl sulfate polyacrylamide gel electrophoresis (SDS-PAGE). The samples are mixed with twice

volume of loading buffer (19:1 of Laemmli sample buffer:β-mercaptoethanol). All mixed samples are incubated in a boiling waterbath for 10 min when β-mercaptoethanol reduces the disulfide bonds and interrupt the proteins tertiary structure and the quatenary structure. The samples are run in duplicates of which one is stained by Coomassie Brilliant Blue R-250 (Figure 2.8a) and the other is transferred onto nitrocellulose membrane for western blot (Figure 2.8b). The transferred membrane is blocked with 5% fat-free milk in PBS and incubated in room temperature for 2 hour each with 9E10 anti-cmyc produced in mouse and anti-mouse HRP-conjugated antibody produced in goat successively. After each step of high-specificity antibody probing, thorough rinse is mandatory. HRP can react with the 3,3'-diaminobenzidine(DAB) to display chromogenic signal.

Soluble scFv purification- After confirming the presence of scFv in supernatant, periplasm and/or lysate of expression culture, load the total volume of each portion (e.g. periplasm) a Ni-NTA agarose beads column (Qiagen,5mL beads for 1L expression culture) in 4 ºC and allow it go through the column driven by gravity. The column is then stringently washed with 0.1% Tween20/2×PBS. The flow-through and the wash are sampled and kept lest loss of scFv. The imidazole eluting buffer is loaded on the column in the order of increasing concentration of 50 mM, 100 mM, 200 mM and 1M imidazole/2×PBS. The 1M imidazole elutes off all the rest of protein staying on the column. For the first purification trial, each elute along with flow-through and wash samples are dispersed on SDS-PAGE and performed Western blot to estimate the scFv concentration and purity. After the first time, the imidazole concentration that elutes off

only and most scFv will be selected as the specific concentration for eluting a certain scFv clone.

2.6 Figures and Tables

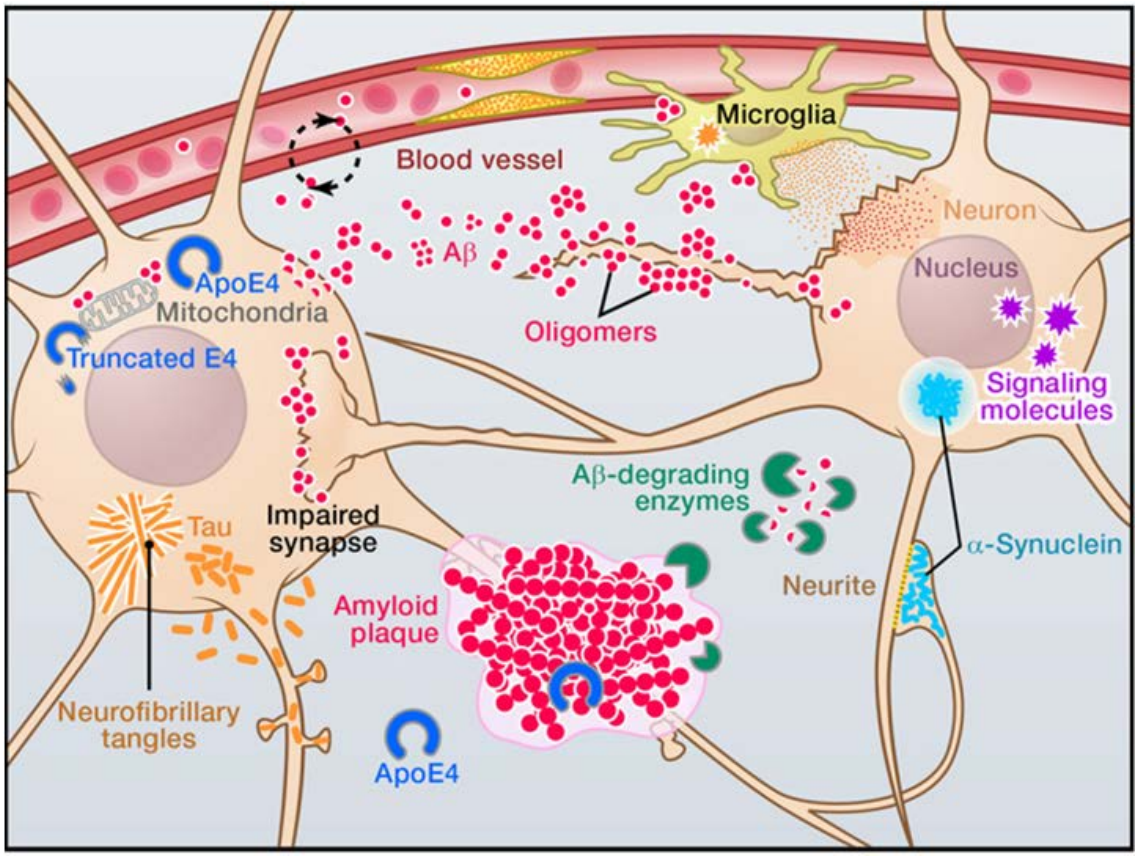

Figure 2.1 Schematic basis of Alzheimer's disease pathogenesis[12]. The neuritic amyloid plaque usually lies extracellular while the tau neurofibrillary tangles can be spot both intracellular detached from microtubule or extracellular after neuronal necrosis.

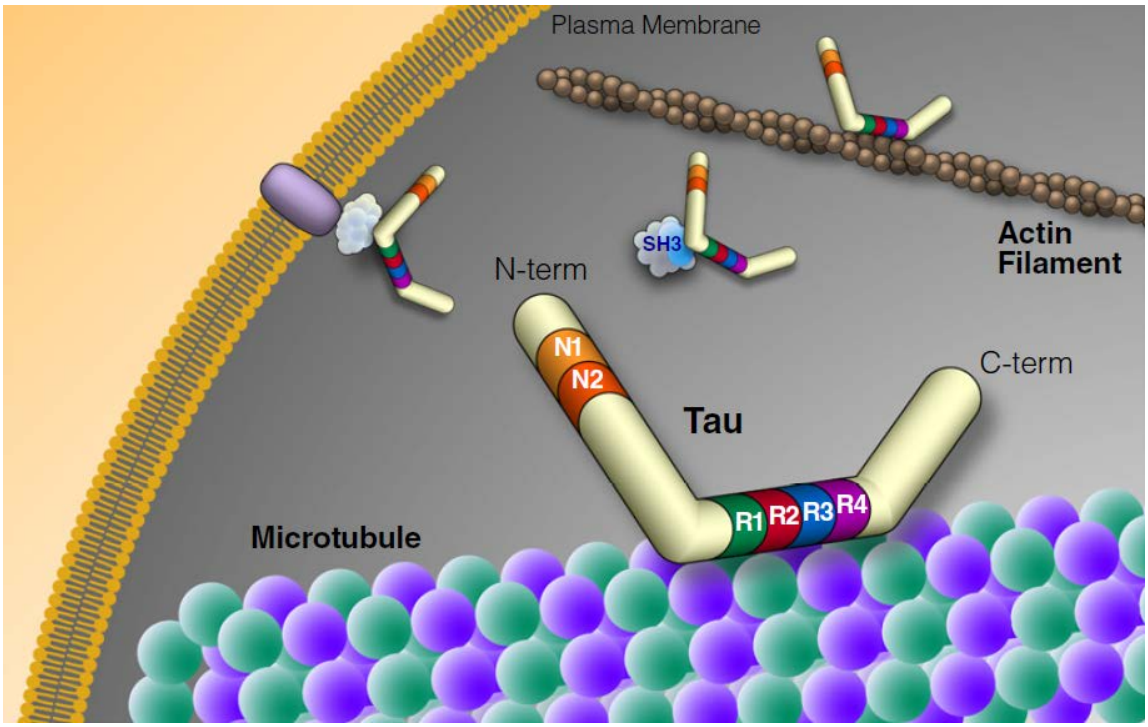

Figure 2.2 Schematic of tau structure, function and possible location[17]. Tau2N4R in the figure is the longest possible isoform. Total six tau isoforms are created by alternative splicing on N terminal exon 2, 3 (N1, N2) and C-terminal microtubule-associated repeats with the presence of absence of exon 10 (3R or 4R).

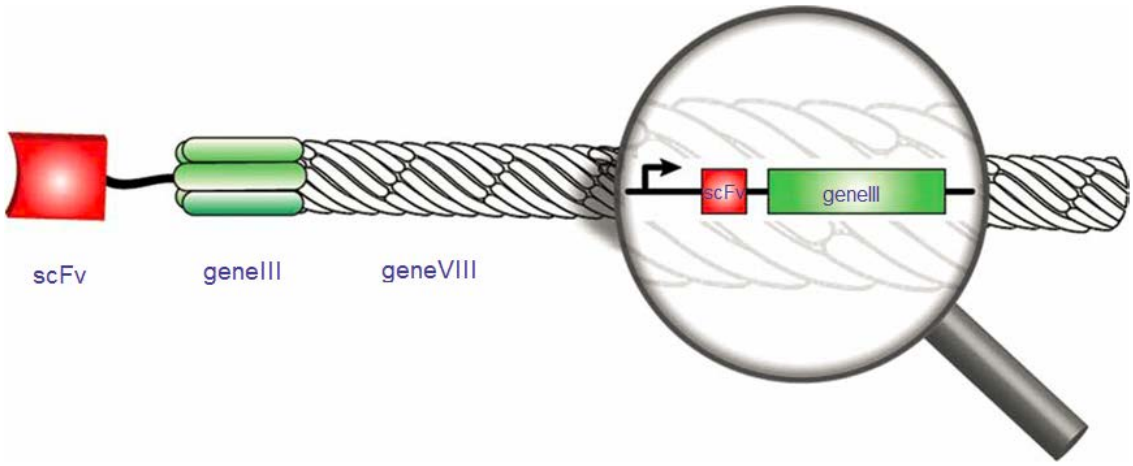

Figure 2.3 Schematic monoclonal scFv display phage particle with phagmid DNA (magnified) encoding scFv and the terminal protein III[60]. After the scFv encoded plasmid host bacteria are infected by M13 family helper phage, they take up phage shell protein gene to express and package them together with scFv. The new generation of phage is a different type with the scFv (red) displayed on its surface as a fusion with the terminal phage gene III protein (a.k.a g3 protein, green). They contain a phagmid DNA (magnified) and expressed both scFv and g3 protein from the same promoter.

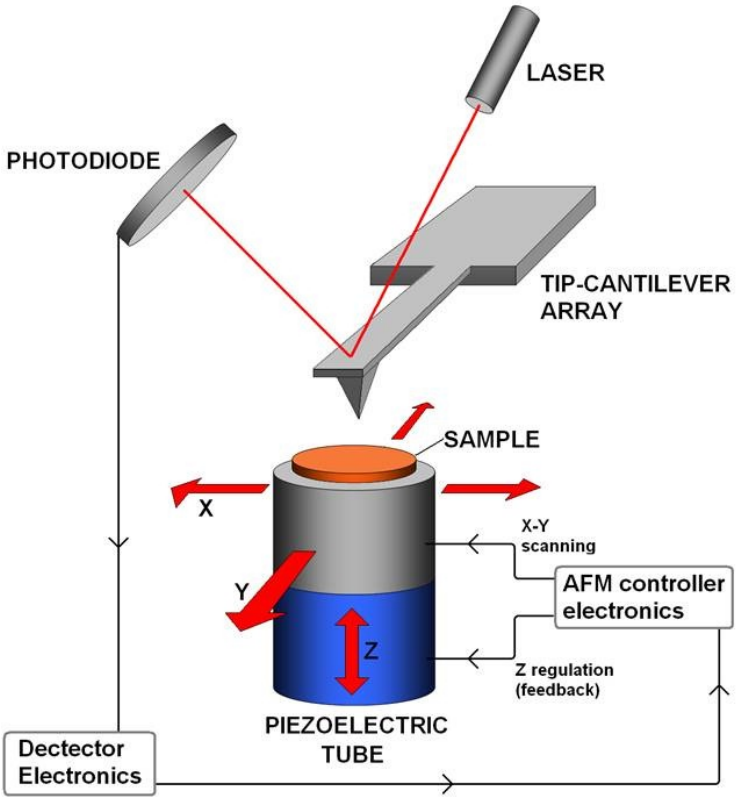

Figure 2.4 Schematic of AFM working principle.

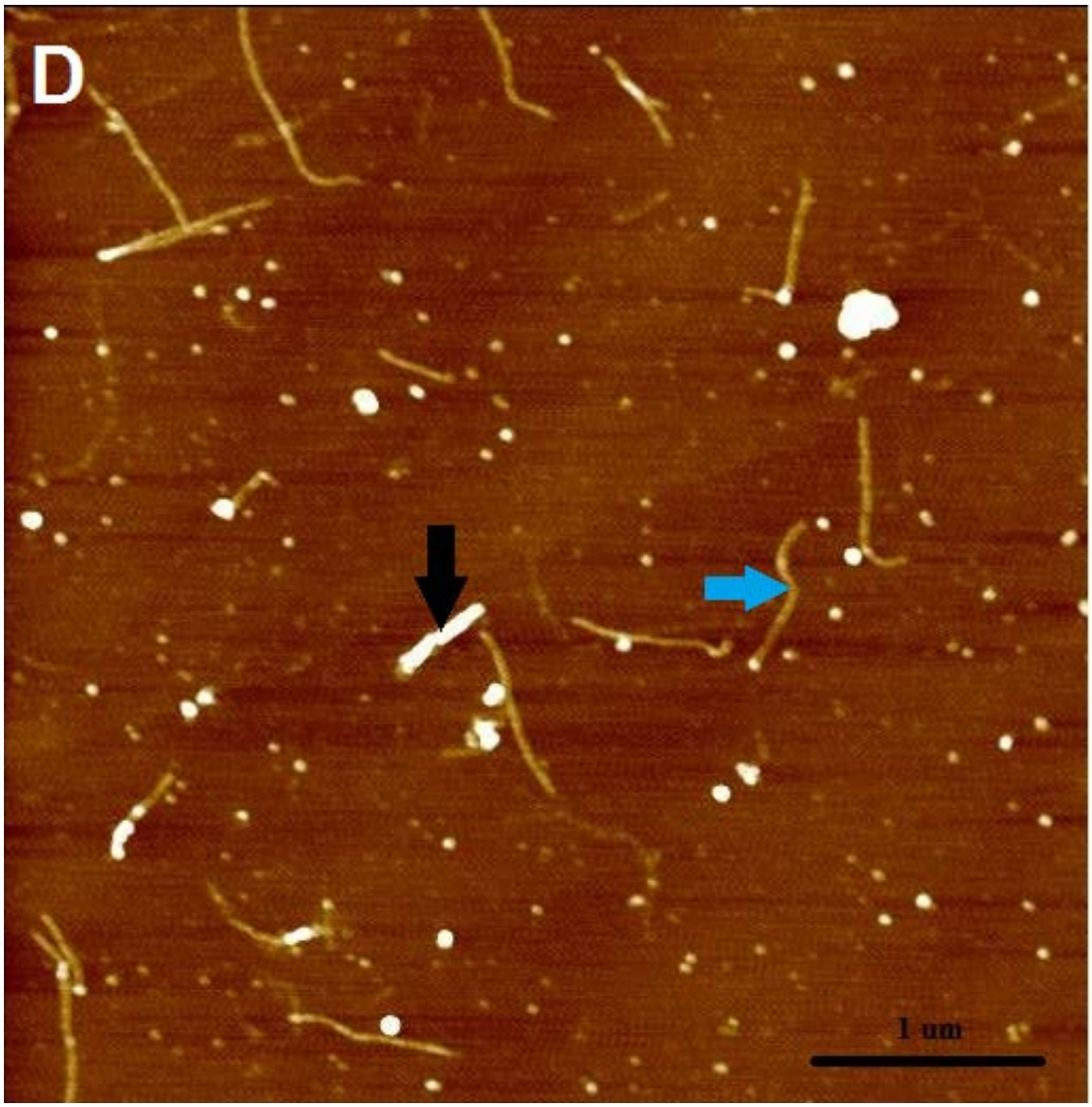

Figure 2.5 AFM image of tau 441 fibril (rod shaped object pointed with a black arrow), bacteriophage of F9T clone (filamentous object pointed with a blue arrow) and tau oligomers with various sizes and location either on one end of the phage or scattered in the background (white dots on the background).

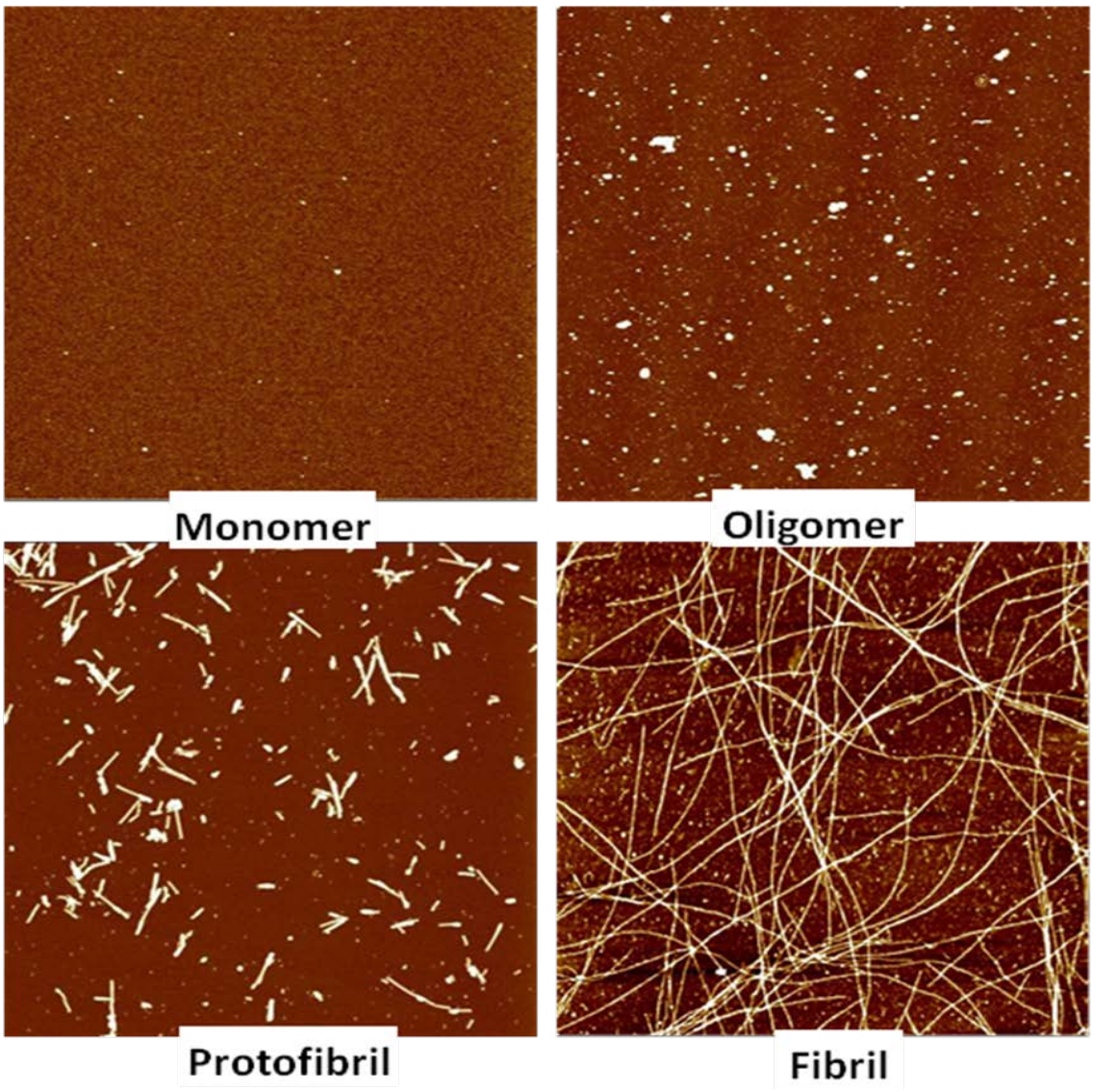

Figure 2.6 AFM can distinguish different size and morphology of α-synuclein from small globular protein monomer, grainy oligomer, rod-like protofibril and long thick fibril. These AFM images directly demonstrate α-synuclein oligomerization and aggregation process.

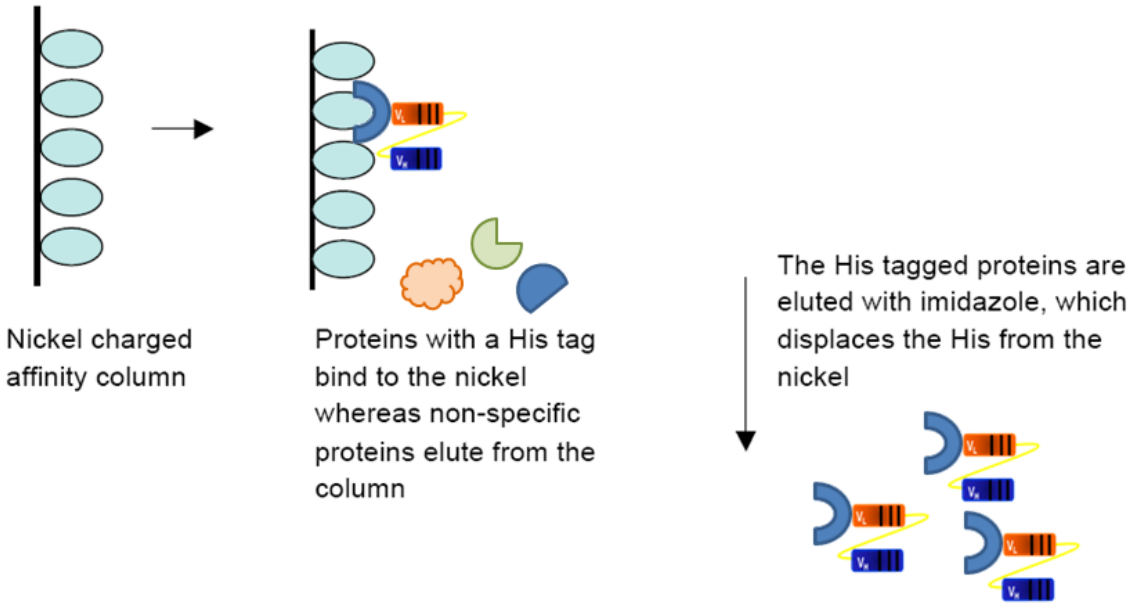

Figure 2.7 Schematic principle of 6-his tag ligated protein purification through nickel charged affinity column.

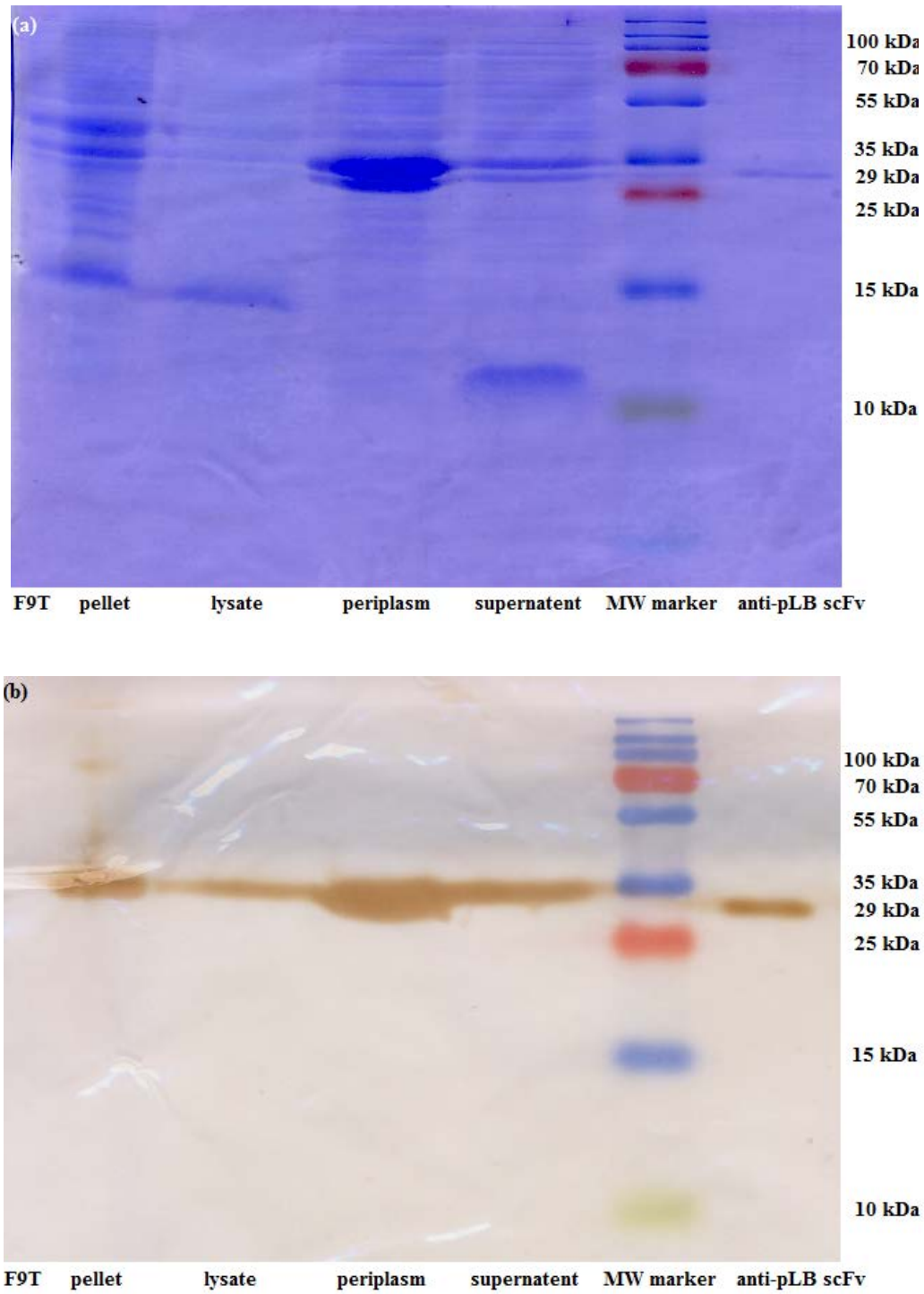

Figure 2. 8 scFv expression and its distribution in culture supernatant, periplasm and cell lysate. The SDS-PAGE (a) demonstrates scFv purity and the other ingredients molecular weights. The western blot (b) confirmed the presence of scFv by detecting cmyc tag on the scFv at its corresponding molecular weight around 29kDa.

2.7 References

1. 2012 Alzheimer's disease facts and figures. Alzheimers Dement, 2012. **8**(2): p. 131-68.

2. Frisoni, G.B., et al., The clinical use of structural MRI in Alzheimer disease. Nat Rev Neurol, 2010. **6**(2): p. 67-77.

3. Putcha, D., et al., Hippocampal hyperactivation associated with cortical thinning in Alzheimer's disease signature regions in non-demented elderly adults. J Neurosci, 2011. **31**(48): p. 17680-8.

4. Marchetti, C. and H. Marie, Hippocampal synaptic plasticity in Alzheimer's disease: what have we learned so far from transgenic models? Rev Neurosci, 2011. **22**(4): p. 373-402.

5. Palop, J.J. and L. Mucke, Amyloid-beta-induced neuronal dysfunction in Alzheimer's disease: from synapses toward neural networks. Nat Neurosci, 2010. **13**(7): p. 812-8.

6. Cummings, J.L., Alzheimer's disease. N Engl J Med, 2004. **351**(1): p. 56-67.

7. Tanzi, R.E. and L. Bertram, Twenty years of the Alzheimer's disease amyloid hypothesis: a genetic perspective. Cell, 2005. **120**(4): p. 545-55.

8. Selkoe, D.J., Alzheimer's disease: genotypes, phenotypes, and treatments. Science, 1997. **275**(5300): p. 630-1.

9. Kamboh, M.I., Molecular genetics of late-onset Alzheimer's disease. Ann Hum Genet, 2004. **68**(Pt 4): p. 381-404.

10. Goedert, M., et al., Tau proteins of Alzheimer paired helical filaments: abnormal phosphorylation of all six brain isoforms. Neuron, 1992. **8**(1): p. 159-68.

11. Spillantini, M.G., et al., Topographical relationship between beta-amyloid and tau protein epitopes in tangle-bearing cells in Alzheimer disease. Proc Natl Acad Sci U S A, 1990. **87**(10): p. 3952-6.

12. Huang, Y. and L. Mucke, Alzheimer mechanisms and therapeutic strategies. Cell, 2012. **148**(6): p. 1204-22.

13. Ward, S.M., et al., Tau oligomers and tau toxicity in neurodegenerative disease. Biochem Soc Trans, 2012. **40**(4): p. 667-71.

14. Haass, C. and D.J. Selkoe, Soluble protein oligomers in neurodegeneration: lessons from the Alzheimer's amyloid beta-peptide. Nat Rev Mol Cell Biol, 2007. **8**(2): p. 101-12.

15. Weingarten, M.D., et al., A protein factor essential for microtubule assembly. Proc Natl Acad Sci U S A, 1975. **72**(5): p. 1858-62.

16. Witman, G.B., et al., Tubulin requires tau for growth onto microtubule initiating sites. Proc Natl Acad Sci U S A, 1976. **73**(11): p. 4070-4.

17. Morris, M., et al., The many faces of tau. Neuron, 2011. **70**(3): p. 410-26.

18. Lee, V.M., M. Goedert, and J.Q. Trojanowski, Neurodegenerative tauopathies. Annu Rev Neurosci, 2001. **24**: p. 1121-59.

19. Takei, Y., et al., Defects in axonal elongation and neuronal migration in mice with disrupted tau and map1b genes. J Cell Biol, 2000. **150**(5): p. 989-1000.

20. Neve, R.L., et al., Identification of cDNA clones for the human microtubule-associated protein tau and chromosomal localization of the genes for tau and microtubule-associated protein 2. Brain Res, 1986. **387**(3): p. 271-80.

21. Mandelkow, E.M. and E. Mandelkow, Tau in Alzheimer's disease. Trends Cell Biol, 1998. **8**(11): p. 425-7.

22. Alonso Adel, C., et al., Promotion of hyperphosphorylation by frontotemporal dementia tau mutations. J Biol Chem, 2004. **279**(33): p. 34873-81.

23. Khatoon, S., I. Grundke-Iqbal, and K. Iqbal, Brain levels of microtubule-associated protein tau are elevated in Alzheimer's disease: a radioimmuno-slot-blot assay for nanograms of the protein. J Neurochem, 1992. **59**(2): p. 750-3.

24. Khatoon, S., I. Grundke-Iqbal, and K. Iqbal, Levels of normal and abnormally phosphorylated tau in different cellular and regional compartments of Alzheimer disease and control brains. FEBS Lett, 1994. **351**(1): p. 80-4.

25. Augustinack, J.C., et al., Specific tau phosphorylation sites correlate with severity of neuronal cytopathology in Alzheimer's disease. Acta Neuropathol, 2002. **103**(1): p. 26-35.

26. Peineau, S., et al., LTP inhibits LTD in the hippocampus via regulation of GSK3beta. Neuron, 2007. **53**(5): p. 703-17.

27. Kimura, T., et al., GSK-3beta is required for memory reconsolidation in adult brain. PLoS One, 2008. **3**(10): p. e3540.

28. Masuda, M., et al., Small molecule inhibitors of alpha-synuclein filament assembly. Biochemistry, 2006. **45**(19): p. 6085-94.

29. Taniguchi, S., et al., Inhibition of heparin-induced tau filament formation by phenothiazines, polyphenols, and porphyrins. J Biol Chem, 2005. **280**(9): p. 7614-23.

30. Lasagna-Reeves, C.A., et al., Alzheimer brain-derived tau oligomers propagate pathology from endogenous tau. Sci Rep, 2012. **2**: p. 700.

31. Lasagna-Reeves, C.A., et al., Identification of oligomers at early stages of tau aggregation in Alzheimer's disease. FASEB J, 2012. **26**(5): p. 1946-59.

32. Check, E., Nerve inflammation halts trial for Alzheimer's drug. Nature, 2002. **415**(6871): p. 462.

33. Clark, M., Antibody humanization: a case of the 'Emperor's new clothes'? Immunol Today, 2000. **21**(8): p. 397-402.

34. Arafat, W.O., et al., Effective single chain antibody (scFv) concentrations in vivo via adenoviral vector mediated expression of secretory scFv. Gene Ther, 2002. **9**(4): p. 256-62.

35. Kipriyanov, S.M., G. Moldenhauer, and M. Little, High level production of soluble single chain antibodies in small-scale Escherichia coli cultures. J Immunol Methods, 1997. **200**(1-2): p. 69-77.

36. Boado, R.J., et al., IgG-single chain Fv fusion protein therapeutic for Alzheimer's disease: Expression in CHO cells and pharmacokinetics and brain delivery in the rhesus monkey. Biotechnol Bioeng, 2010. **105**(3): p. 627-35.

37. Kim, D.J., et al., Production and characterisation of a recombinant scFv reactive with human gastrointestinal carcinomas. Br J Cancer, 2002. **87**(4): p. 405-13.

38. Kasturirangan, S., D. Brune, and M. Sierks, Promoting alpha-secretase cleavage of beta-amyloid with engineered proteolytic antibody fragments. Biotechnol Prog, 2009. **25**(4): p. 1054-63.

39. Dickson, D.W., The pathogenesis of senile plaques. J Neuropathol Exp Neurol, 1997. **56**(4): p. 321-39.

40. Hardy, J. and D.J. Selkoe, The amyloid hypothesis of Alzheimer's disease: progress and problems on the road to therapeutics. Science, 2002. **297**(5580): p. 353-6.

41. Varvel, N.H., et al., Abeta oligomers induce neuronal cell cycle events in Alzheimer's disease. J Neurosci, 2008. **28**(43): p. 10786-93.

42. Hardy, J.A. and G.A. Higgins, Alzheimer's disease: the amyloid cascade hypothesis. Science, 1992. **256**(5054): p. 184-5.

43. Braak, H. and E. Braak, Neuropathological stageing of Alzheimer-related changes. Acta Neuropathol, 1991. **82**(4): p. 239-59.

44. Braak, H. and E. Braak, Demonstration of amyloid deposits and neurofibrillary changes in whole brain sections. Brain Pathol, 1991. **1**(3): p. 213-6.

45. Braak, H. and E. Braak, Evolution of the neuropathology of Alzheimer's disease. Acta Neurol Scand Suppl, 1996. **165**: p. 3-12.

46. Alafuzoff, I., et al., Staging of neurofibrillary pathology in Alzheimer's disease: a study of the BrainNet Europe Consortium. Brain Pathol, 2008. **18**(4): p. 484-96.

47. von Bergen, M., et al., Tau aggregation is driven by a transition from random coil to beta sheet structure. Biochim Biophys Acta, 2005. **1739**(2-3): p. 158-66.

48. Liu, R., et al., Single chain variable fragments against beta-amyloid (Abeta) can inhibit Abeta aggregation and prevent abeta-induced neurotoxicity. Biochemistry, 2004. **43**(22): p. 6959-67.

49. Zameer, A., et al., Single chain Fv antibodies against the 25-35 Abeta fragment inhibit aggregation and toxicity of Abeta42. Biochemistry, 2006. **45**(38): p. 11532-9.

50. Kasturirangan, S., et al., Isolation and characterization of antibody fragmentsselective for specific protein morphologies from nanogram antigensamples. Biotechnol Prog, 2013.

51. Kasturirangan, S., S. Boddapati, and M.R. Sierks, Engineered proteolytic nanobodies reduce Abeta burden and ameliorate Abeta-induced cytotoxicity. Biochemistry, 2010. **49**(21): p. 4501-8.

52. Boddapati, S., Y. Levites, and M.R. Sierks, Inhibiting beta-secretase activity in Alzheimer's disease cell models with single-chain antibodies specifically targeting APP. J Mol Biol, 2011. **405**(2): p. 436-47.

53. Emadi, S., et al., Isolation of a human single chain antibody fragment against oligomeric alpha-synuclein that inhibits aggregation and prevents alpha-synuclein-induced toxicity. J Mol Biol, 2007. **368**(4): p. 1132-44.

54. Emadi, S., et al., Detecting morphologically distinct oligomeric forms of alpha-synuclein. J Biol Chem, 2009. **284**(17): p. 11048-58.

55. Barkhordarian, H., et al., Isolating recombinant antibodies against specific protein morphologies using atomic force microscopy and phage display technologies. Protein Eng Des Sel, 2006. **19**(11): p. 497-502.

56. Kohler, G. and C. Milstein, Continuous cultures of fused cells secreting antibody of predefined specificity. Nature, 1975. **256**(5517): p. 495-7.

57. Glennie, M.J. and P.W. Johnson, Clinical trials of antibody therapy. Immunol Today, 2000. **21**(8): p. 403-10.

58. Marks, J.D., et al., By-passing immunization. Human antibodies from V-gene libraries displayed on phage. J Mol Biol, 1991. **222**(3): p. 581-97.

59. Sheets, M.D., et al., Efficient construction of a large nonimmune phage antibody library: the production of high-affinity human single-chain antibodies to protein antigens. Proc Natl Acad Sci U S A, 1998. **95**(11): p. 6157-62.

60. Lee, C.M., et al., Selection of human antibody fragments by phage display. Nat Protoc, 2007. **2**(11): p. 3001-8.

Chapter 3

Trimeric tau is toxic to human neuronal cells at low nanomolar concentrations

3.1 Abstract

Tau in its monomeric form facilitates polymerization of tubulin into microtubules and helps to maintain their structure in neuronal axons. In Alzheimer's disease (AD) the hallmark neurofibrillary tangles (NFTs) contain aggregated tau in a hyperphosphorylated form. Although hyperphosphorylated tau and NFTs have long been considered as key pathological features of AD, soluble oligomeric tau species may play a more critical role in AD progression since these tau species correlate better with neuronal loss and cognitive dysfunction. Recent studies show that extracellular oligomeric tau can inhibit memory formation and synaptic function and also transmit pathology to neighboring neurons, however the specific forms of oligomeric tau involved in toxicity are still unknown. Tau naturally exists in six major isoforms due to post-transcriptional splicing and also undergoes various post-translational modifications including phosphorylation, all of which greatly complicate studies to determine which tau aggregates are neurotoxic. Recombinant human tau can be generated in single splice variants and without post-translational modification facilitating such studies. Here we used two different splice variants (1N4R and 2N4R) of non-phosphorylated recombinant human tau (NPrhTau) and generated monomeric, dimeric and trimeric fractions of each isoform. The composition of each fraction was verified chromatographically and also by atomic force microscopy (AFM). The toxicity of each fraction toward both human neuroblastoma cells

and cholinergic-like neurons was assessed using a lactate dehydrogenase (LDH) assay. Trimeric but not monomeric or dimeric tau aggregates of both splice variants was neurotoxic at low nanomolar concentrations, with the full length tau isoform having increased toxicity compared to the truncated tau variant.

3.2 Introduction

Alzheimer's disease (AD) is the most common form of dementia, characterized by progressive cognitive impairment, cerebral atrophy and neuronal loss, with death generally occurring four to eight years after diagnosis[1]. Two pathological hallmarks of AD, extracellular neuritic plaques primarily composed of amyloid beta (Aβ) and intracellular neurofibrillary tangles (NFTs) primarily composed of tau protein, were originally identified in 1906 by Dr. Alois Alzheimer[2]. While great strides have been made in understanding the mechanisms that promote aggregation of Aβ and tau into the hallmark plaques and tangles, comparatively little progress has been achieved in halting or curing the disease. Analysis of familial AD cases implicated production of Aβ as a primary factor in progression of AD, leading to the rise of the amyloid cascade hypothesis which states that Aβ misfolding and aggregation initiates AD pathogenesis and triggers other effects such as tau phophorylation, aggregation and tangle formation [3]. The amyloid hypothesis had dominated the field for more than a decade, and has driven numerous clinical studies for therapeutic interventions including several immunization studies targeting Aβ[4-6]. However failure of several clinical trials targeting Aβ has cast doubt on the pathological role of Aβ in AD [7], and increasing evidence indicates that tau also plays an important role in the progression of AD. Tau misfolding and aggregation can take place independently of amyloid formation[8], and in

many cases the presence of tau lesions are associated with AD without presence of Aβ aggregates[9]. Clearance of Aβ plaques without reducing soluble tau levels is insufficient to ameliorate cognitive decline in double transgenic mice overexpressing Aβ and tau P301L[10]. These results among many others indicate that oligomeric tau may be an important therapeutic target for AD.

Tau in its monomeric form is a microtubule-associated protein crucial for microtubule assembly [11-12] and stabilization [13]. Six major tau isoforms can be generated by alternative posttranscriptional splicing of exon 2 and exon 3 on the N-terminal projection domain and of exon 10 (Repeat 2) on the assembly domain (Figure 3.1). Tau contains three or four similar but not identical repeats on the microtubule-binding domain (MBD) that binds to and helps promote microtubule stability and function. For example, Repeat 2 and Repeat 3 contain hexapeptide motifs of PHF6* and PHF6 respectively (Figure 3.1). These motifs increase the tendency to form β-sheet structures that can interact with tubulins to form microtubules and also facilitate self-assembly to generate oligomeric and higher-order aggregates[14-15]. Tau isoforms with or without the second microtubule binding repeat can aggregate, but only the isoforms with the second repeat can form extended oligomeric forms mediated by disulfide linkages due to the additional cysteines in the second repeat (Figure 3.1 and Figure 3.2). Therefore, in this study we utilized tau isoforms containing the second repeat unit to study the role of tau aggregation in neurotoxicity.

Hyperphosphorylation of tau is required for the release of tau from microtubules and its mislocalization to the somatodendritic compartment enabling tau to self-associate

into oligomers and higher order aggregates. However, the toxicity of tau is not directly related to its hyperphosphorylation but rather a mechanism to regulate its interaction with tubulin to stabilize microtubules and to regulate transport along microtubules. Expression of exogenous tau in mature hippocampal neurons leads to blockage of transport along microtubules and degeneration of synapses that can be rescued by phosphorylation of tau by kinase MARK2 to unblock the microtubule tracks[16]. Significantly, tau in the extracellular space is reported to be less phosphorylated than intracellular tau[17-18] and more toxic in its dephosphorylated state[17]. Extracellular oligomers of recombinant full-length human tau protein were shown to be neurotoxic in mice and impair memory consolidation[19], similar work at other labs has shown a similar effects with recombinant tau oligomers and tau oligomers composed of hyperphosphorylated tau from AD brain. Thus, the hyperphosphorylation of tau associated with disease may be a causal factor in tau self-association into oligomers, but the hyperphosphorylation of tau in and of itself may not be the basis for the toxicity of extracellular tau oligomers.

Neurofibrillary tangles (NFTs) have traditionally been correlated with neuronal loss[20] and considered to be key intracellular indicators of AD. Approaches for targeting tau aggregation have focused on inhibiting hyperphosphorylation and fibril formation, reducing total tau levels, or stabilizing microtubules[21]. However, accumulating evidence suggests that soluble oligomeric rather than insoluble fibrillar tau species are neurotoxic and play an important role in the onset and progression of AD [21-24]. Although NFTs are a hallmark feature of AD, they can exist in AD neurons for up to 20 to 30 years[25] before postmortem confirmation and therefore are less likely to induce

immediate toxicity in AD brain[26] . In animal models of tauopathy, the presence of NFTs does not correlate well with neuronal loss and memory deficits[27]. Reduction in neuronal loss and improvement in memory performance are observed despite an increase in NFTs[28]. In addition, the presence of NFT pathology does not localize well with areas of neuronal loss[29-31], synapse loss or dysfunction in the hippocampus along with microglial activation occurs well before the presence of NFTs[32]. In contrast, oligomeric tau was implicated in numerous studies as playing a key role in AD progression[33-35] and to be a primary initiator of neurotoxicity and neurodegeneration[36]. Oligomeric tau has been identified in early stages of neuronal cytopathology in AD and closely correlates with hyperphosphorylation on microtubule binding sites[24]. Tau oligomers can propagate endogenous tau pathology throughout the brain similarly to prions, demonstrating their neuronal toxicity[37]. The presence and concentrations of two tau oligomers (140kDa and 170kDa) correlate with memory loss in various age rTg4510 mice[33]. Oligomeric tau also induces synaptic and mitochondrial dysfunction[19]. Although tau is predominantly intracellular, the role of extracellular tau is gaining attention as extracellular oligomeric tau can have acute effects on long-term potentiation in hippocampal slices and can transmit pathology to healthy neurons [37]. Detection of oligomeric tau levels in human CSF and blood are also promising AD diagnostic biomarkers along with total and hyperphosphorylated tau levels[38]. Because of the important role of oligomeric tau in AD and the recognition of the importance of extracellular tau in disease, it is critical to identify the key toxic tau species in disease etiology. Here we studied the extracellular neurotoxicity of monomeric, dimeric and

trimeric forms of two four-repeat recombinant human tau variants to help identify the key tau species involved in the onset and progression of AD.

3.3 Material and Methods

Recombinant human tau (rhTau) preparation and purification- rhTau was purified as monomers from bacterial (BL21 DE3) clones with tau constructs in the pET21B and pET29a vectors. Standard methods were used to grow and induce the protein with 1 mM IPTG. Pelleted cells were lysed with CelLytic B lysis buffer, lysozyme, benzonase, and protease inhibitors according to the manufacturer's protocol (Sigma-Aldrich, St. Louis, MO)). Cation exchange (GE Healthcare Life Sciences) was used for the first step of purification with SP-Sepharose resin for both tau constructs, and 300 mM NaCl in 25 mM Tris-HCl pH 7.4 was used to elute tau protein. Amicon Ultra Centrifugal Devices (Millipore) were used to buffer exchange the protein preparations into 50 mM Tris-HCl pH 7.4. Protein concentration was determined using a BCA assay (Thermo Fisher Scientific). Tau oligomers were generated by incubating tau monomers at a concentration of 5 μM in 50 mM Tris buffer pH 7.4 with 100 mM NaCl at 37 °C overnight. The monomeric and oligomeric species were resolved by 6% PAGE, eluted, and buffer exchanged into 50 mM Tris-HCl. Fractions were analyzed by non-reducing SDS-PAGE to minimize degradation of oligomeric proteins and silver staining to enhance the signal and to verify the purity of tau variants. Protein concentration was determined using the BCA assay.

Height distribution analysis- AFM sample preparation and imaging were performed as described previously[39-44]. Aliquots of 10 μL 0.50 μM purified tau

variants in 50 mM Tris-HCl buffer were deposited on separate mica pieces for imaging using MultiMode AFM Nanoscope IIIA system (Veeco/Digital instruments, Santa Barbara, CA) which was set in tapping mode and equipped with silicon AFM probes (VISTA probes, nanoscience instruments). Height distribution analysis of the different tau samples was fit a normal distribution probability model using Gwyddion 2.20. All detectable protein molecules were assumed to be spherical and the height values approximate their diameters.

Cell culture and treatments- SH-SY5Y human neuroblastoma cell lines (American Tissue Culture Collection) were cultivated in tissue culture flask (Falcon by Becton Dickinson Labware). Cells were grown in a medium containing 44% v/v Ham's F-12 (IrvineScientific), 44% v/v MEM Earle's salts (IrvineScientific), 10% v/v denatured fetal bovine serum (FBS) (SigmaAldrich), 1% v/v MEM non-essential amino acids (Invitrogen) and 1% v/v antibiotic/antimycotic (Invitrogen). Media were renewed once every two to three days. The cells were passaged to a new flask when they were confluent in the flask. For toxicity studies, the SH-SY5Y cells were seeded in a 48-well cell culture cluster plate (Costar by Corning Incorporated) with 5×10^4 cells/well in 300ul fresh medium. Each experiment was conducted in triplicate. Cell density was estimated by reading a fixed volume on a hemocytometer. After growth in a 37°C incubator for 24 hours, the tissue culture media were replaced with fresh serum-free media for the neurotoxicity test on non-differentiated cells. To investigate tau toxicity on cholinergic neurons, a duplicate set of the cultured cells was induced into cholinergic-like phenotype by incubation with retinoic acid at a final concentration of 10μM for 3 to 5 days[43, 45-47]. The cultivated non-differentiated and cholinergic-like neurons were treated with

monomeric, dimeric and trimeric variants of 1N4R and 2N4R at final concentrations of 2.26 nM, 4.50 nM, 11.15 nM and 15.50 nM. A PBS negative control was used as a standard for subsequent LDH assay analysis. Cultures were incubated with tau species at 37°C and sampled at 3, 18, 24 and 48 hour time points by harvesting 30 ul/well aliquots of culture supernatant.

LDH assay - The LDH protocol is adapted from a commercial kit (Sigma-Aldrich) based on the generic protocol of Decker and Lohmann-Matthes[48]. The LDH assay was performed as described previously[40]. Absorbance was measured at 490nm (reference wavelength 690nm). Relative absorbance values were calculated by subtracting the reference values from the values obtained at 490nm. LDH% values greater than 150 are considered toxic.

Statistical analysis- The relative absorbance value of all samples were normalized to that of controls which were set as 100% for each independent experiment. Group mean values were analyzed by one-way ANOVA with $p<0.05$ standard and LSD post hoc significant differences test. All analyses were performed with SPSS 21.0 (IBM Corp., Armonk, NY).

3.4 Results

rhTau aggregate analysis- We expressed recombinant human tau in a bacterial host system to eliminate any post-translational phosphorylation of tau and therefore remove any potential effects that phosphorylation may have on tau aggregation or loss of function. The resulting non-phosphorylated human recombinant tau (NPrhTau) monomers contain reactive cysteine groups with free thiols, facilitating the formation of intramolecular

disulfide bonds to make stable non-reactive monomers and the formation of intermolecular disulfide bonds to produce tau oligomers and higher degree aggregates(Figure 3.2). The polymerization reaction is controlled by incubation time and protein concentration. The non-reactive monomeric, dimeric and trimeric forms of both the 2N4R and 1N4R splice variants generate stable aggregate morphologies with defined size profiles dependant on the degree of oligomerization and length of the splice variant as evidenced by SDS-PAGE (Figure 3.3) and AFM height distribution analysis (Figure 3.4). The oligomer heights increment for each additional monomeric tau unit is fixed within a certain isoform, which is 0.5nm for 1N4R variants and 1.0nm for the 2N4R variants (Figure 3.4). The size of each respective 2N4R species are also larger than the corresponding 1N4R species (Figure 3.3 and Figure 3.4) as expected given that tau 2N4R contains the extra N-terminal insert compared with the 1N4R variants.

Extracellular rhTau induced neurotoxicity test- While neither the monomeric or dimeric forms of tau from either the 1N or 2N splice variants displayed detectable toxicity, the trimeric form of both variants exerted marked toxicity toward non-differentiated (Figure 3.5A) and retinoic acid induced cholinergic-like neurons (Figure 3.5B) with LDH values well above the toxic threshold of 150 at low nanomolar concentrations (11.15nM and 15.50nM). The full length 2N4R trimeric tau form displayed significantly higher toxicity than the 1N4R trimeric form toward non-differentiated neurons (Figure 3.5A), although the effect is diminished in the cholinergic-like neurons (Figure 3.5B). When trimeric tau was added to non-differentiated SH-SY5Y cells, an increase in toxicity was observed with time at the highest concentrations for both the 1N4R (Figure 3.6A) and 2N4R (Figure 3.6B) trimeric variants. However when

trimeric tau was added to the cholinergic-like neurons, the toxicity of the 1N (Figure 3.6C) and 2N (Figure 3.6D) variants was relatively consistent over the first 24 hours, but increased after 48 hours. Both variants of trimeric tau showed increased toxicity toward the cholinergic-like neurons compared to the non-differentiated neurons at short incubation times (Figure 3.7A) but the reverse was observed at longer incubation times (Figure 3.7B).

3.5 Discussion

While the amyloid cascade hypothesis[49] has dominated studies into the etiology of AD over the last decade or more, the importance of tau in the onset and progression of AD is steadily becoming more apparent. Tau pathology has been observed in the absence of Aβ deposits in children and young adult cases, and tau aggregates in the entorhinal-hippocampal regions precedes the onset of Aβ pathology[8-9]. Numerous studies have shown that various oligomeric forms of Aβ are toxic to neurons and can impair cognitive performance[50-51], thus implicating their potential role as valuable biomarkers for diagnosing AD[42, 52-53]. Similar to the important role of various soluble oligomeric Aβ species in AD, different soluble oligomeric forms of tau may also play a critical role in AD, also causing neuronal loss and cognitive dysfunction[19, 54-55]. Therefore to facilitate diagnoses and therapeutic treatments for AD, it is important to identify the key tau species involved in the onset and progression of the disease. Given that tau has multiple splice variants and post-translational modification sites, we attempted to simplify the complex diversity of tau forms by focusing on two non-phosphorylated human recombinant tau isoforms, 1N4R and 2N4R. These two four-repeat (4R) isoforms of tau both have all four repeats of the microtubule-associated domains and are more

prone to form the aggregates readily phosphorylated by brain protein kinases than those with only three repeats (3R)[56] due to the presence of Repeat 2 with microtubule-affinity enhancing hexapeptide motifs[14-15] and an additional cysteine that forms disulfide linkages to stabilize the aggregates.

The most disease-relevant tau material to use to study toxicity of extracellular tau forms would be well characterized tau oligomers purified from AD cerebrospinal fluid (CSF) using methods to preserve their post-translational modifications, including phosphorylation, glycation, ubiquitination, aggregation and truncation. Preparations from several non-AD and AD cases would be necessary to understand the significance of the results. Here we performed an initial study focused specifically on unmodified tau protein oligomers and control monomer to specifically understand the relevance of oligomer structure to extracellular toxicity.

We determined the toxicity of the different tau variants using both non-differentiated and cholinergic-like neuroblastoma cell lines to determine how aggregate size and cell phenotype affected toxicity. Cholinergic cells are particularly vulnerable in AD with significant neuronal loss in the nucleus basalis of Meynert (NBM), i.e. the hippocampus and the cortex[57]. NBM is enriched in cholinergic cells and undergoes degeneration and a significant decrease of acetylcholine production in AD[58]. Decreased levels of acetylcholine and a number of other cortical cholinergic markers lead to clinical dementia and impairment in cognitive function[58], indicating that cholinergic cells are particularly vulnerable in AD. Here we show that trimeric, but not monomeric or dimeric tau is toxic to neuronal cells at low nano-molar concentrations, and that the full

length 2N tau variant is more toxic than the shorter 1N variant to non-differentiated neurons (Figure 3.5). Both trimeric tau variants cause toxicity to both non-differentiated SH-SY5Y cells and retinoic acid induced cholinergic-like neurons when tau was applied extracellularly at nanomolar levels (Figure 3.6). However the cultured cholinergic-like neurons show increased susceptibility to trimeric tau induced toxicity at short incubation times compared with similar non-differentiated neurons (Figure 3.7A), perhaps partially accounting for the increased vulnerability of cholinergic-like neurons in AD. Since the non-differentiated cells were equally susceptible to trimeric tau induced toxicity at longer incubation times (Figure 3.7B), these results suggest that toxicity of extracellular trimeric tau is not dependent on receptors or proteins specifically associated with cholinergic cells, but that toxicity might be facilitated by them. Our results are consistent with a recent study showing that low molecular weight (LMW) misfolded tau species exclusive of monomeric tau can be endocytosed by neurons and transported both anterograde and retrograde to induce endogenous tau pathology in vivo while fibrillar tau and brain-derived filamentous tau cannot be endocytosed [59]. This suggests that tau toxicity may be spread through cells in certain brain regions by endocytosis of trimeric and larger oligomeric forms of tau and that this uptake is facilitated in cholinergic neurons.

Neuronal toxicity of oligomeric tau may share similar properties to that of oligomeric Aβ where the critical feature involved in neuronal toxicity is the aggregation state of the protein more than post-translational modifications [23, 60]. While there are a wide variety of tau variants that occur in vivo including different post-translational modifications, splice variants and aggregated species, this study begins to more systematically probe the role of selected tau variants in AD. Further studies are needed to

determine the contribution of splice variants and AD-specific post-translational modifications found in extracellular tau to the toxicity of the tau variants and to how these tau variants affect other neuronal models including primary neurons or induced pluripotent stem cells. Well characterized reagents that can selectively identify specific tau variants and morphologies will be useful for these further studies.

3.6 Acknowledgements

We cordially give thanks to Dr. Debra Page Baluch in Keck's bioimaging laboratory for the access to AFM facilities and Dr. Srinath Kasturirangan for the advice and assistance with AFM imagine height distribution analysis. This work was partially supported by NIH; NIA grant # AG029777.

3.7 Figures and Tables

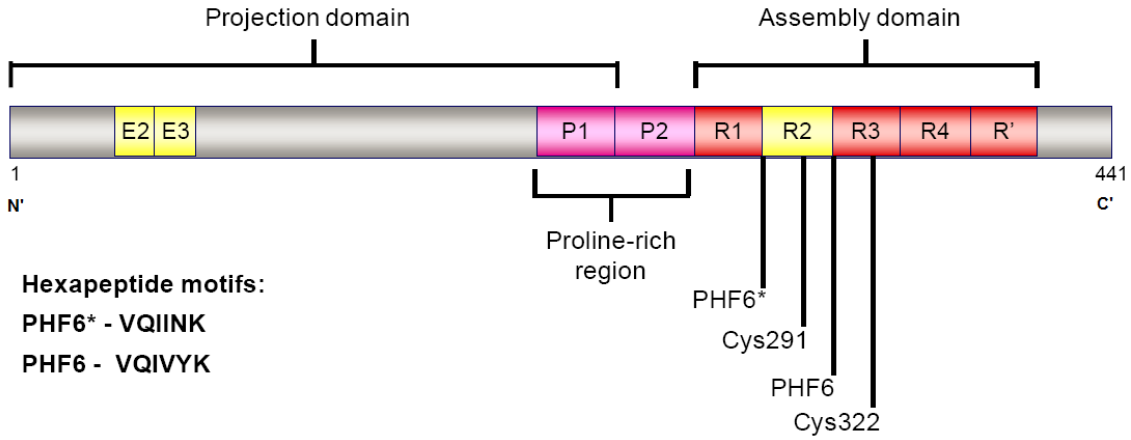

Figure 3.1 Tau protein structural features in linear diagram. A full-length tau protein with 441 amino acids (tau441 or tau 2N4R) is shown. Alternative splicing showed in yellow rectangles results in total of six isoforms, denoted by either their total number of amino acids, or the number of N' terminal exons (Ns) and microtubule-associated repeats (Rs).

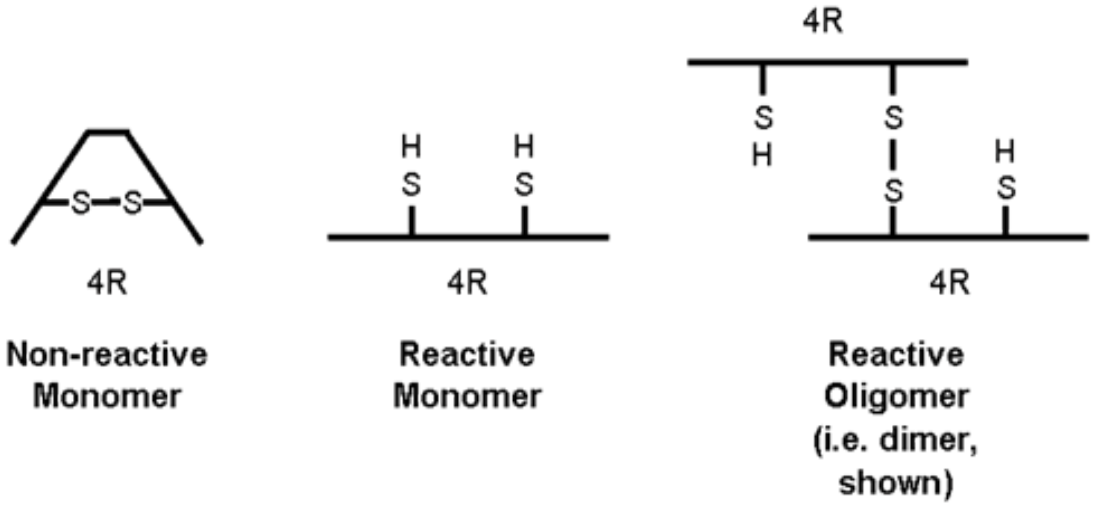

Figure 3.2 Schematic of non-reactive monomer, reactive monomer and reactive oligomer. Reactivity implies the ability to form an intermolecular disulfide linkage. Intramolecular disulfide linkage causes formation of non-reactive tau monomer. The free thiols in a reactive monomer allow formation of an intermolecular or intramolecular disulfide linkage. Reactive oligomer has one or more free thiols readily forming disulfide linkage with reactive monomeric tau for oligomer extension purpose.

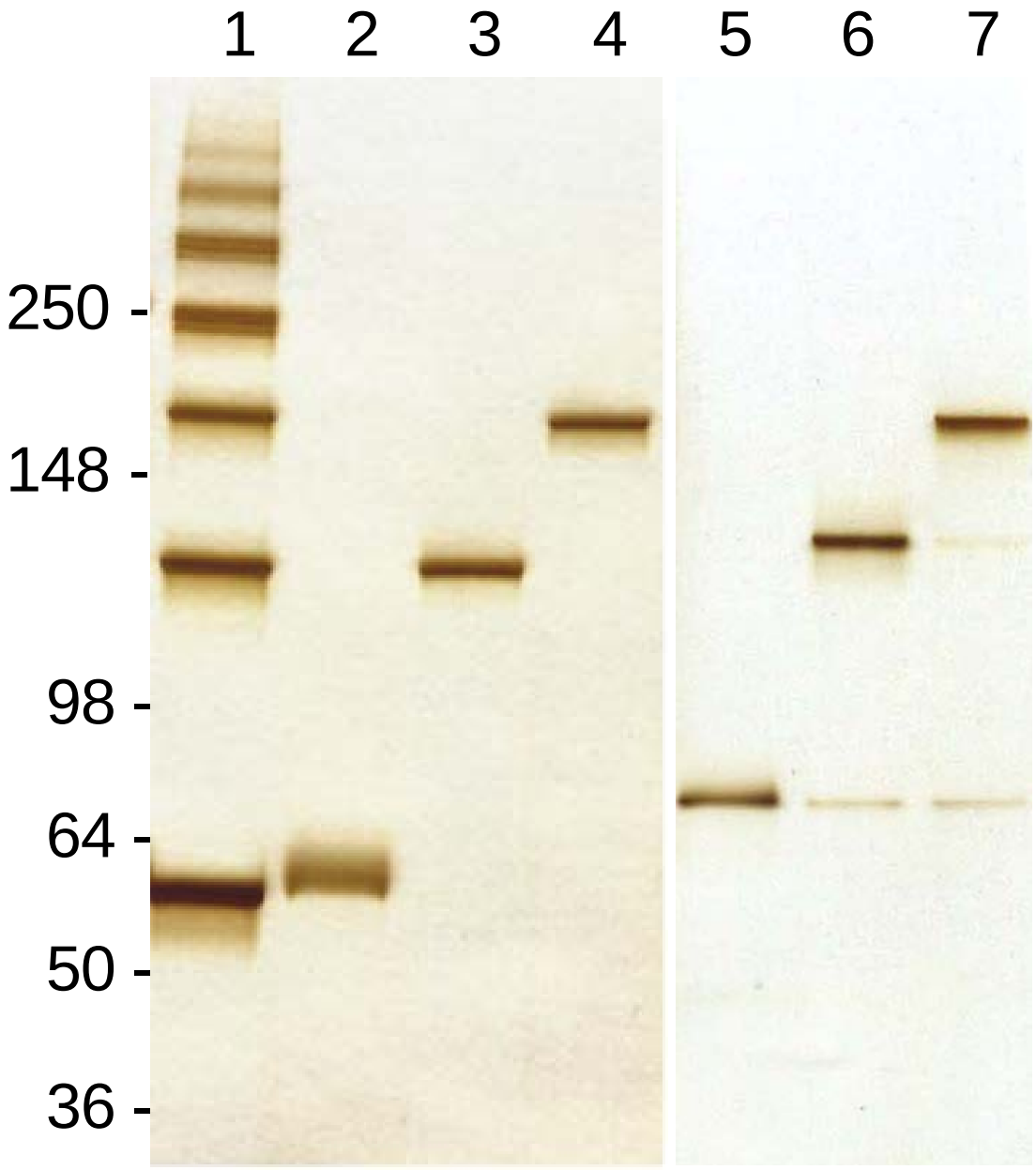

Figure 3.3 Recombinant human tau (rhTau) monomeric and oligomeric species production and purification. rhTau 1N4R enriched with disulfide-mediated tau oligomers (lane 1) was used for the purification of monomeric, dimeric and trimeric tau species (lanes 2-4), rhTau 2N4R purified monomeric, dimeric and trimeric species (lanes 5-7) used in these studies.

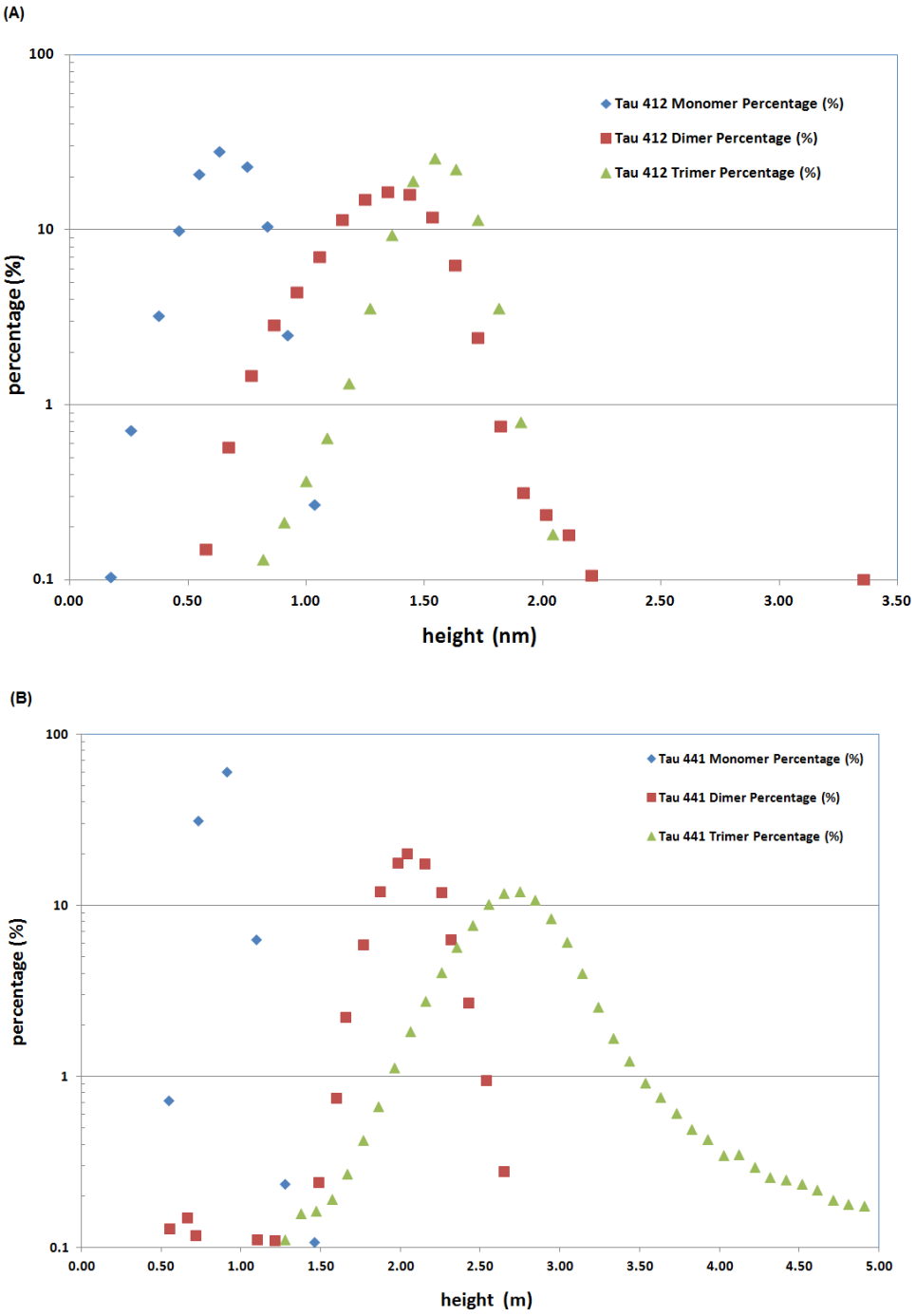

Figure 3.4 Plots of height distribution of monomeric, dimeric and trimeric fractions of rhTau 1N4R (A) and tau 2N4R (B). The height value of each particle was measured using Gwyddion. The numbers of particles falling in continuous size ranges were calculated and normalized into count percentages. The peak values give an approximate value for each tau species particle size. As expected, high-degree oligomers are larger than low-degree oligomers within the same isoform, and corresponding oligomeric aggregates from the longer isoform are larger than aggregates from the shorter isoform.

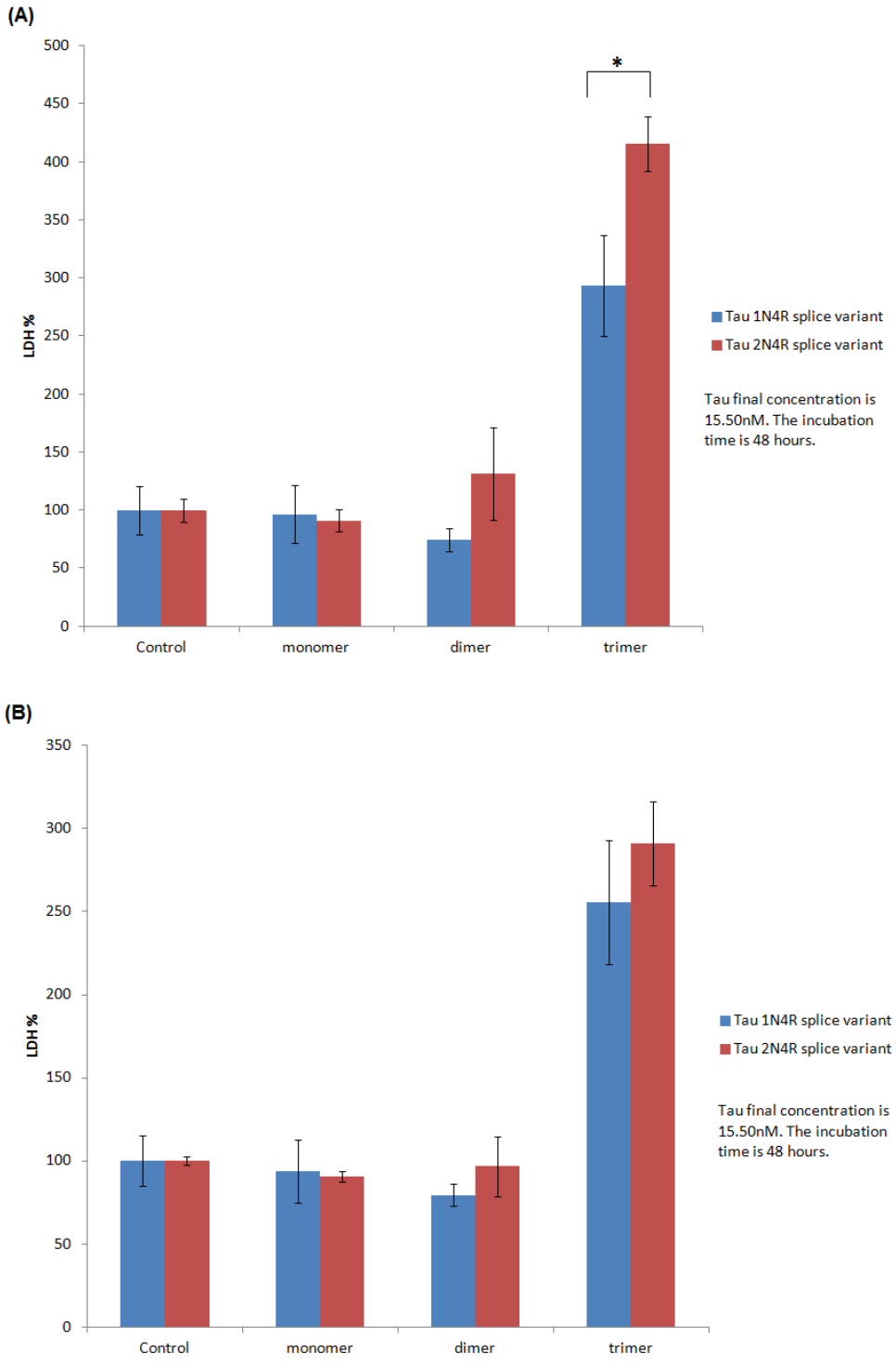

Figure 3.5 Neurotoxicity of extracellular 15.5nM monomeric, dimeric and trimeric forms of 1N4R and 2N4R tau variants toward (A) non-differentiated human neuroblastoma cells (SH-SY5Y) and (B) Retinoic-acid-differentiated SH-SY5Y cells were measured after 48 hour incubation using an LDH assay. For both four-repeat tau isoforms, trimeric form is more neurotoxic than monomeric and dimeric forms ($P<0.001$) on either neuron type. Full-length trimeric rhTau is more neurotoxic than 1N4R trimeric rhTau. ($P<0.05$)

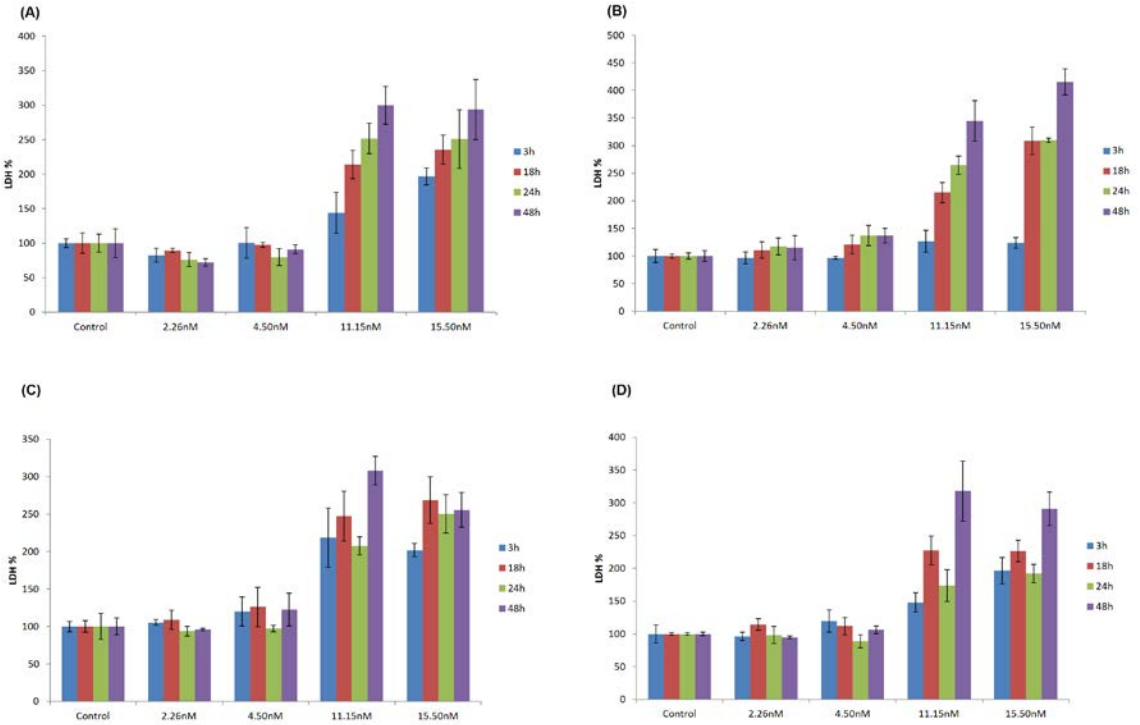

Figure 3.6 Time and concentration dependence of neurotoxicity induced by trimeric rhTau (1N4R and 2N4R) toward neuroblastoma cells measured by LDH assay. Non-differentiated SH-SY5Y cells incubated with (A) 1N4R tau and (B) 2N4R tau; Retinoic-acid-differentiated SH-SY5Y cells incubated with (C) 1N4R tau and (D) 2N4R tau.

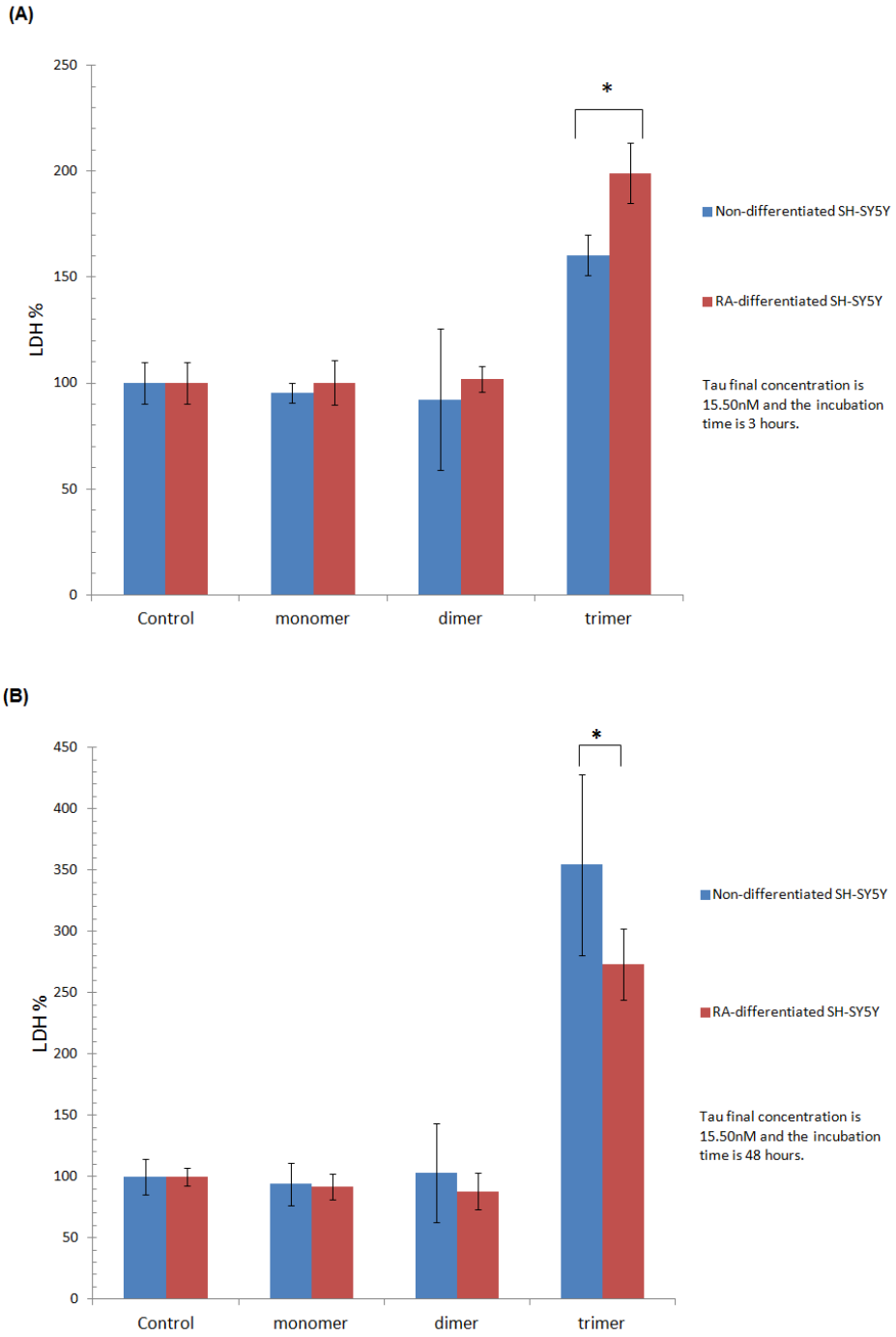

Figure 3.7 Comparison of rhTau-induced neurotoxicity toward non-differentiated SH-SY5Y cells and Retinoic acid (RA)-differentiated SH-SY5Y cells. The data combine toxicity results of 15.5nM monomeric, dimeric and trimeric forms of both 1N4R, 2N4R tau variants. (A) After 3 hours incubation, RA-differentiated SH-SY5Y cells are more vulnerable to extracellular trimeric rhTau toxicity than non-differentiated SHSY-5Y cells are ($P<0.05$). (B)After 48 hours incubation, non-differentiated SH-SY5Y cells are more vulnerable to extracellular trimeric rhTau toxicity than RA-differentiated SH-SY5Y cells ($P<0.05$).

3.8 References

1. 2012 Alzheimer's disease facts and figures. Alzheimers Dement, 2012. **8**(2): p. 131-68.

2. Alzheimer, A., Über eine eigenartige Erkankung der Hirnrinde. Allgemeine Zeitschrift fur Psychiatrie und phychish-Gerichtliche Medizin, (Berlin) 1907(64): p. 146-148.

3. Hardy, J. and D.J. Selkoe, The amyloid hypothesis of Alzheimer's disease: progress and problems on the road to therapeutics. Science, 2002. **297**(5580): p. 353-6.

4. Gilman, S., et al., Clinical effects of Abeta immunization (AN1792) in patients with AD in an interrupted trial. Neurology, 2005. **64**(9): p. 1553-62.

5. Blennow, K., et al., Effect of immunotherapy with bapineuzumab on cerebrospinal fluid biomarker levels in patients with mild to moderate Alzheimer disease. Arch Neurol, 2012. **69**(8): p. 1002-10.

6. Freeman, G.B., et al., 39-week toxicity and toxicokinetic study of ponezumab (PF-04360365) in cynomolgus monkeys with 12-week recovery period. J Alzheimers Dis, 2012. **28**(3): p. 531-41.

7. Check, E., Nerve inflammation halts trial for Alzheimer's drug. Nature, 2002. **415**(6871): p. 462.

8. Braak, H. and K. Del Tredici, The pathological process underlying Alzheimer's disease in individuals under thirty. Acta Neuropathol, 2011. **121**(2): p. 171-81.

9. Braak, H. and E. Braak, Frequency of stages of Alzheimer-related lesions in different age categories. Neurobiol Aging, 1997. **18**(4): p. 351-7.

10. Oddo, S., et al., Reduction of soluble Abeta and tau, but not soluble Abeta alone, ameliorates cognitive decline in transgenic mice with plaques and tangles. J Biol Chem, 2006. **281**(51): p. 39413-23.

11. Weingarten, M.D., et al., A protein factor essential for microtubule assembly. Proc Natl Acad Sci U S A, 1975. **72**(5): p. 1858-62.

12. Witman, G.B., et al., Tubulin requires tau for growth onto microtubule initiating sites. Proc Natl Acad Sci U S A, 1976. **73**(11): p. 4070-4.

13. Mandelkow, E.M. and E. Mandelkow, Tau in Alzheimer's disease. Trends Cell Biol, 1998. **8**(11): p. 425-7.

14. Amos, L.A., Microtubule structure and its stabilisation. Org Biomol Chem, 2004. **2**(15): p. 2153-60.

15. von Bergen, M., et al., Assembly of tau protein into Alzheimer paired helical filaments depends on a local sequence motif ((306)VQIVYK(311)) forming beta structure. Proc Natl Acad Sci U S A, 2000. **97**(10): p. 5129-34.

16. Thies, E. and E.M. Mandelkow, Missorting of tau in neurons causes degeneration of synapses that can be rescued by the kinase MARK2/Par-1. J Neurosci, 2007. **27**(11): p. 2896-907.

17. Diaz-Hernandez, M., et al., Tissue-nonspecific alkaline phosphatase promotes the neurotoxicity effect of extracellular tau. J Biol Chem, 2010. **285**(42): p. 32539-48.

18. Pooler, A.M., et al., Physiological release of endogenous tau is stimulated by neuronal activity. EMBO Rep, 2013. **14**(4): p. 389-94.

19. Lasagna-Reeves, C.A., et al., Tau oligomers impair memory and induce synaptic and mitochondrial dysfunction in wild-type mice. Mol Neurodegener, 2011. **6**: p. 39.

20. Guillozet, A.L., et al., Neurofibrillary tangles, amyloid, and memory in aging and mild cognitive impairment. Arch Neurol, 2003. **60**(5): p. 729-36.

21. Morris, M., et al., The many faces of tau. Neuron, 2011. **70**(3): p. 410-26.

22. Haass, C. and D.J. Selkoe, Soluble protein oligomers in neurodegeneration: lessons from the Alzheimer's amyloid beta-peptide. Nat Rev Mol Cell Biol, 2007. **8**(2): p. 101-12.

23. Kayed, R., et al., Common structure of soluble amyloid oligomers implies common mechanism of pathogenesis. Science, 2003. **300**(5618): p. 486-9.

24. Lasagna-Reeves, C.A., et al., Identification of oligomers at early stages of tau aggregation in Alzheimer's disease. FASEB J, 2012. **26**(5): p. 1946-59.

25. Morsch, R., W. Simon, and P.D. Coleman, Neurons may live for decades with neurofibrillary tangles. J Neuropathol Exp Neurol, 1999. **58**(2): p. 188-97.

26. Kordower, J.H., et al., Loss and atrophy of layer II entorhinal cortex neurons in elderly people with mild cognitive impairment. Ann Neurol, 2001. **49**(2): p. 202-13.

27. Brunden, K.R., J.Q. Trojanowski, and V.M. Lee, Evidence that non-fibrillar tau causes pathology linked to neurodegeneration and behavioral impairments. J Alzheimers Dis, 2008. **14**(4): p. 393-9.

28. Santacruz, K., et al., Tau suppression in a neurodegenerative mouse model improves memory function. Science, 2005. **309**(5733): p. 476-81.

29. Andorfer, C., et al., Hyperphosphorylation and aggregation of tau in mice expressing normal human tau isoforms. J Neurochem, 2003. **86**(3): p. 582-90.

30. Leroy, K., et al., Early axonopathy preceding neurofibrillary tangles in mutant tau transgenic mice. Am J Pathol, 2007. **171**(3): p. 976-92.

31. Spires, T.L., et al., Region-specific dissociation of neuronal loss and neurofibrillary pathology in a mouse model of tauopathy. Am J Pathol, 2006. **168**(5): p. 1598-607.

32. Yoshiyama, Y., et al., Synapse loss and microglial activation precede tangles in a P301S tauopathy mouse model. Neuron, 2007. **53**(3): p. 337-51.

33. Berger, Z., et al., Accumulation of pathological tau species and memory loss in a conditional model of tauopathy. J Neurosci, 2007. **27**(14): p. 3650-62.

34. Maeda, S., et al., Increased levels of granular tau oligomers: an early sign of brain aging and Alzheimer's disease. Neurosci Res, 2006. **54**(3): p. 197-201.

35. Sahara, N., S. Maeda, and A. Takashima, Tau oligomerization: a role for tau aggregation intermediates linked to neurodegeneration. Curr Alzheimer Res, 2008. **5**(6): p. 591-8.

36. Ward, S.M., et al., Tau oligomers and tau toxicity in neurodegenerative disease. Biochem Soc Trans, 2012. **40**(4): p. 667-71.

37. Lasagna-Reeves, C.A., et al., Alzheimer brain-derived tau oligomers propagate pathology from endogenous tau. Sci Rep, 2012. **2**: p. 700.

38. Genius, J., et al., Current application of neurochemical biomarkers in the prediction and differential diagnosis of Alzheimer's disease and other neurodegenerative dementias. Eur Arch Psychiatry Clin Neurosci, 2012. **262 Suppl 2**: p. S71-7.

39. Barkhordarian, H., et al., Isolating recombinant antibodies against specific protein morphologies using atomic force microscopy and phage display technologies. Protein Eng Des Sel, 2006. **19**(11): p. 497-502.

40. Zameer, A., et al., Single Chain Fv Antibodies against the 25-35 Abeta Fragment Inhibit Aggregation and Toxicity of Abeta42. Biochemistry, 2006. **45**(38): p. 11532-9.

41. Emadi, S., et al., Isolation of a human single chain antibody fragment against oligomeric alpha-synuclein that inhibits aggregation and prevents alpha-synuclein-induced toxicity. J Mol Biol, 2007. **368**(4): p. 1132-44.

42. Zameer, A., et al., Anti-oligomeric Abeta single-chain variable domain antibody blocks Abeta-induced toxicity against human neuroblastoma cells. J Mol Biol, 2008. **384**(4): p. 917-28.

43. Emadi, S., et al., Detecting morphologically distinct oligomeric forms of alpha-synuclein. J Biol Chem, 2009. **284**(17): p. 11048-58.

44. Wang, M.S., et al., Characterizing antibody specificity to different protein morphologies by AFM. Langmuir, 2009. **25**(2): p. 912-8.

45. Pahlman, S., et al., Differentiation and survival influences of growth factors in human neuroblastoma. Eur J Cancer, 1995. **31A**(4): p. 453-8.

46. Encinas, M., et al., Sequential treatment of SH-SY5Y cells with retinoic acid and brain-derived neurotrophic factor gives rise to fully differentiated, neurotrophic factor-dependent, human neuron-like cells. J Neurochem, 2000. **75**(3): p. 991-1003.

47. Presgraves, S.P., et al., Terminally differentiated SH-SY5Y cells provide a model system for studying neuroprotective effects of dopamine agonists. Neurotox Res, 2004. **5**(8): p. 579-98.

48. Decker, T. and M.L. Lohmann-Matthes, A quick and simple method for the quantitation of lactate dehydrogenase release in measurements of cellular cytotoxicity and tumor necrosis factor (TNF) activity. J Immunol Methods, 1988. **115**(1): p. 61-9.

49. Hardy, J.A. and G.A. Higgins, Alzheimer's disease: the amyloid cascade hypothesis. Science, 1992. **256**(5054): p. 184-5.

50. Ferreira, S.T., M.N. Vieira, and F.G. De Felice, Soluble protein oligomers as emerging toxins in Alzheimer's and other amyloid diseases. IUBMB Life, 2007. **59**(4-5): p. 332-45.

51. Varvel, N.H., et al., Abeta oligomers induce neuronal cell cycle events in Alzheimer's disease. J Neurosci, 2008. **28**(43): p. 10786-93.

52. Kasturirangan, S., et al., Isolation and characterization of antibody fragmentsselective for specific protein morphologies from nanogram antigensamples. Biotechnol Prog, 2013.

53. Sierks, M.R., et al., CSF levels of oligomeric alpha-synuclein and beta-amyloid as biomarkers for neurodegenerative disease. Integr Biol (Camb), 2011. **3**(12): p. 1188-96.

54. Andorfer, C., et al., Cell-cycle reentry and cell death in transgenic mice expressing nonmutant human tau isoforms. J Neurosci, 2005. **25**(22): p. 5446-54.

55. Belarbi, K., et al., Early Tau pathology involving the septo-hippocampal pathway in a Tau transgenic model: relevance to Alzheimer's disease. Curr Alzheimer Res, 2009. **6**(2): p. 152-7.

56. Alonso Adel, C., et al., Promotion of hyperphosphorylation by frontotemporal dementia tau mutations. J Biol Chem, 2004. **279**(33): p. 34873-81.

57. Braak, H., et al., Vulnerability of cortical neurons to Alzheimer's and Parkinson's diseases. J Alzheimers Dis, 2006. **9**(3 Suppl): p. 35-44.

58. Schliebs, R. and T. Arendt, The cholinergic system in aging and neuronal degeneration. Behav Brain Res, 2011. **221**(2): p. 555-63.

59. Wu, J.W., et al., Small Misfolded Tau Species Are Internalized via Bulk Endocytosis and Anterogradely and Retrogradely Transported in Neurons. J Biol Chem, 2013. **288**(3): p. 1856-70.

60. Glabe, C.G., Common mechanisms of amyloid oligomer pathogenesis in degenerative disease. Neurobiol Aging, 2006. **27**(4): p. 570-5.

Chapter 4

Isolation and Characterization of Single Chain Variable Fragments Selective for Neurotoxic Tau Oligomers

4.1 Abstract

The importance of oligomeric tau in AD has largely been overlooked even though soluble aggregates of tau are neurotoxic and can propagate tau tangle pathology to healthy areas of the brain. Because of the important role of oligomeric tau in AD onset and progression, there is a critical need for well characterized reagents that selectively recognize different key morphologies of tau which can be used as tools to study the etiology of AD and related diseases. We developed a biopanning protocol combining the binding diversity of phage-displayed antibody libraries with the powerful imaging capability of atomic force microscopy (AFM) that enables us to isolate antibody fragments against specific protein variants and determine binding specificity using only minimal amounts of target material without the need for antigen modification or immobilization. Here, we show the use of this panning technology to generate single chain antibody fragments (scFvs) that selectively bind toxic oligomeric tau. We isolated three antibody fragments that each selectively bind oligomeric tau but do not cross-react with monomeric or fibrillar tau. These scFvs differentially bind hippocampal homogenates of 3×TG-AD mice compared to wild type mice and can detect oligomeric tau in these samples at much earlier ages than when neurofibrillary tangles are typically detected. The scFvs also can distinguish human post-mortem AD brain tissue from cognitively normal post-mortem human brain tissue showing increased reactivity with an increase in Braak stage demonstrating the

potential of this approach for developing biomarkers for early detection and progression of AD.

4.2 Introduction

Alzheimer's disease (AD) is a devastating progressive neurodegenerative disease that causes brain atrophy, memory deterioration and cognitive loss in affected individuals. It is the sixth leading cause of death in the United States, currently affecting over 5.4 million Americans with annual costs of over $200 billion in medical care[1]. Although AD was first discovered over a hundred years ago, and substantial progress has been made in understanding the etiology of the disease, there are still no effective therapeutic or definitive diagnostic approaches available. AD is characterized by the presence of two hallmark pathologies: extracellular neuritic plaques containing insoluble fibrillar aggregates of amyloid-beta (Aβ) and intracellular neurofibrillary tangles (NFTs) containing fibrillar aggregates of tau. Although these insoluble aggregated species have long been considered as the primary toxic elements of AD, increasing evidence indicates that small soluble oligomeric forms of both Aβ and tau play more critical roles in the onset and progression of AD than the fibrillar aggregates[2-4]. The role of Aβ aggregation in AD in particular has been extensively studied[5-11], but despite very promising results in animal models, various therapeutic routes of targeting Aβ aggregation have had only very limited success in clinical trials[12-15]. The role of tau in the progression of AD is gaining more attention, including studies to elucidate the roles of different variants and aggregate forms of tau[4, 16-23].

Tau is a microtubule-associated protein, generally located in the axons of neurons, where it is involved in the assembly and stabilization of microtubules from tubulin. Although human tau is encoded by a single gene on chromosome 17q21, six major tau isoforms can be formed by alternative posttranscriptional splicing of exons 2, 3 and 10. Tau can also be post-translationally modified by phosphorylation, glycosylation, ubiquitinylation, or glycation among others[24-26] resulting in a wide variety of different tau species that exist in vivo. Since tau hyperphosphorylation is associated with AD, it has been extensively studied, and inhibition of kinases involved in tau phosphorylation has been pursued as a potential therapeutic approach[27-29]. Levels of phosphorylated variants of tau correlate well with AD and other tauopathies including FTD[30]. Hyperphosphorylation of the microtubule-binding domain (MBD) of tau results in a conformational change that promotes its misfolding and loss of physiological function[31]. However, phosphorylation of tau may also be required for some cellular functions including adult neurogenesis, as new adult-born granule neurons contain a significant amount of a hyperphosphorylated three repeat (3R) tau variants[32]. Therapeutic strategies aimed at regulating kinase activity bear the risk of interrupting normal phosphorylation dependent functions of tau along with other cellular functions. Given the complexity of the many different potential isoforms of tau that can occur in vivo and the uncertainty as to the physiological effects of tau hyperphosphorylation and aggregation, the roles of different hyperphosphorylated and aggregated tau variants in AD remain controversial[19, 29, 33] and the most promising diagnostic or therapeutic targets are still not known.

Similar to the neurotoxic effects observed with soluble oligomeric aggregates of Aβ, numerous studies indicate that soluble aggregates of tau play an important role in the pathology of AD[17]. Both brain derived and recombinant oligomeric tau aggregate species disrupt intracellular calcium levels and are toxic to cultured human neuronal cells when added extracellularly[34-36]. In animal models expressing human tau, neurodegeneration-related phenotypes including behavioral impairments, neuronal loss, and synapse lesions correlate better with the presence of soluble tau oligomers and pre-filament species than with fibrillar NFT levels [37-39]. Neuronal loss also precedes NFT formation suggesting involvement of other species such as oligomeric tau variants [38, 40-42]. In postmortem human brains, high oligomeric tau levels were detected in the frontal lobe cortex at early stages of AD before the presence of NFTs [43-44]. Oligomeric tau may also be responsible for transmission of pathology with a prion-like mechanism as NFT tau pathology spreads from brain regions seeded with oligomeric tau into other regions resulting in aggregation of endogenous tau[45-48]. We have previously shown using recombinant human tau (rhTau) that extracellular trimeric, but not monomeric or dimeric species are toxic to human neuronal cells[49].

Here we describe isolation of antibody based reagents that selectively recognize toxic oligomeric tau species. We used an scFv library[50] as a source of binding diversity and an AFM based biopanning protocol[51-56] as a selection tool to isolate scFvs that selectively bound the trimeric tau species. We utilized several subtractive panning steps in the selection protocol to ensure the removal of all scFvs cross-reactive with monomeric tau and other off-target proteins. We identified three different scFvs that bound trimeric but not monomeric or fibrillar tau. The scFvs react with oligomeric tau in

brain tissue from a transgenic AD mouse model that overexpresses both Aβ and aggregation prone htau P301L and indicate that significant levels of oligomeric tau are present in brain tissue from this mouse model long before NFTs are detected. The scFvs also reacted with oligomeric tau in post-mortem human AD brain tissue. Levels of oligomeric tau in the post-mortem human brain tissue correlate with progression of AD as the amount of oligomeric tau detected with the scFvs increases with Braak stage.

4.3 Material and Methods

scFv Phage Display Library- The Sheets phage display scFv library[50] with an estimated diversity of 6.7×10^9 was generously provided by Dr. Yu Zhou (Department of Anesthesia, University of San Francisco) and used for biopanning. Phage were produced and purified as previously described[57]. A final titer of 10^{13}-10^{14} pfu/mL was used for biopanning.

Aggregated Tau species- Two isoforms (1N4R and 2N4R) of rhTau species were used for the panning protocols. Monomeric and oligomeric forms of tau were generated as described previously[49]. A fibrillar 2N4R aggregate stock was prepared following a heparin fibrillation protocol by mixing rhTau 2N4R monomer (final molarity of 4 μM) and low molecular weight heparin (final molarity of 4 μM) in final 20 mM tris-HCl pH 7.4 and final 5 mM DL-Dithiothreitol (DTT) in deionized water (DI water). The mixture was incubated at 37 °C for 2 weeks with occasional stirring.

Biopanning against rhTau 1N4R trimer- The biopanning process was performed essentially as previously described[55] with the following modifications. The biopanning process was divided into “subtractive panning” and “positive panning” steps (Figure 4. 1).

The subtractive panning steps were designed to remove all scFv-displayed phage from the library pool which bound to non-desired antigens. A control protein bovine serum albumin (BSA) was used to remove non-specific binding phage, and monomeric tau was used to remove all phage binding non-aggregated linear epitopes of tau. The positive panning step recovered any scFv-displayed phage from the remaining phage pool that selectively bound trimeric tau. Each step was monitored by AFM to ensure that essentially all phage binding BSA and monomeric tau were removed and phage binding trimeric tau were recovered.

Subtractive panning step- A set of high affinity immunotubes were coated with 2 mL/tube of 1 mg/mL BSA in carbonate/bicarbonate coating buffer pH 9.6 and another set with 2 mL of 12 µg/mL tau 1N4R monomer in the same coating buffer and incubated overnight at 4 ºC. After antigen immobilization, immunotubes were washed extensively with phosphate buffered saline (PBS) and sealed to keep moist. A total volume of 0.5 mL of the phage display library was added to the first tube coated with BSA. The tube was then sealed and incubated at room temperature for 30 minutes with gentle agitation ensuring that the phage solution did not contact uncoated regions of the immunotube. After incubation, the phage solution was removed and additional unbound phage rinsed off with 100 µl PBS. The phage and rinse solutions were combined and added to a second tube containing BSA and then to sequential tubes following the same procedure for each tube. The final recovered phage solution volume was approximately 1 mL. A 10 µL aliquot of phage solution recovered after incubation with each tube was added to mica containing BSA and imaged by AFM to determine whether any phage remaining in the phage pool that could still bind BSA. If no bound phage were observed, the subtractive

panning step successfully removed essentially all phage binding to the target antigen, in this case BSA. A second subtractive panning round was performed using immunotubes coated with monomeric 1N4R rhTau to remove all phage binding monomeric tau. The process was performed and monitored as described above. After the second round of subtractive panning, the final remaining phage solution was stored in 100 µL aliquots at -80 ºC.

Positive panning- A 10 µl aliquot of 60 µg/mL of positive target antigen, trimeric rhTau 1N4R, was deposited on a piece of freshly cleaved mica, incubated at room temperature for 10 minutes, and then extensively washed with DI water and dried. A 200 µl aliquot of the remaining phage pool obtained after subtractive panning was added to the mica, incubated at room temperature for 10 minutes, and then washed with 2 mL 0.1% Tween20/DI water and at least 10 mL DI water to remove all unbound phage. The positive panning step was performed in duplicate for analysis by AFM to verify the presence of phage binding trimeric tau. Bound phage were eluted with 1.4% triethylamine (TEA) and neutralized after 5 minutes with an equal volume of 1M Tris-HCl pH 7.4 buffer. The eluted phage stock were recovered as described[53]. Single colonies were collected, individually grown and stored at -80 ºC.

Atomic force microscope (AFM) imaging- AFM imaging and analyses were performed as described previously[58]. Aliquots were deposited and incubated for 10 min on freshly cleaved mica at room temperature before the mica surface was washed extensively with DI water and dried with compressed nitrogen flow. To image phage binding specificity for the different tau isoforms, an additional stringent wash with 0.1% Tween20/DI water

was performed to remove non-specific binding phage. The coated mica samples were imaged in air using a MultiMode AFM Nanoscope IIIA system (Veeco/Digital instruments, Santa Barbara, CA) operating in tapping mode using silicon AFM probes (VISTAprobes, nanoscience instruments).

Single clone screening with AFM- Following positive panning, a phage preparation from each individual recovered clone was analyzed for target binding specificity by AFM. Aliquots of each phage were added to mica coated with either BSA, monomeric or trimeric tau. Samples showing the highest binding levels toward trimeric tau, but no reactivity toward BSA or monomeric tau were selected for further characterization.

DNA sequence correction- DNA sequences of recovered clones were obtained and compared with other known scFv sequences[57]. All recovered clones from the positive panning step contained a missing base pair near the amino terminal of the scFv sequence resulting in a shift in the reading frame (Table 4.1). The frameshift was corrected in selected clones using polymerase chain reaction (PCR) with customized primers (Table 4.2). The forward primers encompass the NcoI site (5'-CCATGG-3') upstream of scFv sequence and include the missing base, while the reverse primer encompasses the NotI site (5'-GCGGCCGC-3') downstream of scFv sequence. The corrected scFv gene sequences were ligated into the pGEMT plasmid vector for sequencing to confirm the desired DNA sequence, and then ligated into the pIT2 plasmid vector which contains a hexahistidine tag and c-myc tag for protein expression. The pIT2 plasmids were transformed into either *E. coli* strain HB2151 for scFv expression or TG1 for phage expression.

Phage binding specificity assay- Binding specificities of the sequence corrected phage clones were verified by AFM. Purified phage were deposited and incubated on mica coated with the different tau species and imaged to confirm binding specificity as described above.

Soluble scFv production and purification- Production and purification of the sequence corrected scFv proteins were performed as described previously[51]. Concentrated supernatant, periplasm and cell lysate fractions were prepared separately and tested for presence of scFv. Most of the scFv was located in the periplasmic fraction, with lower amounts excreted to the supernatant as expected[59]. All fractions containing scFv were pooled and purified using a Ni-NTA agarose beads column (Qiagen, 5mL beads for 1L expression culture) and imidazole elution essentially as described [60].

Dot blot assay with human brain tissue- Postmortem human brain samples from the middle temporal gyrus (MTG) of Alzheimer's disease (AD) and cognitively normal non-demented (ND) cases were generously provided by Dr. Thomas Beach (Director of Banner/Sun Health Research Institute Brain Bank). Brain extracts from the MTG of age-matched ND and AD patients were homogenized in Tris-HCl/EDTA buffer with protease inhibitor. The homogenate was spun down to remove solids and the supernatant containing all the soluble protein was collected and adjusted to a total protein concentration of 3 mg/mL. Aliquots of 2 μL 3 mg/mL brain tissue were dotted on gridded nitrocellulose membrane and probed with anti-oligomeric tau scFv essentially as described[61]. Samples were analyzed in triplicate using purified scFv. Reactivity of scFv with brain tissue samples was analyzed using ImageJ and recorded in the form of

densitometric value[55]. Each value was calibrated on a scale of 0 to 1 in which 0 denotes the background and 1 denotes the positive control of anti-phosphorylase b (plb) scFv.

Mouse brain tissue- Brains from 5, 8, 11 months old wild-type mice and 5, 9 and 13 months old 3×transgenic Alzheimer's (3×TG-AD) mice overexpressing human tau P301L[62] were generously provided by Dr. Travis Dunckley (Translational Genomics, Phoenix, AZ). Mouse hippocampus was homogenized as described above for human brain samples.

Phage biotinylation- Phage were biotinylated for enhanced signal detection in ELISA using the EZ-Link Pentylamine-biotin kit (Thermo Scientific). A 10^{11} pfu/mL aliquot of phage stock (0.729mg/ml) was incubated with Pentylamine-Biotin (4.86mM final concentration) and 1-Ethyl-3-[3-dimethylaminopropyl] carbodiimide hydrochloride (EDC) of 0.1M final concentration at room temperature for 2 hours with stirring. Excess Pentylamine-Biotin and EDC were removed with desalting columns.

Capture ELISA- To validate that scFvs were targeting tau and to quantify oligomeric tau present in mouse brain samples, we utilized a capture ELISA where high affinity polystyrene microtiter 96-well plates were first coated with 100 µl/well of 0.3 mg/ml purified scFv (the capture antibody) and incubated at 37 °C for two hours. After the unbound scFvs were removed, the plates were washed three times with 0.1% Tween20/PBS. The plates were then blocked with 2% non-fat milk/PBS at 37 °C for one hour. After a Tween20/PBS wash, an aliquot of 100 µl/well of 0.2 mg/ml mouse brain homogenate (the target analytes) was added, incubated at 37 °C for two hours and then

washed with Tween20/PBS. PBS was used as a negative control. A 100 µL/well aliquot of 10^7 pfu/ml biotinylated phage (the detection antibody) was added at 37 °C for two hours. The wells were washed with Tween20/PBS, and then a 100 µL/well aliquot of 0.5 µg/ml avidin-HRP was added and incubated at 37 °C for one hour. The plates were washed again with Tween20/PBS and binding monitored using a chemiluminescent ELISA kit (SuperSignal ELISA Femto Maximum Sensitivity Substrate (Thermo Scientific)). The chemiluminescent signal was read 1 minute after addition to the mixture. The immunoreactivity signals were normalized by dividing the absolute chemiluminescent readings of the samples by that of PBS control. Within each independent experiment, the mean signal obtained from all the wild-type mice samples was used as a baseline to normalize the signals obtained with the transgenic mice samples.

To verify that the isolated scFvs were binding oligomeric tau in the mouse brain tissue samples, we utilized a capture ELISA where the scFvs were used as the capture antibody and a commercially available anti-tau monoclonal antibody, AT8 (Thermo Scientific), was used as the detection antibody. AT8 targets tau forms with hyperphosphorylated Ser202/Thr205 mainly found in tau aggregates. An anti-mouse antibody conjugated to horseradish peroxidase (HRP) (Thermo Scientific) was used to detect bound AT8.

Size analysis of individual phage target- To determine the size of the target antigen bound by individual phage particles, we deposited a 10 µl aliquot of a fibrillar tau aggregate mixture (19.5 µg/mL, 10×dilution of the original prepared stock) on mica, followed by a 10 µl aliquot of 10^{12} pfu/ml phage, then incubated and rinsed the sample as

described above. The tau aggregate sample contained a mixture of monomeric, oligomeric and fibrillar rhTau 2N4R aggregates. AFM images (5 μm^2) were obtained and processed using Nanoscope Analysis. The diameter of each target antigen particle bound at the tip of the phage was calculated by taking the difference between the maximum height of the particle and the adjusted baseline. At least 6 different antigen particles for each individual clone were measured and averaged to determine the particle height of the target antigen.

Statistical analysis- Samples were analyzed by one-way ANOVA with $p<0.05$ standard and LSD post hoc significant differences test. All analyses were performed with SPSS 21.0 (IBM Corp., Armonk, NY).

4.4 Results and Discussion

Isolation of scFvs selectively binding oligomeric tau

We utilized an AFM based panning protocol incorporating sequential subtractive and positive panning steps (Figure 4. 1A) to isolate scFvs that selectively bind a toxic trimeric tau species. We first eliminated from the scFv library pool essentially all phage containing scFvs binding to the control protein (BSA) (Figure 4. 1B) and then those binding to monomeric tau. After the subtractive panning steps, we isolated scFv-displayed phage that selectively bound toxic oligomeric tau employing a single positive panning step using trimeric rhTau 1N4R as the target antigen. We recovered 96 phage clones from the positive panning step against trimeric tau (Figure 4. 1C). Phage from each of the 96 clones were prepared separately and each sample was assayed for binding specificity to trimeric tau, monomeric tau and BSA by AFM (Figure 4. 2A). We selected

twenty clones that selectively recognized trimeric tau for further study. The DNA sequences were obtained to verify the presence of full length scFv[50, 57], and six distinct full-length scFvs were selected for further analysis (H2, F9, D11, H7, D4 and G12). Although all six clones contained complete scFv sequences, they each lacked a DNA base pair downstream of the N-terminal NcoI site and the methionine start codon (Table 4.1) resulting in a reading frame shift. The pelB leader sequence contains multiple methionine start codons in different reading frames that may facilitate the expression of full length scFvs despite the altered reading frame resulting from the missing base pair at the N-terminal. To enhance soluble scFvs expression efficiency, we corrected the reading frame shift using PCR. We then verified that the each sequence corrected scFv maintained the same binding specificity of the original clone using AFM (Figure 4. 2B). Three sequence corrected clones F9T, D11C and H2A were then selected for further studies based on binding specificity and distinctive CDR sequences.

Verification of binding specificity to tau trimer

To verify that the F9T, D11C and H2A scFvs were selectively binding trimeric tau, we incubated a phage displayed version of each scFv with a sample of aggregated tau and used AFM to determine the average height of the particles bound by each phage particle. We then compared the height of the bound particles to the known height values of different tau aggregate species[49]. A representative AFM image of an F9T scFv phage (blue arrow) binding to a target rhTau 2N4R aggregate (gray arrow) in the mixed monomeric, oligomeric and fibrillar (black arrow) tau sample is shown (Figure 4. 3A). The average height of at least 6 different bound antigens for each scFv was determined and compared to the size of known oligomeric tau aggregates[49]. The target antigen

size for all three scFvs correspond to the size of a rhTau 2N4R trimer[49] (from 2.5 nm to 3.0 nm) providing further evidence that the scFvs selectively target trimeric tau (Figure 4. 3B).

Characterization of binding epitopes

Purified soluble scFv protein for each corrected scFv sequence had the expected 29 kDa full length scFv molecular mass (Figure 4. 2C). Since the scFvs were isolated against a synthetic oligomeric tau variant, we then tested whether the purified F9T, D11C and H2A scFvs could recognize tau aggregates from brain tissue of an AD mouse model and whether they cross-react with other proteins present in brain specimens. All three scFv clones bound oligomeric tau aggregates present in hippocampal tissue homogenates from 9-month old 3×TG-AD mice and none of them showed significant reactivity with wild-type mice (Figure 4. 4). AT8 was used as a detection antibody to verify that the scFvs can also bind tau oligomers that are modified by hyperphosphorylation.

Since the three selected clones (F9T, D11C and H2A) contain distinctive CDR sequences, we tested whether they bind similar or different epitopes on the tau oligomers. A capture ELISA method was performed using the purified scFvs as capture antibodies and the phage displayed version of each scFv as detection antibodies (Figure 4. 5) with the 3×TG-AD mouse brain homogenates as antigen. When F9T-displayed phage was used as the detection antibody, strong signals were obtained for all three capture antibody types. In contrast, when D11C-displayed phage was used as a detection antibody, lower signals were obtained with either D11C or H2A scFv as capture antibody, and no signal with F9T scFv as capture antibody. Similarly, when H2A-displayed phage was used as a

detection antibody, a lower signal was obtained with D11C scFv as the capture antibody and no signal with either F9T or H2A scFv as capture antibody (Figure 4. 5). Since F9T phage produced the strongest immunoreactivity with brain extracts retained by all three scFvs as capture antibody, we used F9T phage as the detection antibody in all further capture ELISAs.

Time dependent tau oligomer accumulation in AD mouse hippocampus

We analyzed how oligomeric tau levels varied with time in the hippocampus of 3×TG-AD mice[63] using the three scFvs against oligomeric tau. The 3×TG-AD mouse model overexpresses human mutant tau_{P301L} (0N4R), which is prone to aggregation in tauopathies[64-66]. Whereas insoluble tau tangles are typically detected around 12-15 months of age in this mouse model[62], oligomeric tau levels are already quite high at 5-months of age, peak around 9-months and are declining by 13-months (Figure 4. 6). Samples from age-matched wild-type mice did not contain any oligomeric tau reactive with these scFvs (Figure 4. 6). Since the scFvs were isolated against 1N4R trimeric tau, but also recognize 2N4R (Figure 4. 3) and 0N4R (Figure 4. 4) oligomeric tau aggregates, but not monomeric or fibrillar tau aggregates, the scFvs target a common conformational feature of the oligomeric tau aggregates and not an isoform specific epitope. Since the concentration of oligomeric tau species increases at early time points (5-9 months) before insoluble tau tangles begin to form, and then decreases after neurofibrillary tangles begin to form (12-15 months), it may be the oligomeric tau species are being incorporated into the NFTs. Since oligomeric tau aggregates are already present at 5-months well before presence of NFTs, these aggregates have promise as an early diagnostic for AD.

Analysis of post-mortem human brain tissue

Since the scFvs effectively detected oligomeric tau species present in brain tissue from an AD mouse model, we next probed post-mortem extracts of human middle temporal gyrus (MTG) specimens at different Braak stages for the presence of oligomeric tau using the F9T scFv using dot blots (Figure 4. 7). In postmortem examination on severe AD brains and ND brains, middle temporal lobe display conspicuous atrophy and weight loss in AD brains[67]. When probed with the anti-oligomeric tau scFvs we could detect only minimal oligomeric tau in the ND Braak stage I-II samples, higher values in the ND Braak stage I-II samples with slight plaques, higher values again in AD samples with moderate plaques (Braak stage III-IV) and the highest signals in AD samples with heavy plaques (Braak stage V-VI). There were significantly higher levels of oligomeric tau in the AD samples compared to both the ND samples without plaques and the ND samples with slight plaques. While NFTs are typically not detected in MTG until Braak stage IV[68-70] we can detect the presence of oligomeric tau aggregates in Braak stage I-II samples that also contain a slight amyloid plaque load again suggesting that the presence of oligomeric tau may be a promising early biomarker for AD.

4.5 Summary

Aggregates of Aβ and tau are the primary protein constituents of the hallmark senile plaques and neurofibrillary tangles of AD[71-73], respectively. While many studies have focused on accumulation and aggregation of Aβ as an initiating factor in AD pathogenesis and neuronal death with tau dysfunction considered to be a downstream event following Aβ aggregation[74-75], other studies suggest that tau interacts with Aβ to accelerate the progression of AD, and that reducing aggregated tau levels is also

important to ameliorate AD symptoms[76]. Aβ and tau aggregation may be linked by separate mechanisms driven by common upstream causes[77]. Numerous studies have implicated the role of soluble oligomeric Aβ species in mediating toxicity in AD[78-80], and evidence now suggests that oligomeric tau may also play toxic roles in AD[17, 44, 81-82]. Recent studies indicate that soluble tau species including oligomeric, prefibrillar and immature pre-filament forms play more crucial roles in AD than the hallmark NFTs which instead may rather play an adaptive and protective role[33, 81]. Oligomeric tau has been shown to have prion-like self-propagating features[48] and can be taken up by endocytosis into neurons where they can induce endogenous tau pathology in vivo[83]. Therefore the roles of oligomeric and fibrillar tau species in AD progression is drawing increased attention and oligomeric tau is a promising therapeutic target for AD[33, 84-85]. Because of the diversity of tau species that may be present in the human brain due to the alternative post-transcriptional splicing and post-translational modifications that may occur, there is a critical need to develop reagents that can selectively identify individual tau aggregate variants to probe the roles of the various forms in disease progression and to assess their value as diagnostic and therapeutic targets.

We previously reported that a trimeric, but not monomeric or dimeric tau species was neurotoxic at low nanomolar levels[49]. Here we isolated three different scFvs (F9T, D11C and H2A) that selectively recognize this toxic trimeric tau species. All three scFvs can detect the presence of oligomeric tau species in an AD mouse model by 5-months of age well before the presence of NFTs. The scFvs can also detect oligomeric tau aggregates in post-mortem human AD brain tissue samples, where levels of oligomeric tau correspond to Braak stage, a classification based on Aβ plaque and abnormal tau

immunohistochemical staining[68-70, 86-89]. . While NFTs are a hallmark feature of AD, oligomeric tau species may play an intermediate role in tau aggregation[44] and have been shown to play an important role in neuronal toxicity. Here we show that oligomeric tau aggregates can be detected much earlier than NFTs in mouse models of AD and levels of these aggregates correlate with progression of AD in human post-mortem tissue. Therefore detection of toxic oligomeric tau aggregates has promise not only as an early diagnostic for AD but also to help stage progression of the disease.

4.6 Acknowledgements

We appreciate the support from Arizona Department of Health Services for the Arizona Department of Health Services for the Arizona Alzheimer's Consortium. We are grateful to the Banner/Sun Health Research Institute Brain Donation Program of Sun City, Arizona for the provision of human brain tissue. The Brain Donation Program is supported by the National Institute on Aging (P30 AG19610 Arizona Alzheimer's Disease Core Center), the Arizona Department of Health Services (contract 211002, Arizona Alzheimer's Research Center), the Arizona Biomedical Research Commission (contracts 4001, 0011, 05-901 and 1001 to the Arizona Parkinson's Disease Consortium) and the Prescott Family Initiative of the Michael J. Fox Foundation for Parkinson's Research. We would also give thanks to Dr. Debra Page Baluch in the ASU Keck's bioimaging laboratory for the access to AFM facilities and Dr. Travis Dunckley from TGen for providing 3×TG-AD mice brains. This work was partially supported by the NIH; NIA grant # AG029777.

Appendix

Conflict of Interest

Eliot Davidowitz, Patricia Lopez, and James Moe are employees of Oligomerix Inc.,3960 Broadway, New York, NY 10032 USA. Partial funding for this work was provided by Oligomerix, Inc. There are no other conflicts of interest.

Abbreviations used

Aβ, amyloid beta; AD, Alzheimer's disease; AFM, atomic force microscopy; ANOVA, analysis of variance; BSA, bovine serum albumin; CDR, complementarity-determining region; DI water, deionized water; DTT, DL-Dithiothreitol; EDC, 1-Ethyl-3-[3-dimethylaminopropyl] carbodiimide hydrochloride; EDTA, Ethylenediaminetetraacetic acid; ELISA, enzyme-linked immunosorbent assay; FTD, frontotemporal dementia; HCFR, heavy chain framework region; HRP, horseradish peroxidase; LSD, lease significant difference; MBD, microtubule-binding domain; MTG, middle temporal gyrus; ND, non-demented; NFT, neurofibrillary tangle; PBS, phosphate buffered saline; PCR, polymerase chain reaction; plb, phosphorylas b; rhTau, recombinant human tau; scFv, single chain variable fragment; TEA, triethylamine; 3×TG-AD mouse, triple transgenic Alzheimer’s mouse.

4.7 Figures and Tables

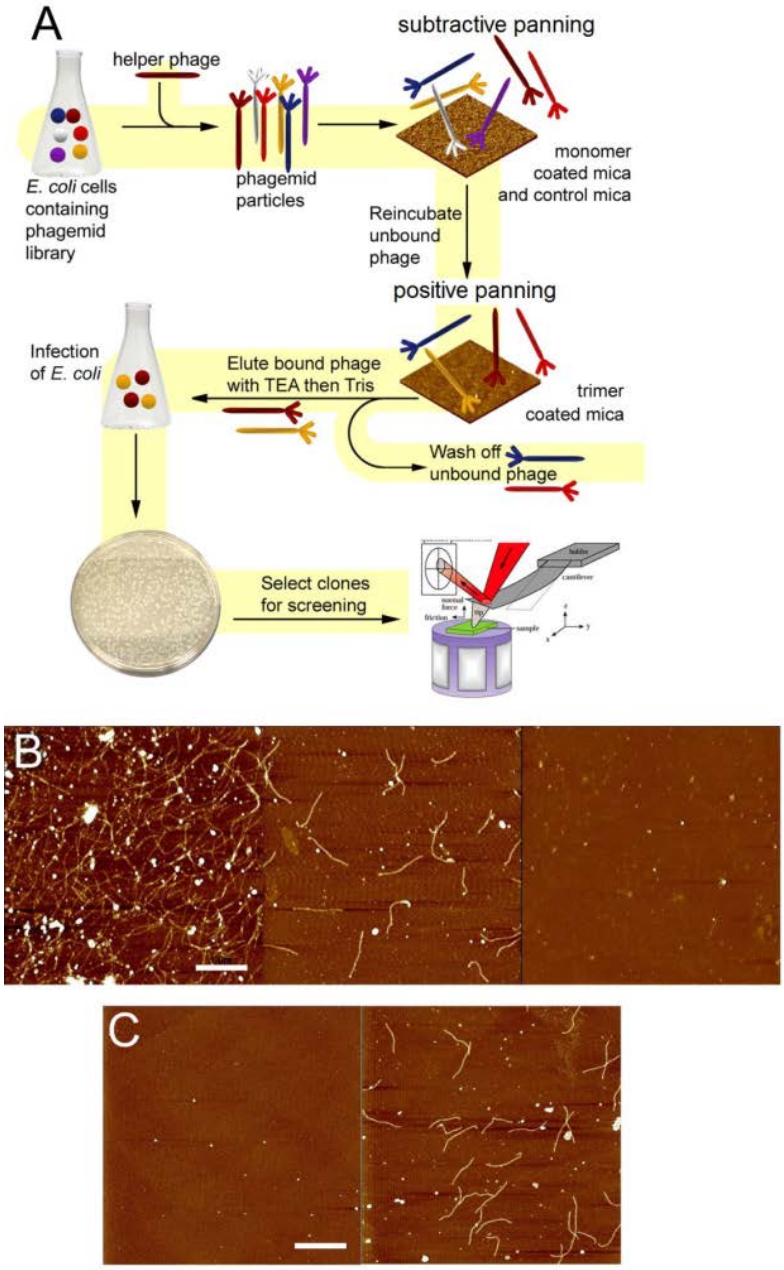

Figure 4. 1 The novel biopanning process combines subtractive panning and positive panning from phagemid scFv library and the single cloning screening using AFM. (A)Schematic of the AFM based panning process. (B) Subtractive panning against BSA after 1 (left), 3 (middle) and 5 (right) rounds of negative panning. The absence of phage after 5 rounds of negative panning indicated that the BSA subtractive panning step was complete. The scale bar of 1 µm applies to all three images. (C) Positive panning against tau trimer was performed and imaged with AFM. Left image: purified trimeric tau 1N4R immobilized on mica; Right image: same sample after addition of the remaining phage pool from subtractive panning and rinse, and it shows phage bound to target antigen. The scale bar of 1 µm applies to both images.

(A)

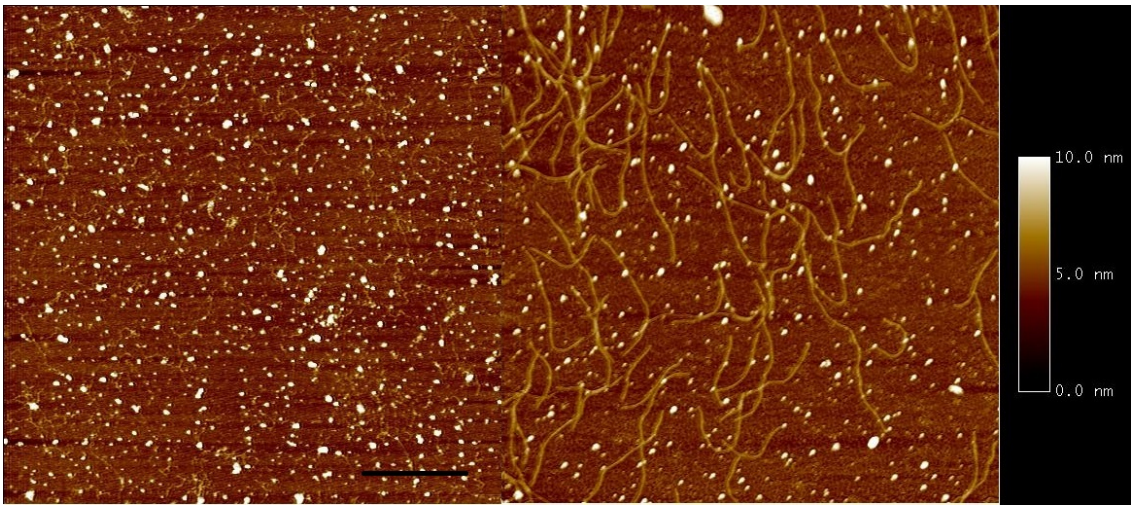

(B)

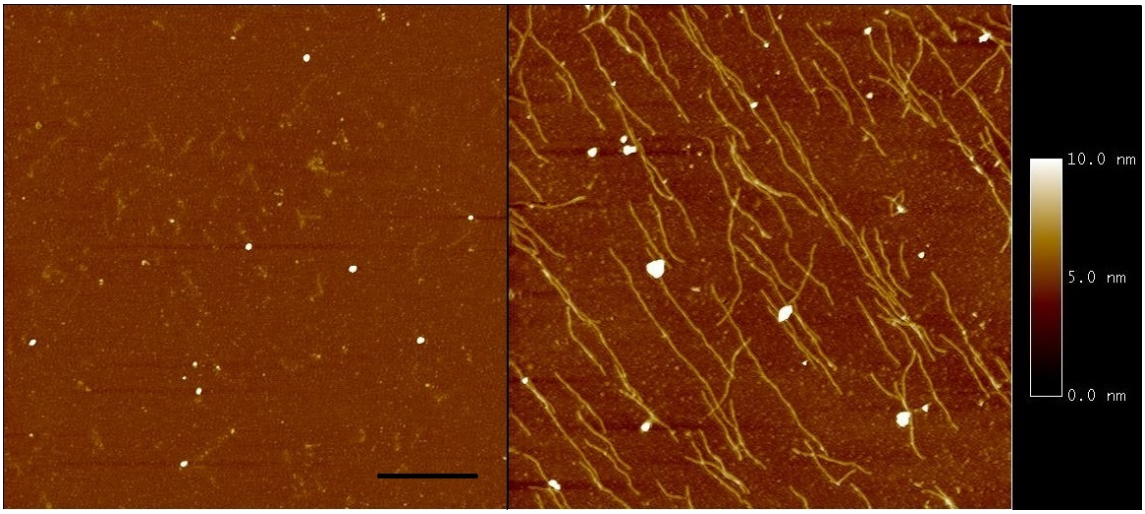

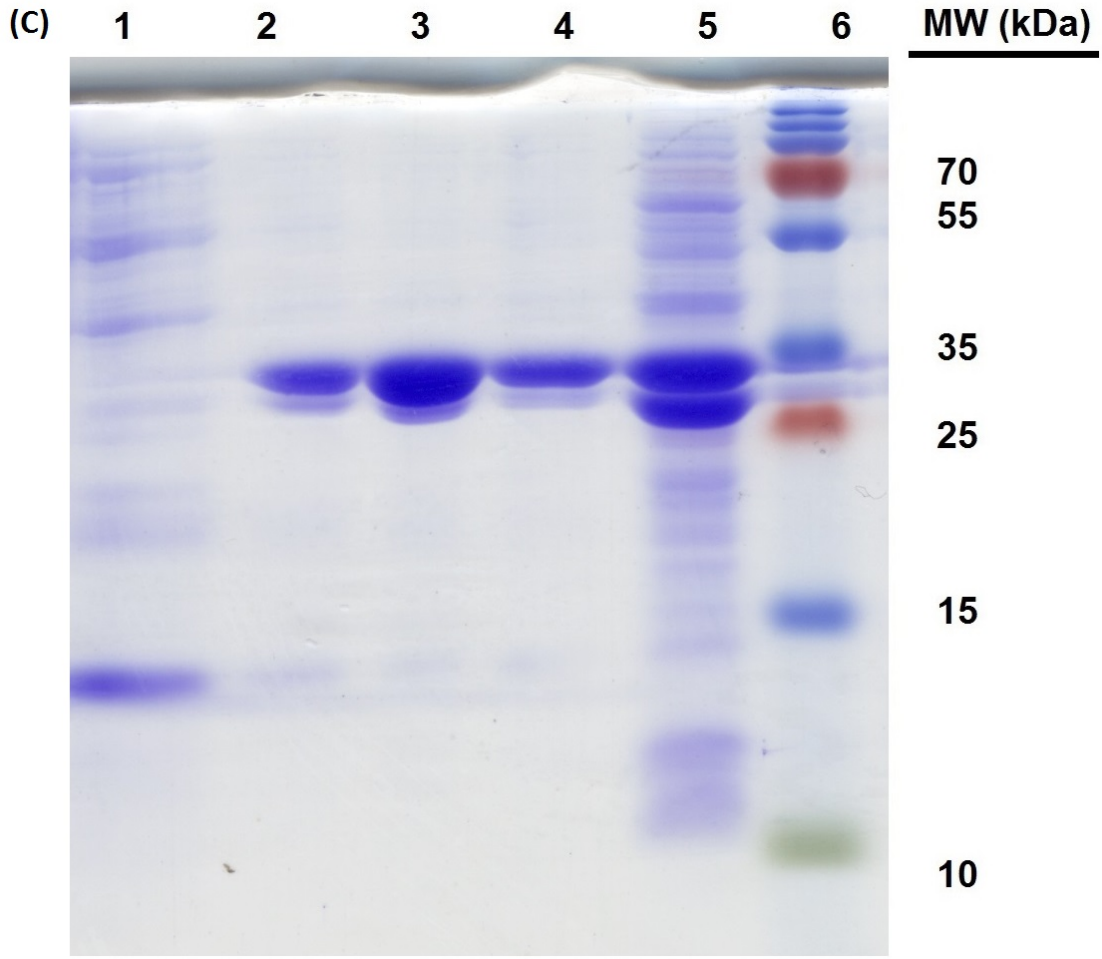

Figure 4. 2 Single clones against trimeric rhTau selection, expression and purification. (A) Representative AFM images of single clone selection based on the specificity to trimeric tau (right) against monomeric (left) and BSA. The scale bar of 1 µm applies to both images. (B) Representative AFM images of sequence corrected phage displayed scFv (F9T) incubated with tau 2N4R monomer (left) and trimer (right). The scale bar of 1 µm applies to both images. (C) SDS-PAGE of F9T scFv periplasmic preparation shows full length 29 kDa protein. Lane 1, wash after scFv loading; lane 2 to lane 4, elution with imidazole of 200 mM, 100 mM and 50 mM; lane 5, periplasm flow through nickel beads column; lane 6, molecular weight standards.

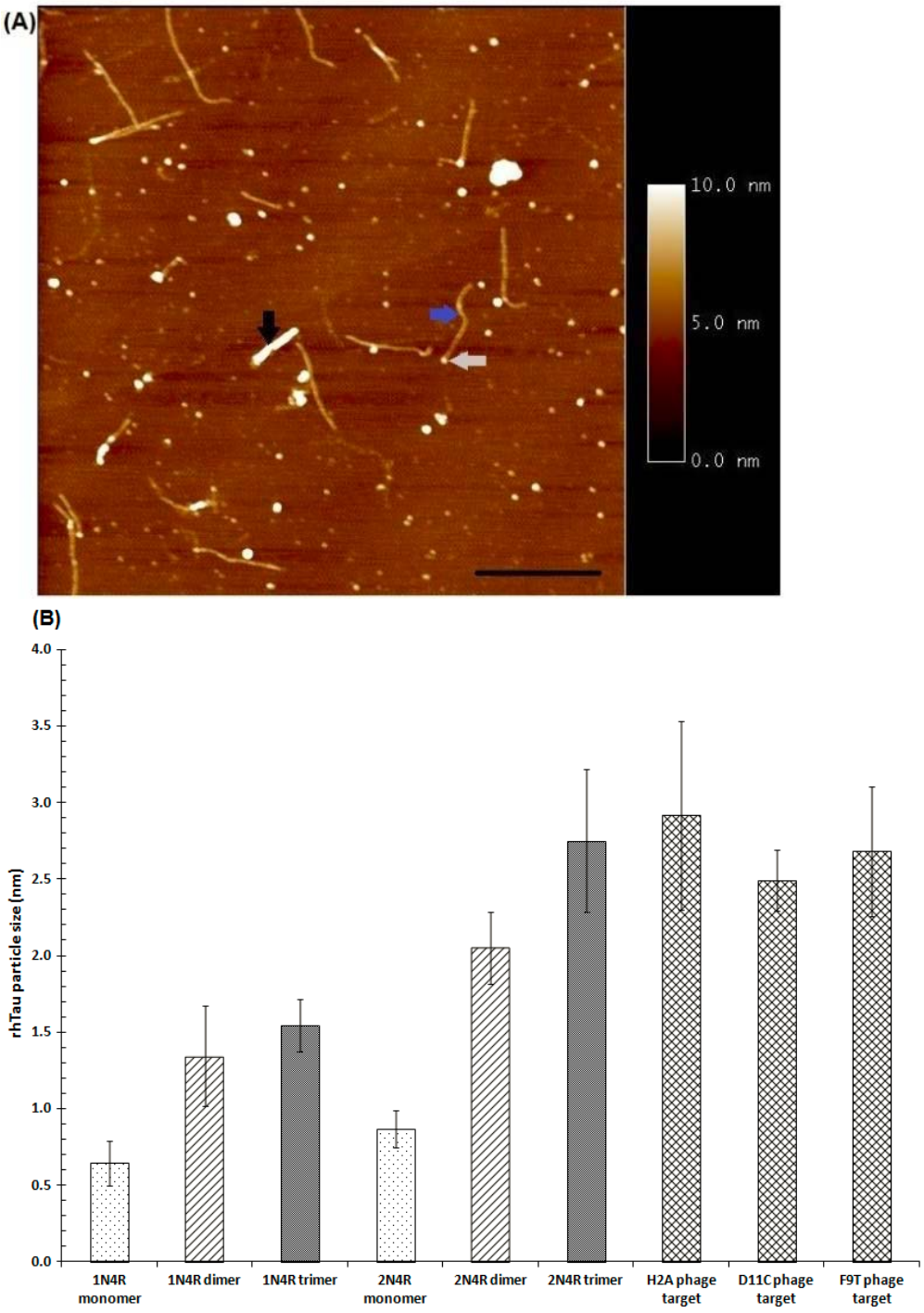

Figure 4. 3 Particle size analysis of oligomeric tau bound to scFv-displayed phage from rhTau 2N4R mixed aggregates. (A) Representative AFM image of F9T phage (blue arrow) interacting with rhTau 2N4R mixed aggregates containing oligomers (gray arrow) and fibrils (black arrow). (B) Size of purified rhTau monomer, dimer and trimer compared to average size of antigens bound by F9T, D11C and H2A phage. The size of each individual particle bound at the tip of a phage particle was measured using the section function in Nanoscope Analysis. The mean value of the particles targeted by each phage is between 2.5 nm and 3.0 nm, consistent with the size of trimeric rhTau 2N4R (Error bar:+/- standard deviation).

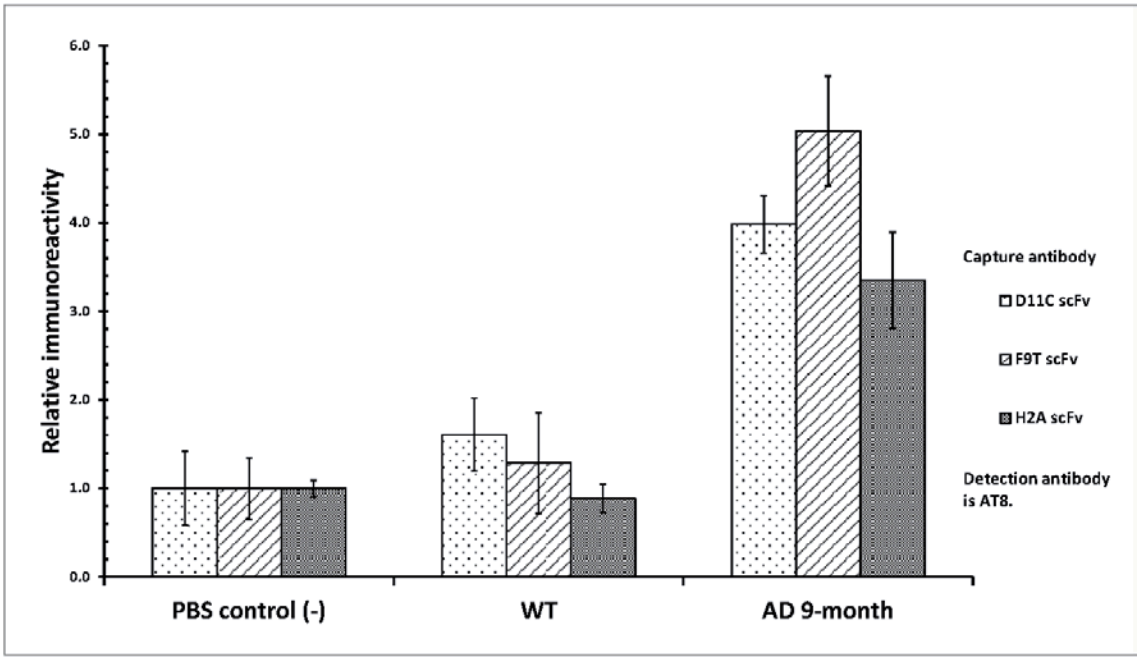

Figure 4. 4 Selective reactivity of F9T, D11C and H2A scFvs with 9-month 3×TG-AD mouse brain tissue. F9T, D11C or H2A scFv were used as capture antibody. Mouse hippocampus homogenates from 3×TG-AD mice and wild-type mice were added as target analytes. PBS was used as the negative control. The bound tau aggregates were detected using anti-tau antibody AT8 conjugated with HRP. Relative immunoreactivities are chemiluminescent signal ratio to the mean value of PBS negative controls. (Error bar:+/- standard deviation)

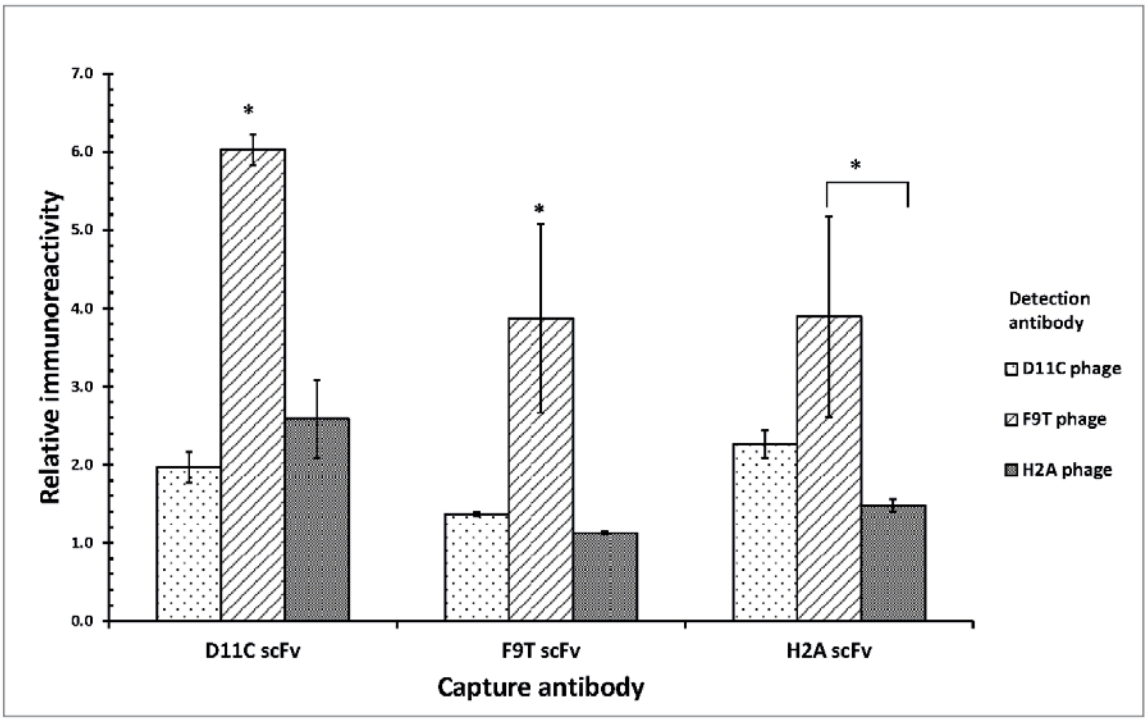

Figure 4. 5 Capture ELISA for detection of oligomeric tau. Each scFv was utilized as a capture antibody in combination with each phage displayed scFv as the detection antibody using 9-month 3×TG-AD mice brain homogenates as antigen. All three scFvs produced the strongest signal when F9T phage was used as detection antibody. The mean comparison was performed within each group of the same capture antibody. Relative immunoreactivities are chemiluminescent signal ratio to the mean value of wild type mice. (Error bar:+/- standard deviation)

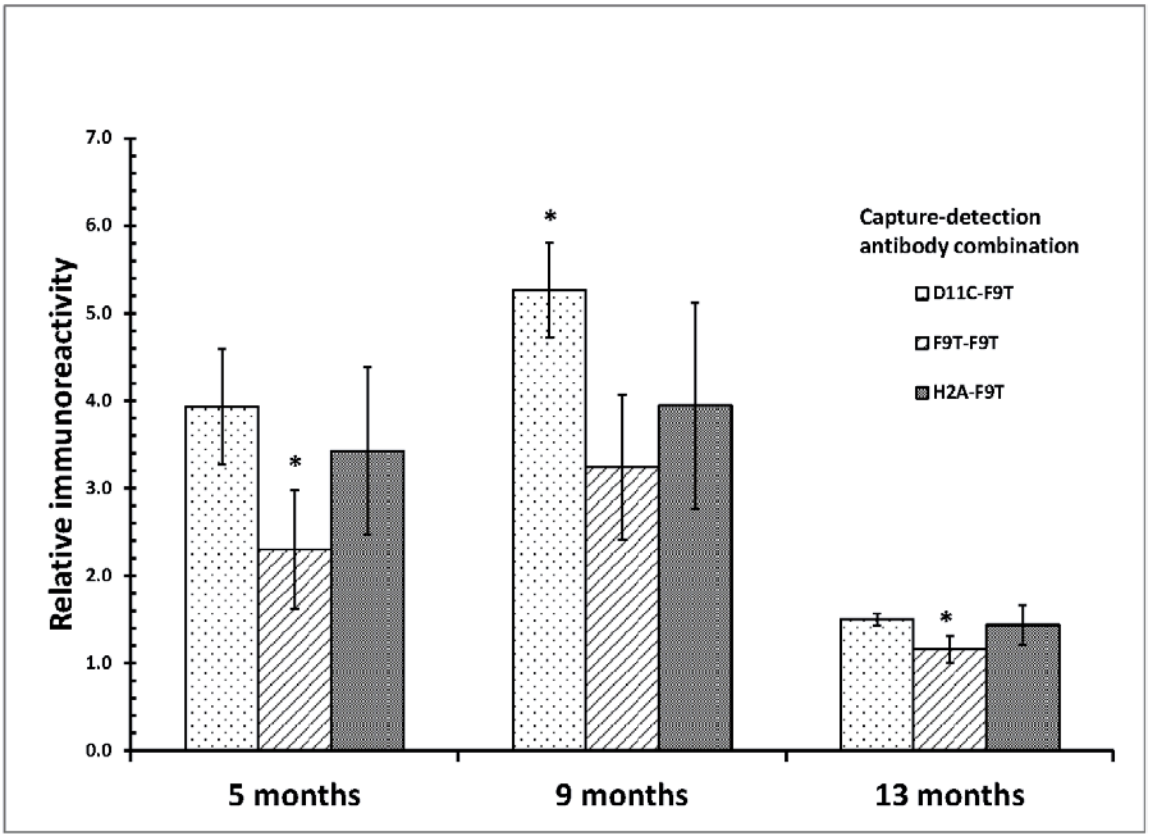

Figure 4. 6 Oligomeric tau levels in different age 3×TG-AD mice brain extracts. The levels of oligomeric tau in the different age 3×TG-AD and wild-type mice were determined using the F9T, D11C and H2A scFvs as the capture antibody and F9T scFv displayed phage as the detection antibody. Two mice for each age group were tested in triplicate. The data were grouped by the age of the mice. The mean comparison was performed within each age matched group. Oligomeric tau levels peak at 9 months and decrease by 13 months. Relative immunoreactivities are chemiluminescent signal ratio to the mean value of wild type mice (Error bar:+/- standard deviation).

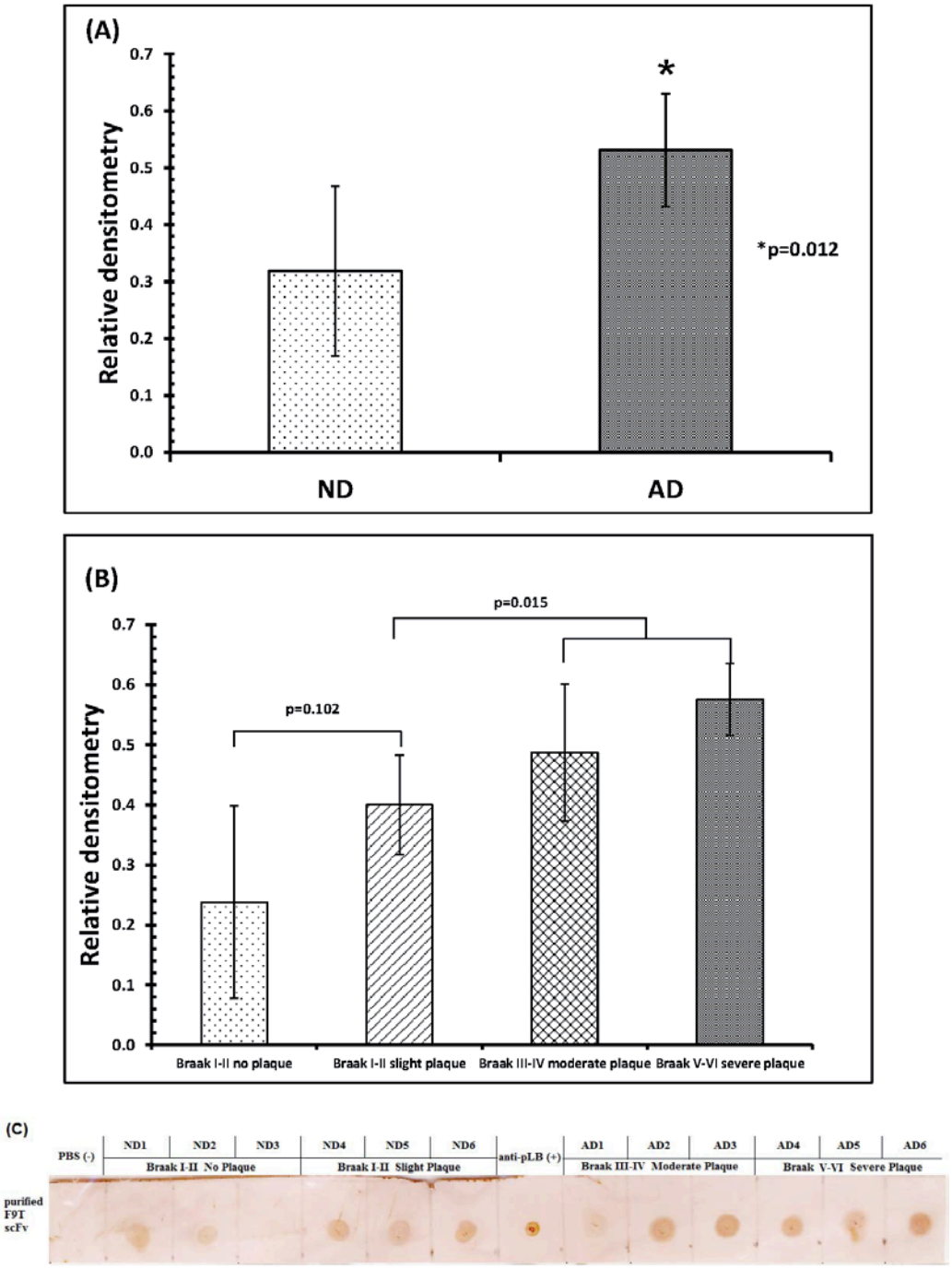

Figure 4. 7 Oligomeric tau levels in post-mortem human brain samples as a function of Braak stage. Brain homogenates from age-matched human middle temporal gyrus (MTG) were blotted on membranes and probed for presence of oligomeric tau using F9T scFv. Signals were scaled between 0 and 1 by ImageJ analysis where 0 is the background signal and 1 is the positive control signal. Statistical analysis was performed in one-way ANOVA comparing means of two groups. (A) non-demented (ND) and Alzheimer's (AD) and (B) Braak stages and neuritic plaque frequencies. Braak stages I-II slight or no plaques; Braak stages III-IV moderate plaques; Braak stages V-VI severe plaques. Oligomeric tau levels as determined by reactivity with F9T correlates directly with Braak stages and plaque frequency with increasing oligomeric tau levels with increasing Braak stage. (C) Sample dot blot affinity assay of homogenized MTG tissue from human non-demented and AD tissue probed with F9T scFv.

Table 4. 1 DNA sequences of the N-terminal region and the first heavy chain framework region (HCFR1) of recovered scFvs after panning compared to known scFvs. F9, H7, D4, D11 and G12 were recovered from the panning protocol, others are published scFv sequences. All recovered scFvs contain similar framework regions as published sequences except for a missing nucleotide near the N-terminal.

SfiI	GGCCCAGCCGGCC					
NcoI		*CCATGG*				
Met start			ATG			HCFR1
αph0x15	GGCCCAGCCGG	*CC*	*ATG*	*G*	CC	CAGGTGCAGCTGGTGCAGTCTGGGGCTGAGGTGAAG
αBSA3	GGCCCAGCCGG	*CC*	*ATG*	*G*	CC	CAGGTGCAGCTGGTGCAGTCTGGGGGAGGCGTGGTC
αTEL9	GGCCCAGCCGG	*CC*	*ATG*	*G*	CC	CAGGTACAGCTGCAGCAGTCAGGCTCAGGACTGGTG
αTEL14	GGCCCAGCCGG	*CC*	*ATG*	*G*	CC	CAGGTGCAGCTGCAGGAGTCGGGGCCAGGACTGGTG
αTEL13	GGCCCAGCCGG	*CC*	*ATG*	*G*	CC	CAGGTGCAGCTGGTGCAGTCTGGAGCAGAGGTGAAA
αTEL16	GGCCCAGCCGG	*CC*	*ATG*	*G*	CC	CAGGTGCAGCTGGTGCAGTCTGGGGCAGAGGTGAAA
F9	GGCCCAGCCGG	*CC*	*ATG*	*G*	CC	CAGGTGCAGCTGCAGGAGTC-GGGGGAGGCGTGGTC
D11	GGCCCAGCCGG	*CC*	*ATG*	*G*	-C	CAGGTGCAGCTGGTGGAGTCTGGGGGAGGCTTGGTA
H2	GGCCCAGCCGG	*CC*	*ATG*	*G*	CC	CAGGTGCAGCTG-TGGAGTCTGGGGGAGGCGTGGTC
D4	GGCCCAGCCGG	*CC*	*ATG*	*G*	CC	CAGGTGCAGCTGGTGC-GTCTGGAGGAGACTTGATC
H7	GGCCCAGCCGG	*CC*	*ATG*	*G*	CC	CAGGTGCAGCTGCAGGAGTC-GGGGGAGACGTGGTC
G12	GGCCCAGCCGG	*CC*	*ATG*	*G*	-C	CGAGTGCAGCTGGTGGAGTCTGGGGCTGAGGTGACG

	HCFR1(Cont'd)
αph0x15	AAGCCTGGGGCCTCAGTGAAGGTCTCCTGCAAGGCTTCTGGTTACACCTTTACC
αBSA3	CAGCCTGGGAGGTCCCTGAGACTCTCCTGTGCAGCCTCTGGATTCACCTTCAGT
αTEL9	AAGCCTTCACAGACCCTGTCCCTCACCTGCTCTGTCTCTGGTGACTCCATCTCC
αTEL14	AAGCCTTCGGAGACCCTGTCCCTCGTCTGCACTGTCTCTGGTGGCTCCCTCAGT
αTEL13	AAGCCCGGGCAGTCTCTGATGATCTCCTGTCAGGGTTCTGGATACAGCTTTAGC
αTEL16	AAGCCCGGGCAGTCTCTGAGGATCTCCTGTAAGGGTGCTGGATACAGCTTTAGC
F9	CAGCCTGGGAGGTCCCTGAGACTCTCCTGTGCAGCGTCTGGATTCACCTTCAGT
D11	CAGCCTGGGGGGTCCCTGAGACTCTCCTGTGCAGCCTCTGGATTCACCTTTAGC
H2	CAGCCTGGGAGGTCCCTGAGACTCTCCTGTGCAGCCTCTGGATTCACCTTCAGT
D4	CAGCCTGGGGGGTCCCTGAGACTCTCCTGTGCAGCCTCTGGATTCACCTTTAAT
H7	CAGCCTGGGAGGTCCCTGAGACTCTCCTGTGCAGCCTCTGGATTCACCTTCAGT
G12	AAGCCTGGGGCCTCAGTAAGGGTCTCCTGCAAGGCTTCTGGATACACCTTCAGC

Table 4.2 Designed primers for correction of missing base pair. Forward primers contain the NcoI (5'-CCATGG-3' in italic) site upstream of scFv sequence and the missing base pair (underlined). The reverse primer includes the NotI (5'-GCGGCCGC-3' in italic) site downstream of scFv sequence.

Primer names	DNA sequences
F9T forward primer	5'-ATA TAT ***CCA TGG*** CCC AGG TGC AGC TGC AGG AGT C<u>T</u>G GGG GAG GCG TGG TCC-3'
D11C forward primer	5'-ATA TAT ***CCA TGG*** <u>C</u>CC AGG TGC AGC TGG TGG AGT CTG GGG GAG GCT TGG TAC-3'
H2A forward primer	5'-GCC GGC ***CAT GGC*** CCA GGT ACA GCT GC<u>A</u> GGA GTC TGG GGG AGG CTT GGT-3'
Reverse primer for all three clones	5'-CCC GTG ATG GTG ATG ATG ATG T***GC GGC CGC*** ACG TTT GAT CTC CAG -3'

4.8 References

1. 2012 Alzheimer's disease facts and figures. Alzheimers Dement, 2012. **8**(2): p. 131-68.

2. Glabe, C.G., Common mechanisms of amyloid oligomer pathogenesis in degenerative disease. Neurobiol Aging, 2006. **27**(4): p. 570-5.

3. Lambert, M.P., et al., Diffusible, nonfibrillar ligands derived from Abeta1-42 are potent central nervous system neurotoxins. Proc Natl Acad Sci U S A, 1998. **95**(11): p. 6448-53.

4. Ward, S.M., et al., Tau oligomers and tau toxicity in neurodegenerative disease. Biochem Soc Trans, 2012. **40**(4): p. 667-71.

5. Gestwicki, J.E., G.R. Crabtree, and I.A. Graef, Harnessing chaperones to generate small-molecule inhibitors of amyloid beta aggregation. Science, 2004. **306**(5697): p. 865-9.

6. Hirohata, M., et al., The anti-amyloidogenic effect is exerted against Alzheimer's beta-amyloid fibrils in vitro by preferential and reversible binding of flavonoids to the amyloid fibril structure. Biochemistry, 2007. **46**(7): p. 1888-99.

7. Ono, K., H. Naiki, and M. Yamada, The development of preventives and therapeutics for Alzheimer's disease that inhibit the formation of beta-amyloid fibrils (fAbeta), as well as destabilize preformed fAbeta. Curr Pharm Des, 2006. **12**(33): p. 4357-75.

8. Ono, K., et al., Curcumin has potent anti-amyloidogenic effects for Alzheimer's beta-amyloid fibrils in vitro. J Neurosci Res, 2004. **75**(6): p. 742-50.

9. Ono, K., et al., Nicotine breaks down preformed Alzheimer's beta-amyloid fibrils in vitro. Biol Psychiatry, 2002. **52**(9): p. 880-6.

10. Sinha, S., et al., Comparison of three amyloid assembly inhibitors: the sugar scyllo-inositol, the polyphenol epigallocatechin gallate, and the molecular tweezer CLR01. ACS Chem Neurosci, 2012. **3**(6): p. 451-8.

11. Sinha, S., et al., Lysine-specific molecular tweezers are broad-spectrum inhibitors of assembly and toxicity of amyloid proteins. J Am Chem Soc, 2011. **133**(42): p. 16958-69.

12. Check, E., Nerve inflammation halts trial for Alzheimer's drug. Nature, 2002. **415**(6871): p. 462.

13. Gilman, S., et al., Clinical effects of Abeta immunization (AN1792) in patients with AD in an interrupted trial. Neurology, 2005. **64**(9): p. 1553-62.

14. Salloway, S., et al., A phase 2 multiple ascending dose trial of bapineuzumab in mild to moderate Alzheimer disease. Neurology, 2009. **73**(24): p. 2061-70.

15. Sperling, R.A., et al., Functional alterations in memory networks in early Alzheimer's disease. Neuromolecular Med, 2010. **12**(1): p. 27-43.

16. Lasagna-Reeves, C.A., et al., Preparation and characterization of neurotoxic tau oligomers. Biochemistry, 2010. **49**(47): p. 10039-41.

17. Berger, Z., et al., Accumulation of pathological tau species and memory loss in a conditional model of tauopathy. J Neurosci, 2007. **27**(14): p. 3650-62.

18. Cohen, T.J., et al., The microtubule-associated tau protein has intrinsic acetyltransferase activity. Nat Struct Mol Biol, 2013. **20**(6): p. 756-62.

19. Cowan, C.M. and A. Mudher, Are tau aggregates toxic or protective in tauopathies? Front Neurol, 2013. **4**: p. 114.

20. Yanamandra, K., et al., Anti-Tau Antibodies that Block Tau Aggregate Seeding In Vitro Markedly Decrease Pathology and Improve Cognition In Vivo. Neuron, 2013.

21. Blair, L.J., et al., Accelerated neurodegeneration through chaperone-mediated oligomerization of tau. J Clin Invest, 2013.

22. Gerson, J.E. and R. Kayed, Formation and propagation of tau oligomeric seeds. Front Neurol, 2013. **4**: p. 93.

23. Lasagna-Reeves, C.A., et al., Identification of oligomers at early stages of tau aggregation in Alzheimer's disease. FASEB J, 2012. **26**(5): p. 1946-59.

24. Avila, J., et al., Role of tau protein in both physiological and pathological conditions. Physiol Rev, 2004. **84**(2): p. 361-84.

25. Hernandez, F. and J. Avila, Tauopathies. Cell Mol Life Sci, 2007. **64**(17): p. 2219-33.

26. Wang, Y.P., et al., Stepwise proteolysis liberates tau fragments that nucleate the Alzheimer-like aggregation of full-length tau in a neuronal cell model. Proc Natl Acad Sci U S A, 2007. **104**(24): p. 10252-7.

27. Alonso, A., et al., Hyperphosphorylation induces self-assembly of tau into tangles of paired helical filaments/straight filaments. Proc Natl Acad Sci U S A, 2001. **98**(12): p. 6923-8.

28. Hanger, D.P., B.H. Anderton, and W. Noble, Tau phosphorylation: the therapeutic challenge for neurodegenerative disease. Trends Mol Med, 2009. **15**(3): p. 112-9.

29. Schneider, A., et al., Phosphorylation that detaches tau protein from microtubules (Ser262, Ser214) also protects it against aggregation into Alzheimer paired helical filaments. Biochemistry, 1999. **38**(12): p. 3549-58.

30. Alonso Adel, C., et al., Promotion of hyperphosphorylation by frontotemporal dementia tau mutations. J Biol Chem, 2004. **279**(33): p. 34873-81.

31. Morris, M., et al., The many faces of tau. Neuron, 2011. **70**(3): p. 410-26.

32. Bullmann, T., et al., Expression of embryonic tau protein isoforms persist during adult neurogenesis in the hippocampus. Hippocampus, 2007. **17**(2): p. 98-102.

33. Congdon, E.E. and K.E. Duff, Is tau aggregation toxic or protective? J Alzheimers Dis, 2008. **14**(4): p. 453-7.

34. Demuro, A., et al., Calcium dysregulation and membrane disruption as a ubiquitous neurotoxic mechanism of soluble amyloid oligomers. J Biol Chem, 2005. **280**(17): p. 17294-300.

35. Gomez-Ramos, A., et al., Extracellular tau is toxic to neuronal cells. FEBS Lett, 2006. **580**(20): p. 4842-50.

36. Gomez-Ramos, A., et al., Extracellular tau promotes intracellular calcium increase through M1 and M3 muscarinic receptors in neuronal cells. Mol Cell Neurosci, 2008. **37**(4): p. 673-81.

37. Andorfer, C., et al., Cell-cycle reentry and cell death in transgenic mice expressing nonmutant human tau isoforms. J Neurosci, 2005. **25**(22): p. 5446-54.

38. Brunden, K.R., J.Q. Trojanowski, and V.M. Lee, Evidence that non-fibrillar tau causes pathology linked to neurodegeneration and behavioral impairments. J Alzheimers Dis, 2008. **14**(4): p. 393-9.

39. Polydoro, M., et al., Age-dependent impairment of cognitive and synaptic function in the htau mouse model of tau pathology. J Neurosci, 2009. **29**(34): p. 10741-9.

40. Meraz-Rios, M.A., et al., Tau oligomers and aggregation in Alzheimer's disease. J Neurochem, 2010. **112**(6): p. 1353-67.

41. Marx, J., Alzheimer's disease. A new take on tau. Science, 2007. **316**(5830): p. 1416-7.

42. Kayed, R., et al., Annular protofibrils are a structurally and functionally distinct type of amyloid oligomer. J Biol Chem, 2009. **284**(7): p. 4230-7.

43. Maeda, S., et al., Increased levels of granular tau oligomers: an early sign of brain aging and Alzheimer's disease. Neurosci Res, 2006. **54**(3): p. 197-201.

44. Maeda, S., et al., Granular tau oligomers as intermediates of tau filaments. Biochemistry, 2007. **46**(12): p. 3856-61.

45. Clavaguera, F., et al., Transmission and spreading of tauopathy in transgenic mouse brain. Nat Cell Biol, 2009. **11**(7): p. 909-13.

46. Liu, L., et al., Trans-synaptic spread of tau pathology in vivo. PLoS One, 2012. **7**(2): p. e31302.

47. de Calignon, A., et al., Propagation of tau pathology in a model of early Alzheimer's disease. Neuron, 2012. **73**(4): p. 685-97.

48. Lasagna-Reeves, C.A., et al., Alzheimer brain-derived tau oligomers propagate pathology from endogenous tau. Sci Rep, 2012. **2**: p. 700.

49. Tian, H., et al., Trimeric tau is toxic to human neuronal cells at low nanomolar concentrations. International Journal of Cell Biology, In press.

50. Sheets, M.D., et al., Efficient construction of a large nonimmune phage antibody library: the production of high-affinity human single-chain antibodies to protein antigens. Proc Natl Acad Sci U S A, 1998. **95**(11): p. 6157-62.

51. Barkhordarian, H., et al., Isolating recombinant antibodies against specific protein morphologies using atomic force microscopy and phage display technologies. Protein Eng Des Sel, 2006. **19**(11): p. 497-502.

52. Emadi, S., et al., Isolation of a human single chain antibody fragment against oligomeric alpha-synuclein that inhibits aggregation and prevents alpha-synuclein-induced toxicity. J Mol Biol, 2007. **368**(4): p. 1132-44.

53. Emadi, S., et al., Detecting morphologically distinct oligomeric forms of alpha-synuclein. J Biol Chem, 2009. **284**(17): p. 11048-58.

54. Kasturirangan, S., et al., Nanobody specific for oligomeric beta-amyloid stabilizes nontoxic form. Neurobiol Aging, 2012. **33**(7): p. 1320-8.

55. Kasturirangan, S., et al., Isolation and characterization of antibody fragments selective for specific protein morphologies from nanogram antigen samples. Biotechnol Prog, 2013. **29**(2): p. 463-71.

56. Zameer, A., et al., Single Chain Fv Antibodies against the 25-35 Abeta Fragment Inhibit Aggregation and Toxicity of Abeta42. Biochemistry, 2006. **45**(38): p. 11532-9.

57. Marks, J.D., et al., By-passing immunization. Human antibodies from V-gene libraries displayed on phage. J Mol Biol, 1991. **222**(3): p. 581-97.

58. Wang, M.S., et al., Characterizing antibody specificity to different protein morphologies by AFM. Langmuir, 2009. **25**(2): p. 912-8.

59. Kipriyanov, S.M., G. Moldenhauer, and M. Little, High level production of soluble single chain antibodies in small-scale Escherichia coli cultures. J Immunol Methods, 1997. **200**(1-2): p. 69-77.

60. Kasturirangan, S., S. Boddapati, and M.R. Sierks, Engineered proteolytic nanobodies reduce Abeta burden and ameliorate Abeta-induced cytotoxicity. Biochemistry, 2010. **49**(21): p. 4501-8.

61. Zameer, A., et al., Anti-oligomeric Abeta single-chain variable domain antibody blocks Abeta-induced toxicity against human neuroblastoma cells. J Mol Biol, 2008. **384**(4): p. 917-28.

62. Oddo, S., et al., Amyloid deposition precedes tangle formation in a triple transgenic model of Alzheimer's disease. Neurobiol Aging, 2003. **24**(8): p. 1063-70.

63. Oddo, S., et al., Triple-transgenic model of Alzheimer's disease with plaques and tangles: intracellular Abeta and synaptic dysfunction. Neuron, 2003. **39**(3): p. 409-21.

64. von Bergen, M., et al., Tau aggregation is driven by a transition from random coil to beta sheet structure. Biochim Biophys Acta, 2005. **1739**(2-3): p. 158-66.

65. Nacharaju, P., et al., Accelerated filament formation from tau protein with specific FTDP-17 missense mutations. FEBS Lett, 1999. **447**(2-3): p. 195-9.

66. Pennanen, L., et al., Accelerated extinction of conditioned taste aversion in P301L tau transgenic mice. Neurobiol Dis, 2004. **15**(3): p. 500-9.

67. Brun, A. and E. Englund, Regional pattern of degeneration in Alzheimer's disease: neuronal loss and histopathological grading. Histopathology, 2002. **41**(3A): p. 40-55.

68. Braak, H., et al., Staging of Alzheimer disease-associated neurofibrillary pathology using paraffin sections and immunocytochemistry. Acta Neuropathol, 2006. **112**(4): p. 389-404.

69. Braak, H. and E. Braak, Staging of Alzheimer's disease-related neurofibrillary changes. Neurobiol Aging, 1995. **16**(3): p. 271-8; discussion 278-84.

70. Braak, H., et al., Vulnerability of cortical neurons to Alzheimer's and Parkinson's diseases. J Alzheimers Dis, 2006. **9**(3 Suppl): p. 35-44.

71. Ballatore, C., V.M. Lee, and J.Q. Trojanowski, Tau-mediated neurodegeneration in Alzheimer's disease and related disorders. Nat Rev Neurosci, 2007. **8**(9): p. 663-72.

72. Goedert, M., Tau protein and neurodegeneration. Semin Cell Dev Biol, 2004. **15**(1): p. 45-9.

73. Gregersen, N., Protein misfolding disorders: pathogenesis and intervention. J Inherit Metab Dis, 2006. **29**(2-3): p. 456-70.

74. Hardy, J. and D. Allsop, Amyloid deposition as the central event in the aetiology of Alzheimer's disease. Trends Pharmacol Sci, 1991. **12**(10): p. 383-8.

75. Hardy, J. and D.J. Selkoe, The amyloid hypothesis of Alzheimer's disease: progress and problems on the road to therapeutics. Science, 2002. **297**(5580): p. 353-6.

76. Oddo, S., et al., Temporal profile of amyloid-beta (Abeta) oligomerization in an in vivo model of Alzheimer disease. A link between Abeta and tau pathology. J Biol Chem, 2006. **281**(3): p. 1599-604.

77. Small, S.A. and K. Duff, Linking Abeta and tau in late-onset Alzheimer's disease: a dual pathway hypothesis. Neuron, 2008. **60**(4): p. 534-42.

78. Harper, J.D., et al., Observation of metastable Abeta amyloid protofibrils by atomic force microscopy. Chem Biol, 1997. **4**(2): p. 119-25.

79. Roher, A.E., et al., Morphological and biochemical analyses of amyloid plaque core proteins purified from Alzheimer disease brain tissue. J Neurochem, 1993. **61**(5): p. 1916-26.

80. Walsh, D.M. and D.J. Selkoe, A beta oligomers - a decade of discovery. J Neurochem, 2007. **101**(5): p. 1172-84.

81. Bretteville, A. and E. Planel, Tau aggregates: toxic, inert, or protective species? J Alzheimers Dis, 2008. **14**(4): p. 431-6.

82. Roberson, E.D., et al., Reducing endogenous tau ameliorates amyloid beta-induced deficits in an Alzheimer's disease mouse model. Science, 2007. **316**(5825): p. 750-4.

83. Wu, J.W., et al., Small Misfolded Tau Species Are Internalized via Bulk Endocytosis and Anterogradely and Retrogradely Transported in Neurons. J Biol Chem, 2013. **288**(3): p. 1856-70.

84. Yoshiyama, Y., et al., Synapse Loss and Microglial Activation Precede Tangles in a P301S Tauopathy Mouse Model. Neuron, 2007. **53**(3): p. 337-351.

85. Honson, N.S. and J. Kuret, Tau aggregation and toxicity in tauopathic neurodegenerative diseases. J Alzheimers Dis, 2008. **14**(4): p. 417-22.

86. Alafuzoff, I., et al., Staging of neurofibrillary pathology in Alzheimer's disease: a study of the BrainNet Europe Consortium. Brain Pathol, 2008. **18**(4): p. 484-96.

87. Braak, H., et al., Staging of brain pathology related to sporadic Parkinson's disease. Neurobiol Aging, 2003. **24**(2): p. 197-211.

88. Braak, H. and E. Braak, Neuropathological stageing of Alzheimer-related changes. Acta Neuropathol, 1991. **82**(4): p. 239-59.

89. Arnold, S.E., et al., The topographical and neuroanatomical distribution of neurofibrillary tangles and neuritic plaques in the cerebral cortex of patients with Alzheimer's disease. Cereb Cortex, 1991. **1**(1): p. 103-16.

Chapter 5

The role of tau oligomer in traumatic brain injury progression in rodent models

5.1 Abstract

In Alzheimer's disease (AD), tau undergoes oligomerization as well as phosphorylation during its transforming from normal monomeric microtubule-associate protein to the main constituent of neurofibrillary tangles (NFTs). Although phosphorylation has been long considered key pathological feature of AD tau, soluble oligomeric tau species may play a more critical role in AD progression as we previously demonstrated that human recombinant tau oligomers are extracellularly toxic to neuroblastoma cells and that non-phosphorylated oligomeric tau was detected AD tau transgenic mouse brain at early stage. We have developed a novel biopanning technique based on AFM to obtain two groups of single chain variable fragments (scFv) targeting toxic tau oligomeric forms and general small molecule tau species respectively. The scFvs recognizing generally all small soluble tau monomer and/or oligomers particularly non-phosphorylated types make a tau antibody detecting or confirming such tau species different from phosphorylated tau conventional tau antibodies do. Combined with these novel tau detecting antibodies, the group of scFvs targeting oligomeric tau makes a useful tool of better understanding the tau aggregating and tau oligomer's role in AD progressions.

5.2 Introduction

Alzheimer's disease (AD) is the most common age-related neurodegenerative disease, of which the main symptoms are loss of brain functions like memory and cognition, brain atrophy and neuron death[1-2]. Tau protein in monomeric form is an important microtubule associated protein in human neurons. However in AD, tau was found in hyperphosphorylated and highly aggregated insoluble form, as the main component of neurofibrillary tangles (NFTs) which is one of the two AD pathological features. Phosphorylation had been the main research focus of tau's effects on AD and potential therapeutic approaches for many years[3-5], since all tau found in NFTs are hyperphosphorylated, markedly different from normal tau phosphorylation level and sites. Also, these phosphorylation sites found in tangled tau are more related to its assembly domain crucial for interaction with microtubule, thus the phosphorylation is considered interrupt tau's normal function. However, oligomeric tau has been recently taking up the share of high attention from tau phosphorylation as a valuable target for studying AD pathogenesis and treating AD, despite the fact that it is not directly discovered in postmortem AD brains. Tau oligomers demonstrate close correlation with neurodegenerative-associated phenotypes such as synapse lesion, neuronal death and behavioral impairment in human tau expressing animal models[6-8]. In postmortem frontal lobe cortex of early AD patients, oligomeric tau species were detected before NFTs' presence[9-10]. Tau oligomers are also detected in middle temporal gyrus of AD patients at different Braak stages with the tau oligomer concentration increasing corresponding to AD progression and preceding the presence and increasing the plaque and tangles, as indicated in Chapter 4. Oligomeric tau was implied in other studies to

follow a prion-like mechanism to transmit AD pathologies, similar as but preceding NFT tau pathology spreading from brain regions seeded with oligomeric tau into other regions resulting in aggregation of endogenous tau[11-14]. These discoveries point out that neuronal toxicity and loss precede the formation of NFTs, which suggests a precursor of NFTs' existence, mostly likely tau oligomers is an early indicator of AD and possible cause for AD pathogenesis and development[7, 15-16].

In our study, we develop two groups of scFvs targeting toxic oligomeric tau and general small molecular tau including tau monomers and oligomers. The former group of scFvs is a potential powerful tool to detect abnormal tau oligomers in trace amount existing in brain tissues from human AD patients and triple transgenic AD-like mice as described in Chapter 4. These later group of scFvs in forms of scFv-displayed phage were tested and confirmed to recognize any small non-aggregated tau species including monomer, dimer, trimer and small oligomers regardless of their phosphorylation conditions, which make them better small tau detectors in our study than commercial phosphorylated tau detecting antibody.

In addition to AD, tau pathology is present in other neurodegenerative diseases. For instance, tau lesions are found as a major feature in repetitive closed head injury including chronic traumatic encephalopathy (CTE)[17] that commonly afflicts professional contact sports athletes such as football players[18] and boxers[19-20]. A recent study using an aged mouse model expressing human tau suggests that repetitive mild traumatic brain injury can augment tau pathology and glial activation based on the presence of hyperphosphorylated or aggregated tau in mouse brain sections[21]. Since we

can selectively detect the presence of oligomeric tau, we would like to determine if oligomeric tau is an early marker of brain injury using rodent models that undergo single or repetitive traumatic brain injury. In this chapter, we test F9T's ability of distinguishing human mutant tau (htau406) knock-in mice and traumatic brain injury (TBI) rodent models by recognizing abnormal tau in their hippocampus sections and brain homogenates, with a novel high sensitivity capture ELISA and immunohistochemical (IHC) staining techniques, respectively. According to the results, we propose that F9T has the potential of recognizing abnormal tau intermediate forms in brain section and thusly diagnosing tau induced brain damage at its early stage.

5.3 Material and Methods

Biopanning against small molecule tau- During the single clone screening process of biopanning against trimeric tau described in Chapter 4, we discovered scFv-displayed phage clones that recognized monomeric tau species as well as trimeric tau from irrelevant antigens such as BSA. Another separate biopanning against monomeric tau using Tomlinson I and J library was also performed to obtain scFv specific to small molecule tau including monomeric tau and low MW oligomeric tau. These scFvs were also confirmed specificity using monoclonal ELISA described as previously[22]. All clones from Sheets library that contain a frameshift in the first framework region in heavy chain region have been fixed following the same procedures as described in Chapter 4 and confirmed it maintained its specificity.

Cell culture and lysis- SH-SY5Y-TMHT441 cells was designed and provided by Dr. Birgit Hutter-Paier group in QPS, Austria. The cells was transfected with stable mutant

human tau enabling this cell line express tau phosphorylated at AD-related sites[23]. It was cultivated using a revised protocol based on that of cultivating SHSY-5Y human neuroblastoma cell lines (American Tissue Culture Collection)[24]. The culture medium contains 44% v/v Ham's F-12 (IrvineScientific), 44% v/v MEM Earle's salts (IrvineScientific), 10% v/v denatured fetal bovine serum (FBS) (SigmaAldrich), 1% v/v MEM non-essential amino acids (Invitrogen) , 1% v/v antibiotic/antimycotic (Invitrogen), and additional 300 μg/mL Geneticin G-418 for first few reviving passages, compared with culturing SH-SY5Y cells. Both SH-SY5Y and SH-SY5Y-TMHT441 were cultured in multiple 250mL Falcon sterile tissue culture flasks with vented caps. After the cell cultures grew confluent in the flask, the media were collected and centrifuge to collect the cell culture supernatant. The cells were also scraped off the flasks and washed twice with PBS. NP40 cell lysis buffer (invitrogen) freshly mixed with 1/10 volume of protease inhibitor cocktail (Sigma Cat.#P-2714) were added to cell pellet at the ratio of 10^8 cells/mL buffer to resuspend for lysis. The cell and lysis buffer mixture were ice incubated for 30 min with vortexing at 10 min intervals, then centrifuged at 13,000 rpm for 10 min at 4°C to collect supernatant as neuronal lysate, which should be store as aliquots in -80 °C.

Tau406+/TauKO mouse model- It is a genetically modified mouse model base on mouse tau knock out model. The experiment group is mutant human tau (4R) transgenic mouse (*Tau406+/TauKO*), while the negative control group is without mutant human tau knock-in(*Tau406-/TauKO*). This humanized transgenic mouse model is provided by Dr. Paul Fraser (Cleveland Clinic, Cleveland, OH). Human cortex and hippocampus from tau-associated dementia patients and non-demented controls are provided by Banner/Sun

Health Research Institute. The brain tissue homogenization follows the same protocol described in Chapter 4.

Traumatic brain injury (TBI) mouse model- The TBI mouse models and the control mice treated with corresponding times of anesthesia were generously provided by Dr. Fiona Crawford from Roskamp Institute, Sarasota, FL. All these mouse models were constructed from wild type (C57BL6) mice. The TBI mouse were injured at the age of 8-10 weeks and euthanatized 6 months post-injury, therefore the brains were essentially 8 to 8.5 months old. This time point was selected because we saw evidence for tau phosphorylation (CP13) in injured mice at this time point. The TBI mice have undergone either single mild injury (s-mTBI) or repetitive injury (r-mTBI), while the control mice (s-sham and r-sham) were treated at the same time points as TBI mouse with isoflurane alternated with oxygen as described previously[21]. The brain sections were provided from two mice per group and kept anonymous until the IHC staining result comes out.

Traumatic brain injury (TBI) rat model- The TBI rats model were created and provided by Dr. Sarah Stabenfeldt, Arizona State University. TBI rats were sacrificed 7 days or 14 days after head concussive treatment, with wild type TBI treated with anesthesia as negative control (sham). Selected brain sections (I-cortex, I-hippocampus, cerebel) of these two different rat age groups and control rats were homogenized shortly after sacrifice, and only the homogenates were provided for potential abnormal tau detection.

High sensitivity capture ELISA- We developed a high sensitivity capture ELISA based on the capture ELISA protocol described in Chapter 3, to evaluate scFvs' ability of detecting trace amount of oligomer tau in neuronal lysate, brain homogenate, CSF or serum

samples. scFv was produced using in scFv encoded E.coli culture at the early exponential phage (OD_{600}=0.3) with IPTG expressing soluble scFv at room temperature overnight. The expression culture was centrifuged and the supernatant containing active scFv was added 0.1% Tween20 and used as the capture antibody to coat the high affinity polystyrene microtiter 96-well plates. The plates were incubated at 50rpm slow shaking 37 °C for one hour for thorough coating before the unbound scFvs were removed. The plates were then washed three times with 0.1% Tween20/PBS and blocked with 2% non-fat milk/PBS at 50rpm slow shaking 37 °C for one hour. After repeating the Tween20/PBS wash, an aliquot of 100 µl/well of 2.5 µg/ml target analyte (brain homogenate, neuroblastoma lysate, serum etc.) was added, incubated at 50rpm slow shaking 37 °C for one hour and then washed with Tween20/PBS. PBS replaces target analytes to act as a negative control. A 100 µL/well aliquot of 0.35mg/ml monomeric tau targeting phage (the detection antibody) was added and incubated at 37 °C slow shaking for one hour. The wells were washed four times with Tween20/PBS for thorough removal of detecting phage. The remaining bound phage were then detected by 100 µL/well aliquots of 1:2000 dilution anti-M13 conjugated with HRP (GE) by incubation at 37 °C slow shaking for one hour. After four times wash with Tween20/PBS, the plates binding condintion were monitored using a chemiluminescent ELISA kit (SuperSignal ELISA Femto Maximum Sensitivity Substrate (Thermo Scientific)). The chemiluminescent signal peaks at 1 minute after the addition of the substrate mixture and was recorded then. The immunoreactivity signals were normalized by dividing the absolute chemiluminescent readings of the samples by that of PBS control within each independent experiment.

Immunohistochemical (IHC) staining- TBI and wild-type mouse brains were sectioned and immunohistochemcial stained following IHC-paraffin protocol. F9T scFv was used as the primary antibody to incubate with brain sections in 4°C overnight. After thorough rinse 3 times for 5 minutes each with TBS + 0.025 % Triton × 100, the remaining scFv due to the specific binding was detected with 9E10 mouse anti-cmyc antibody, goat anti-mouse antibody conjugated with HRP, which reacts with the substrate DAB, in order to visualize it chromogenically.

5.4 Results and discussion

ScFv selection against small molecule tau- We performed high sensitivity capture ELISA to select the most specific and sensitive scFv against small molecule tau (i.e. monomeric and low MW oligomeric tau) from the pool of scFvs obtained from biopanning, by using them as the detection antibody and comparing their sensitivity. We used F9T scFv as capture antibody, because this scFv previously proved its ability to capture abnormal tau species from tau transgenic mice brain homogenates. We used SHSY5Y-TMHT441 cell lysate and supernatant as two of the target analytes as it contains human tau aggregates detectable by AT8 and F9T(Figure 5.1). SHSY5Y cell lysate and supernatant were used as negative analytes, while PBS was used as negative control and background. Among all scFvs targeting small molecular tau, F3A, 3B5, 4H3 and WX5 display strong reaction with tau species captured by F9T in SHSY5Y-TMHT441 lysate, which was confirmed by detecting 10 times dilution of the lysate returning a significant lower signal (Figure 5.2). These four clones were further confirmed valid detecting antibody when they were used to comparing the pathological oligomeric tau contents in SHSY5Y-TMHT441 and wild type SHSY5Y lysates and supernatant. As the results show, SHSY5Y-TMHT441 lysate

(protein concentration 0.137mg/ml) contains large amount small tau oligomers that can be captured by F9T and recognized by scFv targeting all small tau molecules regardless of its phosphorylation condition, while SHSY5Y-TMHT441 supernatant doesn't despite its high protein contents(1.426mg/ml or 3.215mg/ml) (Figure 5.3). Wild type SHSY5Y doesn't contain such tau oligomers either in lysate (0.137mg/ml) or supernatant (1.426mg/ml) when tested at the equal corresponding protein concentration (Figure 5.3). All four selected clones display the ability of distinguish SHSY5Y-TMHT441 lysate from other three types of analytes, and thus were used in our tests of the existence of abnormal tau oligomers in human tau transgenic mice brain homogenates.

Detection of tau oligomers in mutant human tau transgenic mouse model- In high sensitivity capture ELISA, F9T scFv captured all available tau oligomers it recognized in mutant human tau transgenic mice (Tau406+/TauKO mouse) brain homogenates, therefore the amount of tau oligomers later detectable by F3A scFv-displayed phage reflects the tau oligomers concentration in the brain of this particular mouse. As shown in Figure 5.4, Tau406+/TauKO mouse group of 3-month age displays no significant different signal from its Tau406-/TauKO control mouse group. However, Tau406+/TauKO mouse group of 6-month age shows a significantly higher signal than Tau406-/TauKO control mouse group ($p<0.05$), indicating a positive result for oligomeric tau presence in the Tau406+/TauKO mice. This implies that between 3 months and 6 months of Tau406+/TauKO mice, human mutant tau related oligomerization starts to take place and gets ready to form into other types of pathological tau detectable by F9T and F3A.

Detection of abnormal tau species in TBI rodent models- We performed immunohistochemical staining on hippocampus sections from TBI mice and have shown that oligomeric tau is selectively present in single and repetitive mild TBI mouse hippocampus sections (Figure 5.5) suggesting that oligomeric tau is a promising biomarker for patients suffering from TBI and CTE. We further analyzed F9T's affinity to another TBI rat model determine the time course profile and the various brain parts profile of oligomeric tau following traumatic brain injury. We performed high sensitivity capture ELISA of oligomeric tau targeting scFv capturing potential target in TBI rats' brain homogenates detected by small tau targeting scFv-displayed phage clones. In the test group of F9T scFv as capture antibody and 3B5 phage as detecting antibody, all three brain sections of 7 day after TBI treatment displays a distinct increase in oligomeric tau concentration compared with corresponding section from sham negative control. On the contrary, rats sacrificed 14 day after TBI treatment contains lower oligomeric tau concentration than sham negative control rats in all three corresponding brain sections(Figure 5.6). This trend suggests a process of tau oligomer appearing and aggregating into other forms undetectable by F9T.

5.5 Summary

Tau has been studied as a key factor to AD pathogenesis, for the presence of its hyperphosphorylated aggregated form found in neurofibrillary tangles (NFTs). The research are mainly focused on hyperphosphorylation until recently discoveries point out that tau oligomer are more responsible for neuronal toxicity and tau pathology spreading onto healthy brain sections. Clearance of NFTs can't alleviate the AD progress or reduce neuronal loss. Therefore, a reagent targeting tau oligomers or general small molecules

regardless of its phosphorylation degree is a promising tool for scientists to better understanding of tau oligomeric structure's role in neurotoxicity and AD progression. We previous identified trimeric recombinant human tau (rhTau) is the most extracellular toxic to neuroblastom cells SHSY5Y and to its cholinergic-like differentiated form, comparing with monomeric and dimeric rhTau[24]. Therefore, we took trimeric rhTau as the target to development a scFv specifically recognizes and captures it. Tested with AFM, immunoblotting assays and monoclonal capture ELISA assays, These scFvs (F9T, D11C and H2A) proved to recognize all forms of dimeric, trimeric and small oligomeric tau including those with typical sites phorphorylated tau found in AD pathology from AD-tau transgenic animal and AD human brain tissues. One could tell from Figure 5.1 that F9T scFv and AT8 anti-phosphorylated-tau antibody detect distinct amount but different variants of tau in SHSY5Y-TMHT441 cells that expressing mutant human tau related to AD, while they failed to detect anything in wild type SHSY5Y. The detected tau in two images may have overlap but one would never know unless another small tau antibody is introduced in the test. Therefore, to confirm the abnormal tau species distinguished by trimeric tau scFvs are soluble oligomeric tau not fibrillar tau, we develop another group of scFvs targeting small molecular tau including monomer, dimer and oligomers, with the same biopanning protocol. These small tau scFvs (F3A, 3B5 etc.) are better detecting antibodies in our capture ELISA assays than commercial tau antibodies specific to a certain mutant hyperphosphorylated tau, because they are more specific to the tau monomeric and oligomeric structure instead of phosphorylation. It minimized the possibility that the toxic tau oligomeric captured by tau oligomer scFvs failed to be detected by the commercial antibody because of its lack of phosphorylation.

Such group of tau oligomers happens to be the one that is of most interest, as it is the evidence that pathological tau oligomers are not necessarily phosphorylated and the oligomeric structure of tau variants are of equal if not less critical factor than tau phosphorylated aggregates for AD pathogenesis and progression.

We used the supernatant and cell lysate of both wild type and mutant htau expressing SHSY5Y to screening out anti-small-tau scFvs that can detect anti-trimeric-tau scFv (i.e. F9T) targets, because these two neuronal cells prove to have a comparison of F9T targeted tau's absence and presence. WX5, 3B5, 4H3 and F3A are four anti-small-tau scFvs that can detect tau variants captured by F9T scFv (Figure 5.2) from the lysate of SHSY5Y-TMHT441 which contains highest concentration of F9T's target (Figure 5.3).

In the case of mutant human tau transgenic mice on the base of mouse tau knockout, we discovered that the abnormal tau oligomer level increase significant from 3-month to 6-month in test group age, relative to negative control of each age group (Figure 5.4). We also identified F9T scFv's target in the hippocampus section of single and repetitive mild TBI mice compared with none in that of control mice(Figure 5.5). These TBI mice prove to have chronic neuropathological and neurobehavioral changes [21, 25]. F9T scFv can also differentiate TBI rats as soon as 7 days after TBI treatments compared with negative control of each time frame (Figure5.6). Such rodent models without human tau transgenic suffered from traumatic brain injury (TBI) are good tools of studying tau oligomer's role in TBI progression, although the animal tau is different

from human tau. It implicates tau oligomers as the early form of tau aggregation that possibly propels the aggregation process.

5.6 Acknowledgements

We appreciate the support from Arizona Department of Health Services for the Arizona Department of Health Services for the Arizona Alzheimer's Consortium. We are grateful to Dr. Sarah Stabenfeldt, Arizona State University and Dr. Fiona Crawford Roskamp Institute, Sarasota, FL for the generous gift of TBI rodent models; We would also give thanks to Prof. Paul Fraser from University of Toronto, Canada for Tau406+/TauKO mouse model with negative controls; Dr. Birgit Hutter-Paier group in QPS, Austria for the SHSY5Y neuroblastoma cells stably transfected with human mutant tau. This work was partially supported by the NIH; NIA grant # AG029777.

5.7 Figures and tables

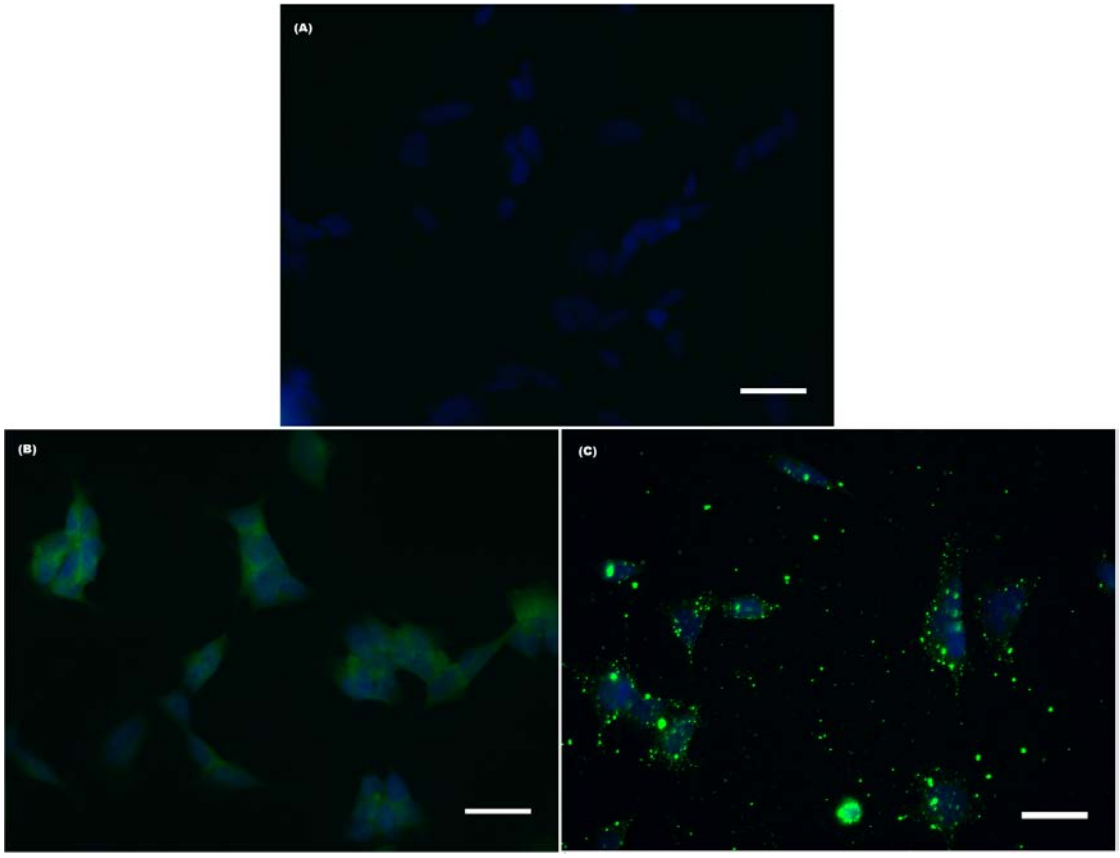

Figure 5.1 F9T and AT8 can identify different forms of tau in SH-SY5Y-TMHT441 neuroblastoma cells using immunofluorescence techniques. The remaining anti-oligomeiric tau antibody F9T was detected by successive coincubation with 9E10 c-Myc antibody produced in mice and Alexa Fluor® 488 Goat Anti-Mouse IgG (H+L) Antibody. AT8 was commercially produced in mouse and was detected directly by Alexa Fluor® 488 Goat Anti-Mouse IgG (H+L) Antibody, which was excited to emit fluorescent light of 515nm to 530nm (green). The neuronal nuclei were counterstained with DAPI (blue). F9T and AT8 displayed no obvious affinity to non-differentiated neuroblastoma SHSY-5Y cells(A), while show strong yet different pattern and intensity of immunoreactivity to SH-SY5Y-TMHT441, which was transfected a stable mutant human gene to expresses hyperphosphorylated tau. Such hyperphosphorylated tau can exist in various forms like monomer, oligomer and mostly in higher degree aggregates, detectable by AT8 (B). On the other hand, F9T was screened and engineered with an enhanced specificity to oligomeric tau. Compared with AT8 staining pattern, F9T detected discreet spots in neuronal culture with higher intensity possibly due to the repetitive epitopes of F9T existing in one molecule of tau oligomer(C).

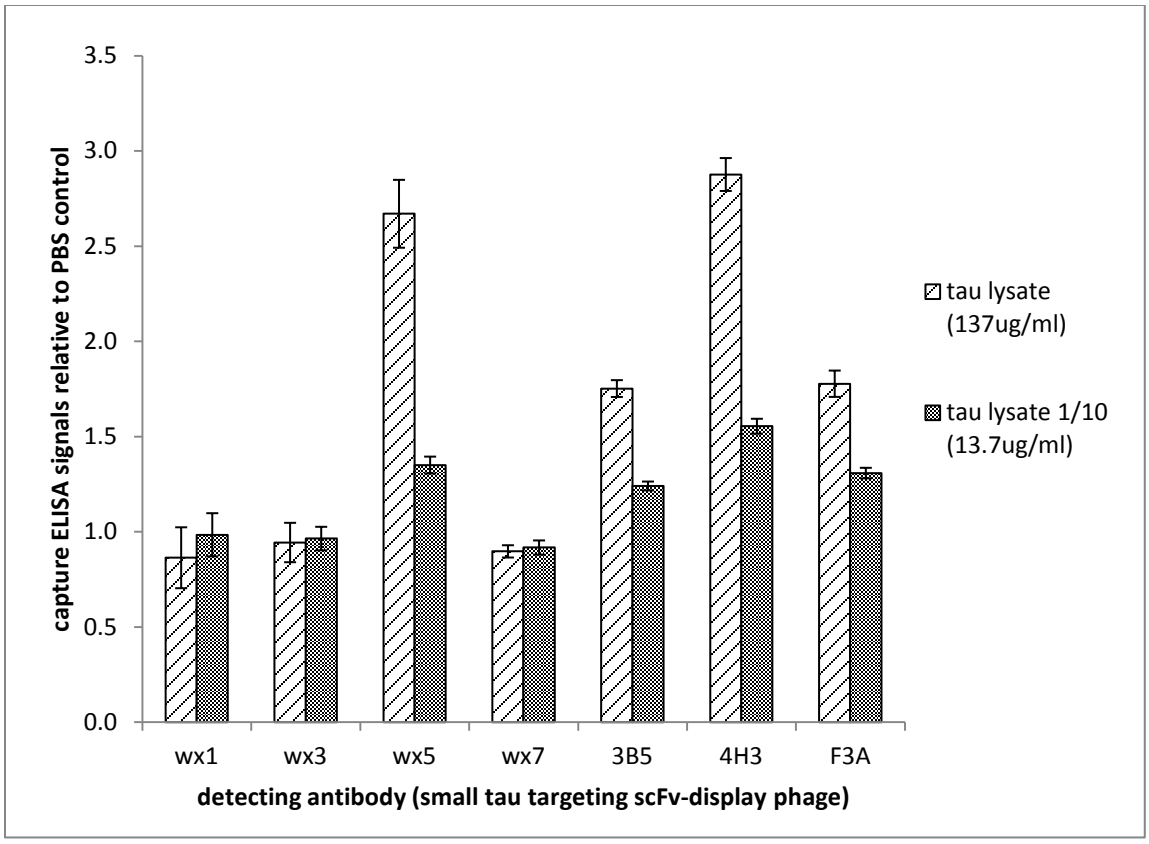

Figure 5.2 small tau targeting scFvs screening using capture ELISA with SHSY5Y-TMHT441 lysate as analyte. This high sensitive capture ELISA test was performed using F9T scFv as capture antibody, SHSY5Y-TMHT441 lysate as analytes and all obtained small tau targeting scFv-displayed phage as detecting antibody. Predicted according to the result in Figure 5.1, some abnormal small molecular tau will be captured by F9T and retain in the wells at the amount proportional to the applied neuron lysate concentration. WX5, 3B5, 4H3 and F3A display a higher signal on original lysate than on 1/10 concentration lysate while others display no distinct difference. Therefore, these four clones are valid detecting antibodies to work with F9T scFv and most favorably D11C scFv in analyzing animal tissues possibly containing pathological oligomeric tau.

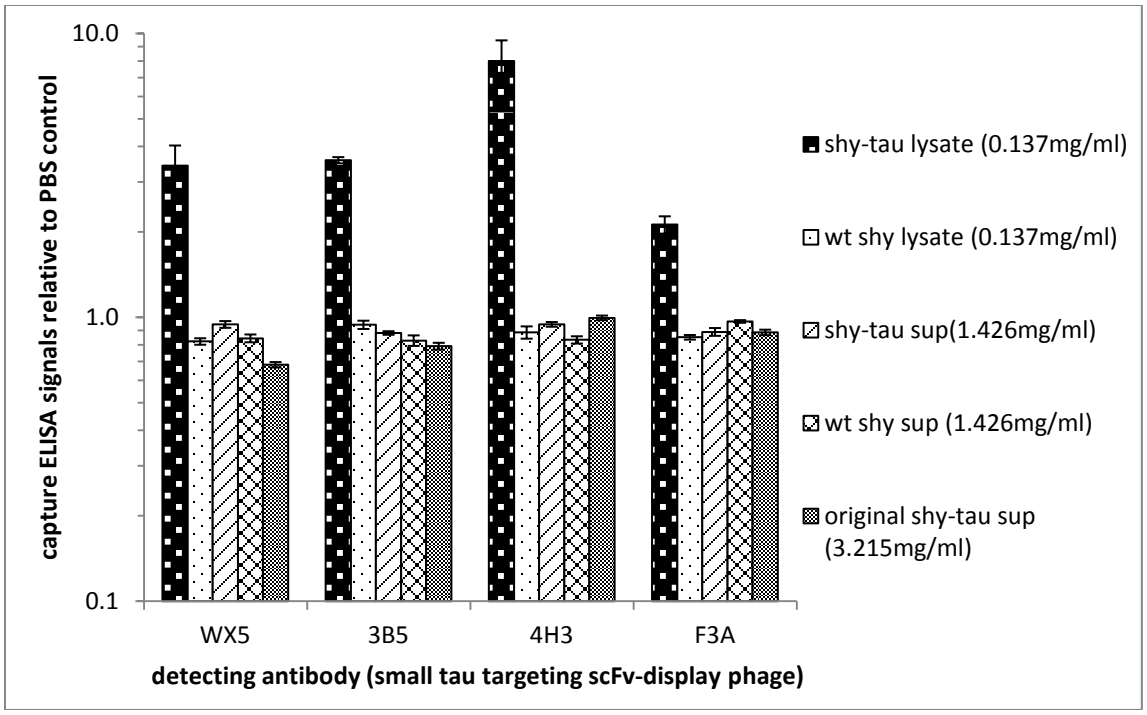

Figure 5.3 Affinity analysis of small tau targeting scFvs to SHSY5Y-TMHT441 and wild-type SHSY5Y lysate portion captured by F9T scFv. We selected 4 potential valid small tau targeting scFvs in the form of display phage to detect the tau species F9T scFv captures from SHSY5Y-TMHT441 lysate (shy-tau lysate), wild type SHSY5Y lysate (wt shy lysate), wild type SHSY5Y supernatant (wt shy sup), SHSY5Y-TMHT441 supernatant (shy-tau sup) and its original high protein supernatant. All four clones display a strong recognition of abnormal tau in SHSY5Y-TMHT441 lysate while they reaction with the other three types of analytes are low, below the PBS negative control.

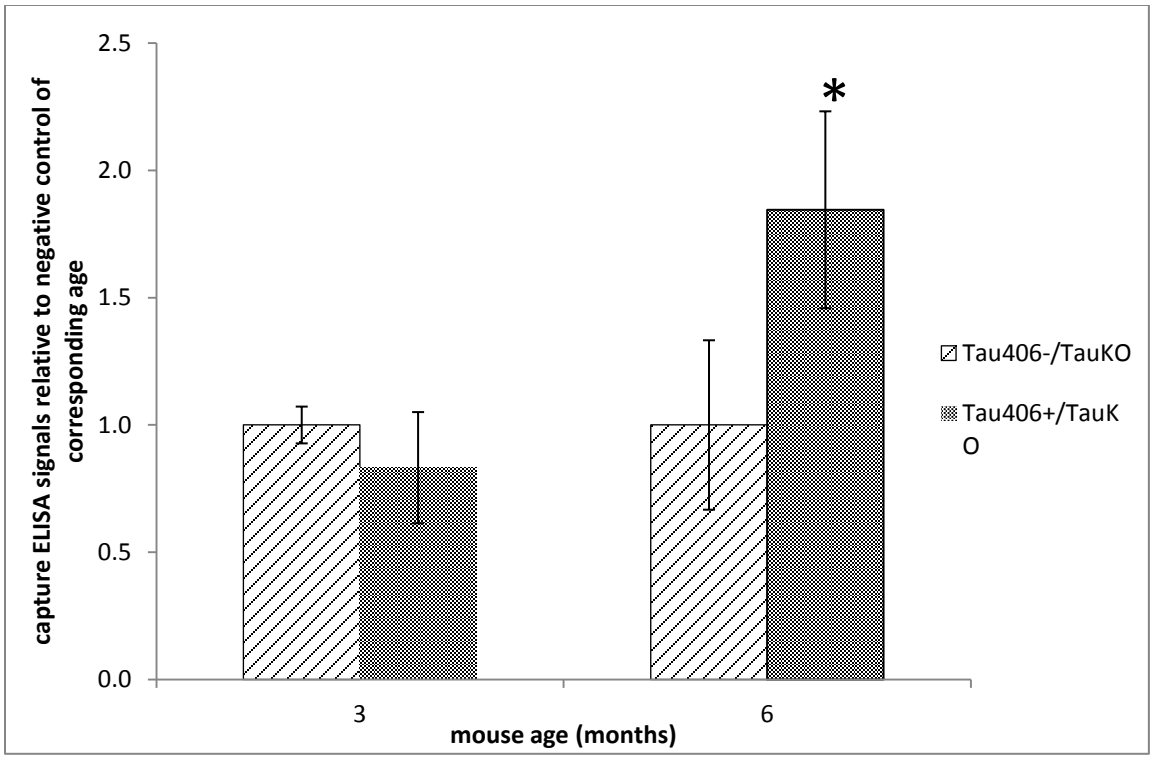

Figure 5.4 Mutant human tau knockin mouse (Tau406+/TauKO) at different ages have a varying oligomeric tau amount compared with negative control(Tau406-/TauKO). The high sensitivity capture ELISA was performed with F9T scFv as capture antibody and F3A phage as detecting antibody to investigate mutant human tau transgenic mouse brain on the correlation of oligomeric tau concentration and mouse age indirectly indicating tau-related AD pathology development. The signals of test group (Tau406+/TauKO) are displayed as the relative value of the signals of negative control group (Tau406+/TauKO) of corresponding ages.

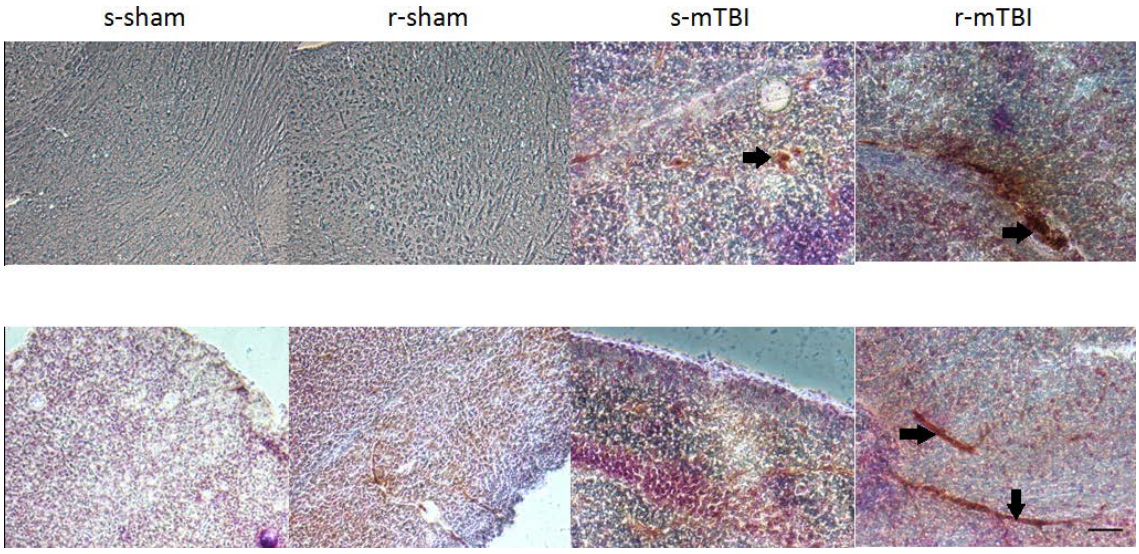

Figure 5.5 F9T scFv detects abnormal tau lesion in hippocampal sections of wild type mice after single or repetitive traumatic brain injuries. Mice are of two independent groups (top and bottom) of which TBI mice brain has strong immunoreativity with F9T scFv compared with the control mice, reacted with 9E10 anti-cmyc IgG produced in mouse, anti-mouse IgG conjugated with HRP, which was chromogenic detected by 3,3'-diaminobenzidine tetrahydrochloride(DAB). (s-single; r-repetitive; sham-anesthesia control; mTBI-mild traumatic brain injury; scale bar=50μm)

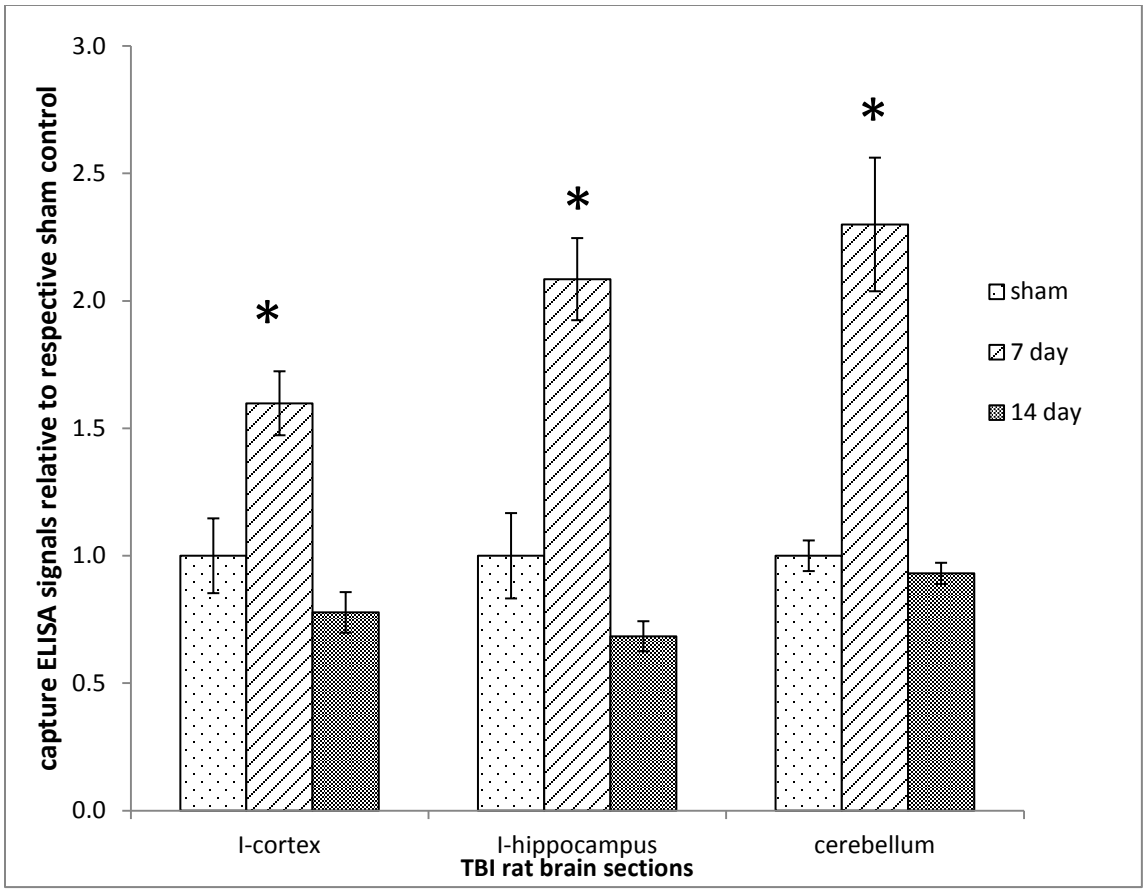

Figure 5.6 Plots of affinity difference of F9T to TBI mice in different brain regions and different time after TBI treatment. The high sensitivity capture ELISA was performed with F9T scFv as capture antibody and 3B5 phage as detecting antibody to investigate TBI mice brain and its abnormal tau concentration with similar structure with human tau oligomers. All signals of test cases are relative to the sham control of sham negative control of each brain sections, which are set as 1.

5.8 References

1. Alzheimer, A., Über eine eigenartige Erkankung der Hirnrinde. Allgemeine Zeitschrift fur Psychiatrie und phychish-Gerichtliche Medizin, (Berlin) 1907(64): p. 146-148.

2. 2012 Alzheimer's disease facts and figures. Alzheimers Dement, 2012. **8**(2): p. 131-68.

3. Alonso, A., et al., Hyperphosphorylation induces self-assembly of tau into tangles of paired helical filaments/straight filaments. Proc Natl Acad Sci U S A, 2001. **98**(12): p. 6923-8.

4. Hanger, D.P., B.H. Anderton, and W. Noble, Tau phosphorylation: the therapeutic challenge for neurodegenerative disease. Trends Mol Med, 2009. **15**(3): p. 112-9.

5. Schneider, A., et al., Phosphorylation that detaches tau protein from microtubules (Ser262, Ser214) also protects it against aggregation into Alzheimer paired helical filaments. Biochemistry, 1999. **38**(12): p. 3549-58.

6. Andorfer, C., et al., Cell-cycle reentry and cell death in transgenic mice expressing nonmutant human tau isoforms. J Neurosci, 2005. **25**(22): p. 5446-54.

7. Brunden, K.R., J.Q. Trojanowski, and V.M. Lee, Evidence that non-fibrillar tau causes pathology linked to neurodegeneration and behavioral impairments. J Alzheimers Dis, 2008. **14**(4): p. 393-9.

8. Polydoro, M., et al., Age-dependent impairment of cognitive and synaptic function in the htau mouse model of tau pathology. J Neurosci, 2009. **29**(34): p. 10741-9.

9. Maeda, S., et al., Granular tau oligomers as intermediates of tau filaments. Biochemistry, 2007. **46**(12): p. 3856-61.

10. Maeda, S., et al., Increased levels of granular tau oligomers: an early sign of brain aging and Alzheimer's disease. Neurosci Res, 2006. **54**(3): p. 197-201.

11. Clavaguera, F., et al., Transmission and spreading of tauopathy in transgenic mouse brain. Nat Cell Biol, 2009. **11**(7): p. 909-13.

12. Liu, L., et al., Trans-synaptic spread of tau pathology in vivo. PLoS One, 2012. **7**(2): p. e31302.

13. de Calignon, A., et al., Propagation of tau pathology in a model of early Alzheimer's disease. Neuron, 2012. **73**(4): p. 685-97.

14. Lasagna-Reeves, C.A., et al., Alzheimer brain-derived tau oligomers propagate pathology from endogenous tau. Sci Rep, 2012. **2**: p. 700.

15. Marx, J., Alzheimer's disease. A new take on tau. Science, 2007. **316**(5830): p. 1416-7.

16. Meraz-Rios, M.A., et al., Tau oligomers and aggregation in Alzheimer's disease. J Neurochem, 2010. **112**(6): p. 1353-67.

17. McKee, A.C., et al., Chronic traumatic encephalopathy in athletes: progressive tauopathy after repetitive head injury. J Neuropathol Exp Neurol, 2009. **68**(7): p. 709-35.

18. Nowinski, C., Head Games: Football's Concussion Crisis From the NFL to Youth Leagues. Drummond Publishing Group, 2006.

19. Geddes, J.F., et al., Neurofibrillary tangles, but not Alzheimer-type pathology, in a young boxer. Neuropathol Appl Neurobiol, 1996. **22**(1): p. 12-6.

20. Tokuda, T., et al., Re-examination of ex-boxers' brains using immunohistochemistry with antibodies to amyloid beta-protein and tau protein. Acta Neuropathol, 1991. **82**(4): p. 280-5.

21. Ojo, J.O., et al., Repetitive Mild Traumatic Brain Injury Augments Tau Pathology and Glial Activation in Aged hTau Mice. J Neuropathol Exp Neurol, 2013. **72**(2): p. 137-51.

22. Emadi, S., et al., Isolation of a human single chain antibody fragment against oligomeric alpha-synuclein that inhibits aggregation and prevents alpha-synuclein-induced toxicity. J Mol Biol, 2007. **368**(4): p. 1132-44.

23. Loffler, T., et al., Stable mutated tau441 transfected SH-SY5Y cells as screening tool for Alzheimer's disease drug candidates. J Mol Neurosci, 2012. **47**(1): p. 192-203.

24. Tian, H., et al., Trimeric tau is toxic to human neuronal cells at low nanomolar concentrations. Int J Cell Biol, 2013. **2013**: p. 260787.

25. Mouzon, B.C., et al., Chronic neuropathological and neurobehavioral changes in a repetitive mild traumatic brain injury model. Ann Neurol, 2014. **75**(2): p. 241-54.

Chapter 6

Proposed future work

6.1 Introduction

The incidence of Alzheimer's disease doubles every five years after the age of 65. By the age of 85, nearly 50% of people still alive have AD. This fact is critically important in the United States since the baby boomers have entered this AD high-risk age range and the total number of AD patients in US will grow rapidly. Therefore, a reliable and convenient diagnostic approach for preclinical AD and mild cognitive impairment (MCI) is in dire need. Antibody fragments such as scFvs that can selectively detect the presence of protein variants associated with AD in patient tissue or fluid samples are a promising tool to facilitate early and accurate diagnoses of AD. scFvs have been developed against a variety of different protein targets involved in neurodegenerative diseases and shown to have diagnostic and therapeutic value. We expect that the tau trimer targeting scFvs isolated in this study will be similarly useful for helping to define the role of soluble aggregated tau in neurodegenerative disease.

The hallmark extracellular senile plaques and intracellular neurofibrillary tangles (NFTs) of AD were first discovered by Dr. Alois Alzheimer more than a century ago and have been the definition of the disease thereafter. Much effort has been made to detect and quantify the presence of these plaques and tangles in brain tissue in vivo. For example, Amyvid, a drug approved by US FDA recently, is a radioactive dye capable of staining amyloid plaques on a PET scan[1]. However, many studies indicate oligomeric amyloid or tau are the more toxic species and are the precursors of the insoluble plaques

and tangles[2-5]. Rather than detecting the plaques and tangles, a more reliable and earlier diagnosis might be facilitated by identifying and quantifying the presence of key oligomeric protein species. Determining the levels of oligomeric tau present in brain tissues including cortex, hippocampus and CSF could be a very useful tool to facilitate early and accurate diagnoses of AD or other dementias.

In addition to AD, tau pathology is present in other neurodegenerative diseases including Parkinson's disease (PD), frontotemporal dementia with Parkinsonism (FTDP-17) and progressive supranulear palsy (PSP). Tau lesions are also a major feature in repetitive closed head injury including chronic traumatic encephalopathy (CTE)[6] that commonly happens to professional athletes engaging in contact sports such as football[7] or boxing[8-9]. A recent study using an aged mouse model expressing human tau suggests that repetitive mild traumatic brain injury can augment tau pathology and glial activation based on the presence of hyperphosphorylated or aggregated tau in mouse brain sections [10]. Since we can selectively detect the presence of oligomeric tau, we would like to determine if oligomeric tau is an early marker of brain injury using a mouse model that undergoes single or repetitive traumatic brain injury. We propose that F9T has the potential of recognizing abnormal tau intermediate forms in brain section and thusly diagnosing tau induced brain damage at its early stage.

As demonstrated in Chapter 3, trimeric tau species of either 2N4R or 1N4R displayed higher toxicity when applied extracellular than tau monomer, dimer and expectedly PBS negative controls. We observed that the rhTau stably transfected SHSY-5Y-TMHT441[11] generally grows slower and displays early apoptosis compared with

its wild-type form SHSY-5Y neurons. These results suggest that tau oligomers may be responsible of propagating tau lesions and impairing the host neuron physiological functions[12-13]. By adding scFvs that selectively target tau oligomers to cultured neuronal cells and measuring the difference of neurotoxicity or viability compared to controls, we can better understand how scFv would affect its targets, i.e. tau oligomers, and tau-induced toxicity.

Although there is no direct evidence of cause-effect relations between AD development with tau polymerization and aggregation, time correlation of tau aggregation with the neurodegeneration process has been observed as that of Aβ. scFv targeting tau oligomers would be of great value if it's tested and proved to bear negative influence on tau oligomer formation or aggregation.

6.2 Material and methods

Preparation of human tau- Tau was purified from the cortex of a 44 year old male with severe Familiar Alzheimer's Disease with tau pathology (AD tau) characterized by numerous argyrophilic neuronal tangles (Bielschowsky staining), and innumerable AT8-labeled neurons present throughout the cerebral cortex including the motor cortex (BA4), and visual cortex (BA17). Tissue was provided by the New York Brain Bank – The Taub Institute, Columbia University. This tissue was prepared as previously described[14][14]with the modification that size fractionation was used in place of the immunoaffinity column for the final purification step. An advantage of this method is that tau phosphorylation is preserved using homogenization buffer containing 1% perchloric

acid. Reductant was used during purification and fractions containing monomeric tau were pooled, concentrated and buffer exchanged into 50 mM Tris-HCl pH 7.4.

Atomic Force microscopy (AFM)- For AFM sample preparation, a 10 µl aliquot of 10 µg/µl Tau protein solution was deposited on a freshly cleaved mica substrate (Spruce Pine, NC), incubated for 5 min at room temperature, rinsed extensively with 0.2 µm filtered deionized water (18.1 MΩ, Millipore, MA), and dried under a gentle stream of N_2 gas. All AFM height images were recorded in tapping mode with scan rates of 2.5 Hz and 512x512 pixels resolution with commercial AFMs in air at room temperature. AFM images for height distribution calculations were acquired using the Nanoscope IIIa AFM (Veeco, Santa Barbara, CA) equipped with oxide sharpened Si_3N_4 AFM tips (k = 40 N/m, f_o ~ 300kHz) (Model: OTESPA, Veeco, Santa Barbara, CA) and analyzed with the Scanning Probe Imaging Processor software (SPIP, Image Metrology) in order to reduce the effect of bowing and tilt mica surface on background, a second-order polynomial flattening was performed.

Height Distribution Analysis- The AFM files of each Tau sample can be analyzed to generate the particle height distribution with Gwyddion. The flattened background of each image was set to zero, and every detected particle on the imaged was categorized according to its size determined by pixels on the AFM image. A statistical analysis of the particle height distribution was also generated by Gwyddion. The particle counts were added up within each height range. The total number of the particles in the image was also calculated, and depends on the image size and sample concentration. Therefore, the

percentage of particles in certain height range taking up of the total number can represent the distribution. It also makes it convenient to compare between different samples.

Cell culture and treatments- SHSY5Y-TMHT441 cells was designed and provided by Dr. Birgit Hutter-Paier group in QPS, Austria. The cells was transfected with stable mutant human tau to express tau phosphorylated at AD-related sites[11]. It was cultivated using a revised protocol based on that of cultivating SHSY5Y human neuroblastoma cell lines (American Tissue Culture Collection)[15]. The culture medium contains 44% v/v Ham's F-12 (IrvineScientific), 44% v/v MEM Earle's salts (IrvineScientific), 10% v/v denatured fetal bovine serum (FBS) (SigmaAldrich), 1% v/v MEM non-essential amino acids (Invitrogen), 1% v/v antibiotic/antimycotic (Invitrogen), and additional 300 μg/mL Geneticin G-418 for first few reviving passages.

Immunocytofluorescent staining- The human neuroblastoma cells SHSY5Y wild-type and human mutant tau transfected type (SHSY5Y-TMHT441) were seeded and cultured in 8-well chamber for 24 h. Cells were washed with PBS buffer and then fixed with 4% PFA. Cells were incubated with polyclonal rabbit antibody against human tau (Catalog: PA1-18272, Thermo-scientific, 1:400), or scFv against tau oligomers (D11C and F9T scFv with tag c-Myc) overnight in 4^{o}C. The rabbit anti-c-myc antibody (Abcam, 1:1500) was followed and then fluorescent goat anti-rabbit IgG were applied for 30 min.

Oligomeric tau toxicity assay- SHSY5Y-TMHT441 is cultivated and plated as described previously[15]. Different concentrations of anti-oligomeric tau and control scFvs will be added to cells. Cell toxicity and viability will be measured using LDH assay[15-17].

scFv effects on extracellular tau induced neurotoxicity- We will determine whether the anti-oligomeric tau scFvs can block spread of toxicity induced by different tau variants. We will add samples containing various tau forms to SH-SY5Y cells with or without added scFv. Sample to be tested will include supernatant and cell lysates from tau overexpressing Sh-SY5Y cells and brain homogenates from AD mouse models and post-mortem human AD and control tissue. Toxicity will be monitored by LDH assay as described[15].

6.3 Preliminary results and future work plan

6.3.1 Preliminary diagnosis of AD using AFM and size distribution

AFM has been long used to investigate material morphological features at molecular level including biomolecules. In our study, it also plays an important role in preliminary diagnosis of AD based on the analysis result of tau aggregation conditions. The healthy control human brain contains normal monomeric tau only that displayed as a single peak at 1.5nm to 2.0nm, while the AD human brain contains monomeric, dimer, trimer and all types of oligomers of different isoforms that displayed as multiple peaks including HC peak as the lowest MW(Figure 6.1A). Due to the different isoforms at different oligomeric level, the molecular weights at the peaks in AD combined curve are hard to interpreted or defined. However, the bright side is that a healthy human brain contains only monomeric tau falls in a small MW range for all isoforms. We can use it as a calibration (Figure 6.1B) to diagnose if the patient is healthy or inclined to develop AD. As this technique matures similar as mass spectrometry did, we can know more about the tau contents and their features in AD.

6.3.2 Detection of tau oligomers in tissue implies early diagnostic potential

We will assay human CSF and serum samples for the presence of oligomeric tau using the anti-oligomeric tau scFvs. Preliminary data generated using AFM to image binding of anti-oligomeric tau scFvs displayed on the surface of a phage particle to post-mortem human CSF samples indicate that we can detect oligomeric tau in CSF samples. Although AFM based F9T phage affinity test assay is a promising tool for detecting the presence of low concentrations of target antigens in human samples, we have developed a sensitive capture ELISA in our lab which facilitates analysis of multiple samples. We will use this capture ELISA to analyze post-mortem human CSF and serum samples.

Another effective way of tau oligomer detection at cellular-level is immunocytofluorescence assay. Tau oligomers were targeted and bound by F9T scFv in SHSY5Y cells transfected with human mutant tau (Figure 6.2). The results showed a negative immunostaining of total tau (A) and Oligomer Tau with clone D11C (B) and clone F9T (C) in SH-SY5Y cells. However, in SHSY5Y-TMHT441, the immunopositive staining were observed with total tau (D) and oligomeric tau aggregates (arrows in E and F, clone D11C and F9T, respectively).

We have also shown in Chapter 5 that oligomeric tau is selectively present in single and repetitive mild TBI mouse hippocampus sections using immunohistochemcal staining suggesting that oligomeric tau is a promising biomarker for patients suffering from TBI and CTE. F9T also target a much younger sacrificed TBI rats from negative controls. We will analyze various different brain samples from mice that have suffered TBI to determine the time course profile of oligomeric tau following traumatic brain

injury. We will also assay CSF samples taken from patients suffering TBI in collaboration with Dr. Leslie Baxter and Dr. Nicholas Theodore (Barrow Neurological Institute).

6.3.3 Therapeutic potential of anti-oligomeric tau scFvs

The anti-oligomeric tau scFv, F9T, shows strong immunoreactivity with the tau expressing neuron model SHSY-5Y-TMHT441 but essentially no reaction with wild-type SHSY-5Y(Figure 6. 2 (A) versus (C)). The monoclonal antibody AT8 which binds phosphorylated aggregates of tau also preferentially stains SHSY-5Y-TMHT441 cells (Figure 6. 2 (B)), although with a different pattern than that observed with F9T. We hypothesize that scFv targeting tau oligomers can ameliorate neurotoxicity induced by either extracellular or endogenous aggregates of tau. We will determine whether the anti-oligomeric tau scFvs can block tau induced toxicity by adding cell supernatant and lysate samples from the tau overexpressing SHSY-5Y-TMHT441 cells to healthy SHSY-5Y cells. We will add different concentrations of anti-oligomeric tau scFv to the samples to determine how efficiently the scFvs can block tau induced toxicity. We will perform similar studies with brain homogenates from different AD mouse models and from post-mortem human AD tissue to determine whether the scFvs can block spread of tau toxicity from brain samples as well.

These studies should demonstrate whether the anti-oligomeric tau scFvs isolated here have potential diagnostic and therapeutic value for neurodegenerative diseases including AD, TBI and other tauopathies.

6.4 Figures and tables

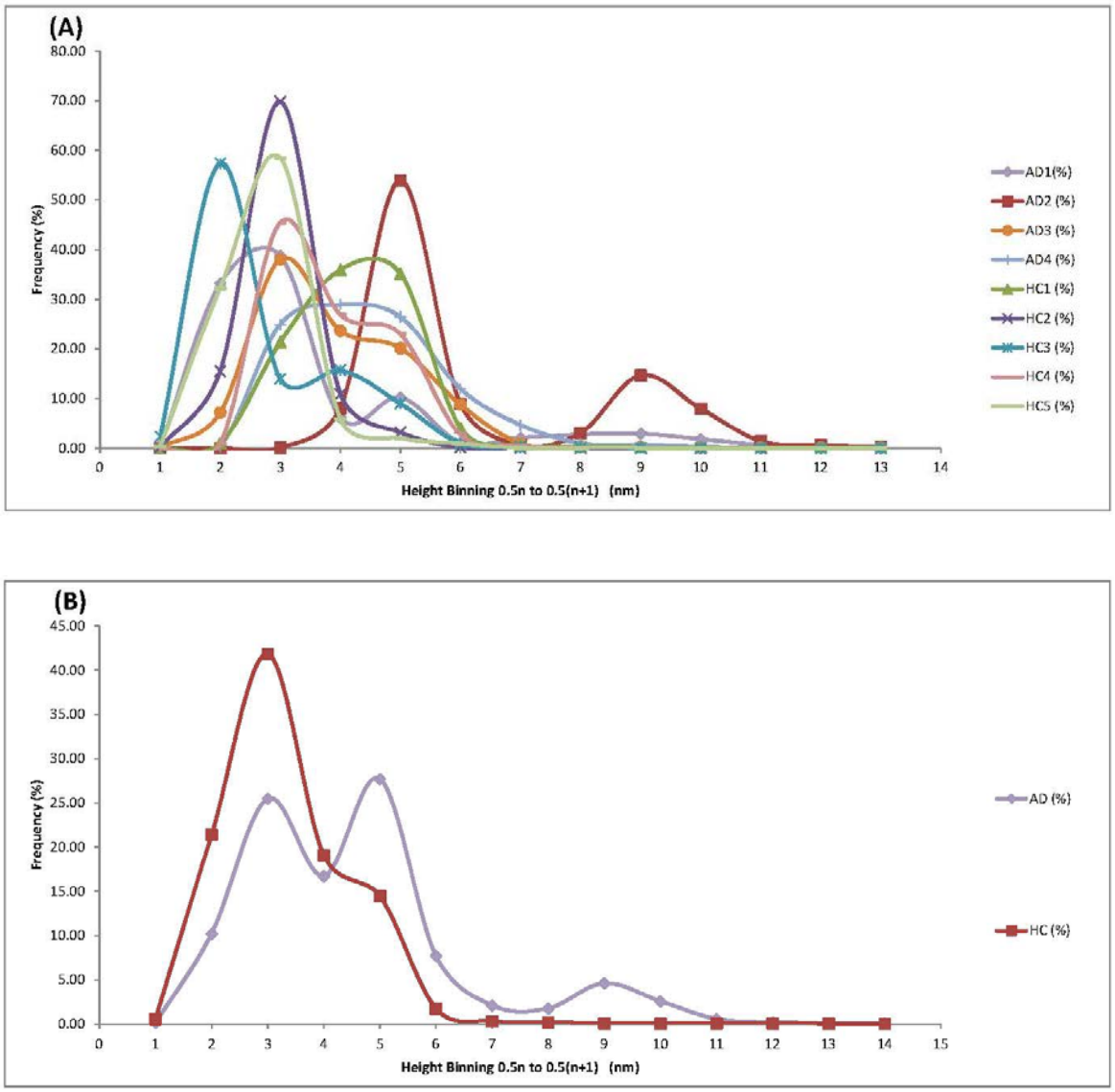

Figure 6. 1 Human brain derived tau analyzed by AFM on the particle size distribution. (A) Size distribution results of four Alzheimer's (AD) patients and five healthy control (HC) human cases separately; (B) Size distribution results of combined AD and HC human groups. The HC human brain contains normal monomeric tau only that displayed as a single peak at 1.5nm to 2.0nm, while the AD human brain contains monomeric, dimer, trimer and all types of oligomers of different isoforms that displayed as multiple peaks including HC peak as the lowest MW.

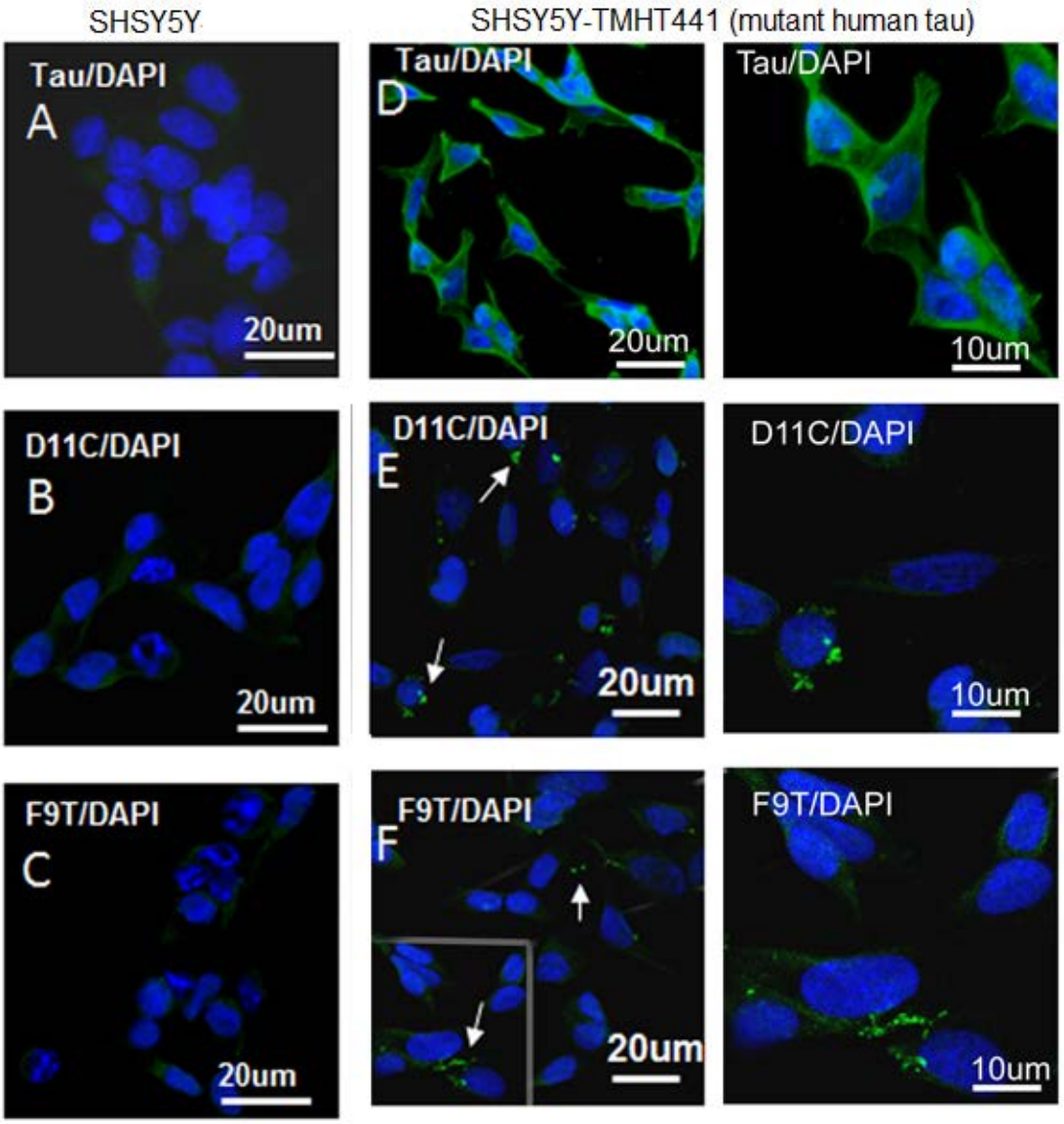

Figure 6. 2 Tau oligomers observed by F9T and D11C scFv in SHSY5Y-TMHT441 expressing mutant human tau. SHSY5Y(A,B,C) and SHSY5Y-TMHT441(D,E,F) were seeded and cultured in 8-well chamber for 24 h. Cells were washed with PBS buffer and then fixed with 4% PFA. Cells were incubated with polyclonal rabbit antibody against human tau (Catalog: PA1-18272, Thermo-scientific, 1:400) targeting all tau (A and D), or scFv against tau oligomers overnight in 4^{o}C.These tau oligomer targeting scFv are tagged with c-myc and named as D11C (B and E) and F9T (C and F). The rabbit anti-c-myc antibody (Abcam, 1:1500) was followed and then fluorescent goat anti-rabbit IgG were applied for 30 min. Goat anti-rabbit IgG was commercially produced in mouse and was detected directly by Alexa Fluor® 488 Goat Anti-Mouse IgG (H+L) Antibody, which was excited to emit fluorescent light of 515nm to 530nm (green). The neuronal nuclei were counterstained with DAPI (blue). This figure showed a negative immunostaining of total tau (A) and oligomer tau with clone D11C (B) and clone F9T (C) in SHSY5Y cells. However, in SHSY5Y-TMHT441 expressing human mutant tau, the positive immunostaining were observed with total Tau (D) and oligomer tau aggregates (arrows in E and F, clone D11C and F9T, respectively).

6.5 References

1. Furst, A.J. and G.A. Kerchner, From Alois to Amyvid: seeing Alzheimer disease. Neurology, 2012. **79**(16): p. 1628-9.

2. Glabe, C.G., Common mechanisms of amyloid oligomer pathogenesis in degenerative disease. Neurobiol Aging, 2006. **27**(4): p. 570-5.

3. Kayed, R., et al., Common structure of soluble amyloid oligomers implies common mechanism of pathogenesis. Science, 2003. **300**(5618): p. 486-9.

4. Oddo, S., et al., Temporal profile of amyloid-beta (Abeta) oligomerization in an in vivo model of Alzheimer disease. A link between Abeta and tau pathology. J Biol Chem, 2006. **281**(3): p. 1599-604.

5. Ferreira, S.T., M.N. Vieira, and F.G. De Felice, Soluble protein oligomers as emerging toxins in Alzheimer's and other amyloid diseases. IUBMB Life, 2007. **59**(4-5): p. 332-45.

6. McKee, A.C., et al., Chronic traumatic encephalopathy in athletes: progressive tauopathy after repetitive head injury. J Neuropathol Exp Neurol, 2009. **68**(7): p. 709-35.

7. Nowinski, C., Head Games: Football's Concussion Crisis From the NFL to Youth Leagues. Drummond Publishing Group, 2006.

8. Geddes, J.F., et al., Neurofibrillary tangles, but not Alzheimer-type pathology, in a young boxer. Neuropathol Appl Neurobiol, 1996. **22**(1): p. 12-6.

9. Tokuda, T., et al., Re-examination of ex-boxers' brains using immunohistochemistry with antibodies to amyloid beta-protein and tau protein. Acta Neuropathol, 1991. **82**(4): p. 280-5.

10. Ojo, J.O., et al., Repetitive Mild Traumatic Brain Injury Augments Tau Pathology and Glial Activation in Aged hTau Mice. J Neuropathol Exp Neurol, 2013. **72**(2): p. 137-51.

11. Loffler, T., et al., Stable mutated tau441 transfected SH-SY5Y cells as screening tool for Alzheimer's disease drug candidates. J Mol Neurosci, 2012. **47**(1): p. 192-203.

12. Lasagna-Reeves, C.A., et al., Alzheimer brain-derived tau oligomers propagate pathology from endogenous tau. Sci Rep, 2012. **2**: p. 700.

13. Wu, J.W., et al., Small Misfolded Tau Species Are Internalized via Bulk Endocytosis and Anterogradely and Retrogradely Transported in Neurons. J Biol Chem, 2013. **288**(3): p. 1856-70.

14. Ivanovova, N., et al., High-yield purification of fetal tau preserving its structure and phosphorylation pattern. J Immunol Methods, 2008. **339**(1): p. 17-22.

15. Tian, H., et al., Trimeric tau is toxic to human neuronal cells at low nanomolar concentrations. Int J Cell Biol, 2013. **2013**: p. 260787.

16. Zameer, A., et al., Single chain Fv antibodies against the 25-35 Abeta fragment inhibit aggregation and toxicity of Abeta42. Biochemistry, 2006. **45**(38): p. 11532-9.

17. Decker, T. and M.L. Lohmann-Matthes, A quick and simple method for the quantitation of lactate dehydrogenase release in measurements of cellular cytotoxicity and tumor necrosis factor (TNF) activity. J Immunol Methods, 1988. **115**(1): p. 61-9.

REFERENCES

1. 2012 Alzheimer's disease facts and figures. Alzheimers Dement, 2012. 8(2): p. 131-68.

2. Goedert, M., et al., Tau proteins of Alzheimer paired helical filaments: abnormal phosphorylation of all six brain isoforms. Neuron, 1992. 8(1): p. 159-68.

3. Spillantini, M.G., et al., Topographical relationship between beta-amyloid and tau protein epitopes in tangle-bearing cells in Alzheimer disease. Proc Natl Acad Sci U S A, 1990. 87(10): p. 3952-6.

4. Hardy, J. and D.J. Selkoe, The amyloid hypothesis of Alzheimer's disease: progress and problems on the road to therapeutics. Science, 2002. 297(5580): p. 353-6.

5. Mandelkow, E.M. and E. Mandelkow, Tau in Alzheimer's disease. Trends Cell Biol, 1998. 8(11): p. 425-7.

6. Emadi, S., et al., Isolation of a human single chain antibody fragment against oligomeric alpha-synuclein that inhibits aggregation and prevents alpha-synuclein-induced toxicity. J Mol Biol, 2007. 368(4): p. 1132-44.

7. Liu, R., et al., Single chain variable fragments against beta-amyloid (Abeta) can inhibit Abeta aggregation and prevent abeta-induced neurotoxicity. Biochemistry, 2004. 43(22): p. 6959-67.

8. Zameer, A., et al., Single Chain Fv Antibodies against the 25-35 Abeta Fragment Inhibit Aggregation and Toxicity of Abeta42. Biochemistry, 2006. 45(38): p. 11532-9.

9. Sheets, M.D., et al., Efficient construction of a large nonimmune phage antibody library: the production of high-affinity human single-chain antibodies to protein antigens. Proc Natl Acad Sci U S A, 1998. 95(11): p. 6157-62.

10. Check, E., Nerve inflammation halts trial for Alzheimer's drug. Nature, 2002. 415(6871): p. 462.

11. Pardridge, W.M., Alzheimer's disease drug development and the problem of the blood-brain barrier. Alzheimers Dement, 2009. 5(5): p. 427-32.

12. Pardridge, W.M. and R.J. Boado, Pharmacokinetics and safety in rhesus monkeys of a monoclonal antibody-GDNF fusion protein for targeted blood-brain barrier delivery. Pharm Res, 2009. 26(10): p. 2227-36.

13. Frisoni, G.B., et al., The clinical use of structural MRI in Alzheimer disease. Nat Rev Neurol, 2010. 6(2): p. 67-77.

14. Putcha, D., et al., Hippocampal hyperactivation associated with cortical thinning in Alzheimer's disease signature regions in non-demented elderly adults. J Neurosci, 2011. 31(48): p. 17680-8.

15. Marchetti, C. and H. Marie, Hippocampal synaptic plasticity in Alzheimer's disease: what have we learned so far from transgenic models? Rev Neurosci, 2011. 22(4): p. 373-402.

16. Palop, J.J. and L. Mucke, Amyloid-beta-induced neuronal dysfunction in Alzheimer's disease: from synapses toward neural networks. Nat Neurosci, 2010. 13(7): p. 812-8.

17. Cummings, J.L., Alzheimer's disease. N Engl J Med, 2004. 351(1): p. 56-67.

18. Tanzi, R.E. and L. Bertram, Twenty years of the Alzheimer's disease amyloid hypothesis: a genetic perspective. Cell, 2005. 120(4): p. 545-55.

19. Selkoe, D.J., Alzheimer's disease: genotypes, phenotypes, and treatments. Science, 1997. 275(5300): p. 630-1.

20. Kamboh, M.I., Molecular genetics of late-onset Alzheimer's disease. Ann Hum Genet, 2004. 68(Pt 4): p. 381-404.

21. Huang, Y. and L. Mucke, Alzheimer mechanisms and therapeutic strategies. Cell, 2012. 148(6): p. 1204-22.

22. Ward, S.M., et al., Tau oligomers and tau toxicity in neurodegenerative disease. Biochem Soc Trans, 2012. 40(4): p. 667-71.

23. Haass, C. and D.J. Selkoe, Soluble protein oligomers in neurodegeneration: lessons from the Alzheimer's amyloid beta-peptide. Nat Rev Mol Cell Biol, 2007. 8(2): p. 101-12.

24. Weingarten, M.D., et al., A protein factor essential for microtubule assembly. Proc Natl Acad Sci U S A, 1975. 72(5): p. 1858-62.

25. Witman, G.B., et al., Tubulin requires tau for growth onto microtubule initiating sites. Proc Natl Acad Sci U S A, 1976. 73(11): p. 4070-4.

26. Morris, M., et al., The many faces of tau. Neuron, 2011. 70(3): p. 410-26.

27. Lee, V.M., M. Goedert, and J.Q. Trojanowski, Neurodegenerative tauopathies. Annu Rev Neurosci, 2001. 24: p. 1121-59.

28. Takei, Y., et al., Defects in axonal elongation and neuronal migration in mice with disrupted tau and map1b genes. J Cell Biol, 2000. 150(5): p. 989-1000.

29. Neve, R.L., et al., Identification of cDNA clones for the human microtubule-associated protein tau and chromosomal localization of the genes for tau and microtubule-associated protein 2. Brain Res, 1986. 387(3): p. 271-80.

30. Alonso Adel, C., et al., Promotion of hyperphosphorylation by frontotemporal dementia tau mutations. J Biol Chem, 2004. 279(33): p. 34873-81.

31. Khatoon, S., I. Grundke-Iqbal, and K. Iqbal, Brain levels of microtubule-associated protein tau are elevated in Alzheimer's disease: a radioimmuno-slot-blot assay for nanograms of the protein. J Neurochem, 1992. 59(2): p. 750-3.

32. Khatoon, S., I. Grundke-Iqbal, and K. Iqbal, Levels of normal and abnormally phosphorylated tau in different cellular and regional compartments of Alzheimer disease and control brains. FEBS Lett, 1994. 351(1): p. 80-4.

33. Augustinack, J.C., et al., Specific tau phosphorylation sites correlate with severity of neuronal cytopathology in Alzheimer's disease. Acta Neuropathol, 2002. 103(1): p. 26-35.

34. Peineau, S., et al., LTP inhibits LTD in the hippocampus via regulation of GSK3beta. Neuron, 2007. 53(5): p. 703-17.

35. Kimura, T., et al., GSK-3beta is required for memory reconsolidation in adult brain. PLoS One, 2008. 3(10): p. e3540.

36. Masuda, M., et al., Small molecule inhibitors of alpha-synuclein filament assembly. Biochemistry, 2006. 45(19): p. 6085-94.

37. Taniguchi, S., et al., Inhibition of heparin-induced tau filament formation by phenothiazines, polyphenols, and porphyrins. J Biol Chem, 2005. 280(9): p. 7614-23.

38. Lasagna-Reeves, C.A., et al., Alzheimer brain-derived tau oligomers propagate pathology from endogenous tau. Sci Rep, 2012. 2: p. 700.

39. Lasagna-Reeves, C.A., et al., Identification of oligomers at early stages of tau aggregation in Alzheimer's disease. FASEB J, 2012. 26(5): p. 1946-59.

40. Clark, M., Antibody humanization: a case of the 'Emperor's new clothes'? Immunol Today, 2000. 21(8): p. 397-402.

41. Arafat, W.O., et al., Effective single chain antibody (scFv) concentrations in vivo via adenoviral vector mediated expression of secretory scFv. Gene Ther, 2002. 9(4): p. 256-62.

42. Kipriyanov, S.M., G. Moldenhauer, and M. Little, High level production of soluble single chain antibodies in small-scale Escherichia coli cultures. J Immunol Methods, 1997. 200(1-2): p. 69-77.

43. Boado, R.J., et al., IgG-single chain Fv fusion protein therapeutic for Alzheimer's disease: Expression in CHO cells and pharmacokinetics and brain delivery in the rhesus monkey. Biotechnol Bioeng, 2010. 105(3): p. 627-35.

44. Kim, D.J., et al., Production and characterisation of a recombinant scFv reactive with human gastrointestinal carcinomas. Br J Cancer, 2002. 87(4): p. 405-13.

45. Kasturirangan, S., D. Brune, and M. Sierks, Promoting alpha-secretase cleavage of beta-amyloid with engineered proteolytic antibody fragments. Biotechnol Prog, 2009. 25(4): p. 1054-63.

46. Dickson, D.W., The pathogenesis of senile plaques. J Neuropathol Exp Neurol, 1997. 56(4): p. 321-39.

47. Varvel, N.H., et al., Abeta oligomers induce neuronal cell cycle events in Alzheimer's disease. J Neurosci, 2008. 28(43): p. 10786-93.

48. Hardy, J.A. and G.A. Higgins, Alzheimer's disease: the amyloid cascade hypothesis. Science, 1992. 256(5054): p. 184-5.

49. Braak, H. and E. Braak, Neuropathological stageing of Alzheimer-related changes. Acta Neuropathol, 1991. 82(4): p. 239-59.

50. Braak, H. and E. Braak, Demonstration of amyloid deposits and neurofibrillary changes in whole brain sections. Brain Pathol, 1991. 1(3): p. 213-6.

51. Braak, H. and E. Braak, Evolution of the neuropathology of Alzheimer's disease. Acta Neurol Scand Suppl, 1996. 165: p. 3-12.

52. Alafuzoff, I., et al., Staging of neurofibrillary pathology in Alzheimer's disease: a study of the BrainNet Europe Consortium. Brain Pathol, 2008. 18(4): p. 484-96.

53. von Bergen, M., et al., Tau aggregation is driven by a transition from random coil to beta sheet structure. Biochim Biophys Acta, 2005. 1739(2-3): p. 158-66.

54. Kasturirangan, S., et al., Isolation and characterization of antibody fragmentsselective for specific protein morphologies from nanogram antigensamples. Biotechnol Prog, 2013.

55. Kasturirangan, S., S. Boddapati, and M.R. Sierks, Engineered proteolytic nanobodies reduce Abeta burden and ameliorate Abeta-induced cytotoxicity. Biochemistry, 2010. 49(21): p. 4501-8.

56. Boddapati, S., Y. Levites, and M.R. Sierks, Inhibiting beta-secretase activity in Alzheimer's disease cell models with single-chain antibodies specifically targeting APP. J Mol Biol, 2011. 405(2): p. 436-47.

57. Emadi, S., et al., Detecting morphologically distinct oligomeric forms of alpha-synuclein. J Biol Chem, 2009. 284(17): p. 11048-58.

58. Barkhordarian, H., et al., Isolating recombinant antibodies against specific protein morphologies using atomic force microscopy and phage display technologies. Protein Eng Des Sel, 2006. 19(11): p. 497-502.

59. Kohler, G. and C. Milstein, Continuous cultures of fused cells secreting antibody of predefined specificity. Nature, 1975. 256(5517): p. 495-7.

60. Glennie, M.J. and P.W. Johnson, Clinical trials of antibody therapy. Immunol Today, 2000. 21(8): p. 403-10.

61. Marks, J.D., et al., By-passing immunization. Human antibodies from V-gene libraries displayed on phage. J Mol Biol, 1991. 222(3): p. 581-97.

62. Lee, C.M., et al., Selection of human antibody fragments by phage display. Nat Protoc, 2007. 2(11): p. 3001-8.

63. Alzheimer, A., Über eine eigenartige Erkankung der Hirnrinde. Allgemeine Zeitschrift fur Psychiatrie und phychish-Gerichtliche Medizin, (Berlin) 1907(64): p. 146-148.

64. Hardy, J. and D.J. Selkoe, The amyloid hypothesis of Alzheimer's disease: progress and problems on the road to therapeutics. Science, 2002. 297(5580): p. 353-6.

65. Gilman, S., et al., Clinical effects of Abeta immunization (AN1792) in patients with AD in an interrupted trial. Neurology, 2005. 64(9): p. 1553-62.

66. Blennow, K., et al., Effect of immunotherapy with bapineuzumab on cerebrospinal fluid biomarker levels in patients with mild to moderate Alzheimer disease. Arch Neurol, 2012. 69(8): p. 1002-10.

67. Freeman, G.B., et al., 39-week toxicity and toxicokinetic study of ponezumab (PF-04360365) in cynomolgus monkeys with 12-week recovery period. J Alzheimers Dis, 2012. 28(3): p. 531-41.

68. Check, E., Nerve inflammation halts trial for Alzheimer's drug. Nature, 2002. 415(6871): p. 462.

69. Braak, H. and K. Del Tredici, The pathological process underlying Alzheimer's disease in individuals under thirty. Acta Neuropathol, 2011. 121(2): p. 171-81.

70. Braak, H. and E. Braak, Frequency of stages of Alzheimer-related lesions in different age categories. Neurobiol Aging, 1997. 18(4): p. 351-7.

71. Oddo, S., et al., Reduction of soluble Abeta and tau, but not soluble Abeta alone, ameliorates cognitive decline in transgenic mice with plaques and tangles. J Biol Chem, 2006. 281(51): p. 39413-23.

72. Amos, L.A., Microtubule structure and its stabilisation. Org Biomol Chem, 2004. 2(15): p. 2153-60.

73. von Bergen, M., et al., Assembly of tau protein into Alzheimer paired helical filaments depends on a local sequence motif ((306)VQIVYK(311)) forming beta structure. Proc Natl Acad Sci U S A, 2000. 97(10): p. 5129-34.

74. Thies, E. and E.M. Mandelkow, Missorting of tau in neurons causes degeneration of synapses that can be rescued by the kinase MARK2/Par-1. J Neurosci, 2007. 27(11): p. 2896-907.

75. Diaz-Hernandez, M., et al., Tissue-nonspecific alkaline phosphatase promotes the neurotoxicity effect of extracellular tau. J Biol Chem, 2010. 285(42): p. 32539-48.

76. Pooler, A.M., et al., Physiological release of endogenous tau is stimulated by neuronal activity. EMBO Rep, 2013. 14(4): p. 389-94.

77. Lasagna-Reeves, C.A., et al., Tau oligomers impair memory and induce synaptic and mitochondrial dysfunction in wild-type mice. Mol Neurodegener, 2011. 6: p. 39.

78. Guillozet, A.L., et al., Neurofibrillary tangles, amyloid, and memory in aging and mild cognitive impairment. Arch Neurol, 2003. 60(5): p. 729-36.

79. Kayed, R., et al., Common structure of soluble amyloid oligomers implies common mechanism of pathogenesis. Science, 2003. 300(5618): p. 486-9.

80. Morsch, R., W. Simon, and P.D. Coleman, Neurons may live for decades with neurofibrillary tangles. J Neuropathol Exp Neurol, 1999. 58(2): p. 188-97.

81. Kordower, J.H., et al., Loss and atrophy of layer II entorhinal cortex neurons in elderly people with mild cognitive impairment. Ann Neurol, 2001. 49(2): p. 202-13.

82. Brunden, K.R., J.Q. Trojanowski, and V.M. Lee, Evidence that non-fibrillar tau causes pathology linked to neurodegeneration and behavioral impairments. J Alzheimers Dis, 2008. 14(4): p. 393-9.

83. Santacruz, K., et al., Tau suppression in a neurodegenerative mouse model improves memory function. Science, 2005. 309(5733): p. 476-81.

84. Andorfer, C., et al., Hyperphosphorylation and aggregation of tau in mice expressing normal human tau isoforms. J Neurochem, 2003. 86(3): p. 582-90.

85. Leroy, K., et al., Early axonopathy preceding neurofibrillary tangles in mutant tau transgenic mice. Am J Pathol, 2007. 171(3): p. 976-92.

86. Spires, T.L., et al., Region-specific dissociation of neuronal loss and neurofibrillary pathology in a mouse model of tauopathy. Am J Pathol, 2006. 168(5): p. 1598-607.

87. Yoshiyama, Y., et al., Synapse loss and microglial activation precede tangles in a P301S tauopathy mouse model. Neuron, 2007. 53(3): p. 337-51.

88. Berger, Z., et al., Accumulation of pathological tau species and memory loss in a conditional model of tauopathy. J Neurosci, 2007. 27(14): p. 3650-62.

89. Maeda, S., et al., Increased levels of granular tau oligomers: an early sign of brain aging and Alzheimer's disease. Neurosci Res, 2006. 54(3): p. 197-201.

90. Sahara, N., S. Maeda, and A. Takashima, Tau oligomerization: a role for tau aggregation intermediates linked to neurodegeneration. Curr Alzheimer Res, 2008. 5(6): p. 591-8.

91. Genius, J., et al., Current application of neurochemical biomarkers in the prediction and differential diagnosis of Alzheimer's disease and other neurodegenerative dementias. Eur Arch Psychiatry Clin Neurosci, 2012. 262 Suppl 2: p. S71-7.

92. Zameer, A., et al., Anti-oligomeric Abeta single-chain variable domain antibody blocks Abeta-induced toxicity against human neuroblastoma cells. J Mol Biol, 2008. 384(4): p. 917-28.

93. Wang, M.S., et al., Characterizing antibody specificity to different protein morphologies by AFM. Langmuir, 2009. 25(2): p. 912-8.

94. Pahlman, S., et al., Differentiation and survival influences of growth factors in human neuroblastoma. Eur J Cancer, 1995. 31A(4): p. 453-8.

95. Encinas, M., et al., Sequential treatment of SH-SY5Y cells with retinoic acid and brain-derived neurotrophic factor gives rise to fully differentiated, neurotrophic factor-dependent, human neuron-like cells. J Neurochem, 2000. 75(3): p. 991-1003.

96. Presgraves, S.P., et al., Terminally differentiated SH-SY5Y cells provide a model system for studying neuroprotective effects of dopamine agonists. Neurotox Res, 2004. 5(8): p. 579-98.

97. Decker, T. and M.L. Lohmann-Matthes, A quick and simple method for the quantitation of lactate dehydrogenase release in measurements of cellular cytotoxicity and tumor necrosis factor (TNF) activity. J Immunol Methods, 1988. 115(1): p. 61-9.

98. Ferreira, S.T., M.N. Vieira, and F.G. De Felice, Soluble protein oligomers as emerging toxins in Alzheimer's and other amyloid diseases. IUBMB Life, 2007. 59(4-5): p. 332-45.

99. Sierks, M.R., et al., CSF levels of oligomeric alpha-synuclein and beta-amyloid as biomarkers for neurodegenerative disease. Integr Biol (Camb), 2011. 3(12): p. 1188-96.

100. Andorfer, C., et al., Cell-cycle reentry and cell death in transgenic mice expressing nonmutant human tau isoforms. J Neurosci, 2005. 25(22): p. 5446-54.

101. Belarbi, K., et al., Early Tau pathology involving the septo-hippocampal pathway in a Tau transgenic model: relevance to Alzheimer's disease. Curr Alzheimer Res, 2009. 6(2): p. 152-7.

102. Braak, H., et al., Vulnerability of cortical neurons to Alzheimer's and Parkinson's diseases. J Alzheimers Dis, 2006. 9(3 Suppl): p. 35-44.

103. Schliebs, R. and T. Arendt, The cholinergic system in aging and neuronal degeneration. Behav Brain Res, 2011. 221(2): p. 555-63.

104. Wu, J.W., et al., Small Misfolded Tau Species Are Internalized via Bulk Endocytosis and Anterogradely and Retrogradely Transported in Neurons. J Biol Chem, 2013. 288(3): p. 1856-70.

105. Glabe, C.G., Common mechanisms of amyloid oligomer pathogenesis in degenerative disease. Neurobiol Aging, 2006. 27(4): p. 570-5.

106. Lambert, M.P., et al., Diffusible, nonfibrillar ligands derived from Abeta1-42 are potent central nervous system neurotoxins. Proc Natl Acad Sci U S A, 1998. 95(11): p. 6448-53.

107. Gestwicki, J.E., G.R. Crabtree, and I.A. Graef, Harnessing chaperones to generate small-molecule inhibitors of amyloid beta aggregation. Science, 2004. 306(5697): p. 865-9.

108. Hirohata, M., et al., The anti-amyloidogenic effect is exerted against Alzheimer's beta-amyloid fibrils in vitro by preferential and reversible binding of flavonoids to the amyloid fibril structure. Biochemistry, 2007. 46(7): p. 1888-99.

109. Ono, K., H. Naiki, and M. Yamada, The development of preventives and therapeutics for Alzheimer's disease that inhibit the formation of beta-amyloid fibrils (fAbeta), as well as destabilize preformed fAbeta. Curr Pharm Des, 2006. 12(33): p. 4357-75.

110. Ono, K., et al., Curcumin has potent anti-amyloidogenic effects for Alzheimer's beta-amyloid fibrils in vitro. J Neurosci Res, 2004. 75(6): p. 742-50.

111. Ono, K., et al., Nicotine breaks down preformed Alzheimer's beta-amyloid fibrils in vitro. Biol Psychiatry, 2002. 52(9): p. 880-6.

112. Sinha, S., et al., Comparison of three amyloid assembly inhibitors: the sugar scyllo-inositol, the polyphenol epigallocatechin gallate, and the molecular tweezer CLR01. ACS Chem Neurosci, 2012. 3(6): p. 451-8.

113. Sinha, S., et al., Lysine-specific molecular tweezers are broad-spectrum inhibitors of assembly and toxicity of amyloid proteins. J Am Chem Soc, 2011. 133(42): p. 16958-69.

114. Salloway, S., et al., A phase 2 multiple ascending dose trial of bapineuzumab in mild to moderate Alzheimer disease. Neurology, 2009. 73(24): p. 2061-70.

115. Sperling, R.A., et al., Functional alterations in memory networks in early Alzheimer's disease. Neuromolecular Med, 2010. 12(1): p. 27-43.

116. Lasagna-Reeves, C.A., et al., Preparation and characterization of neurotoxic tau oligomers. Biochemistry, 2010. 49(47): p. 10039-41.

117. Cohen, T.J., et al., The microtubule-associated tau protein has intrinsic acetyltransferase activity. Nat Struct Mol Biol, 2013. 20(6): p. 756-62.

118. Cowan, C.M. and A. Mudher, Are tau aggregates toxic or protective in tauopathies? Front Neurol, 2013. 4: p. 114.

119. Yanamandra, K., et al., Anti-Tau Antibodies that Block Tau Aggregate Seeding In Vitro Markedly Decrease Pathology and Improve Cognition In Vivo. Neuron, 2013.

120. Blair, L.J., et al., Accelerated neurodegeneration through chaperone-mediated oligomerization of tau. J Clin Invest, 2013.

121. Gerson, J.E. and R. Kayed, Formation and propagation of tau oligomeric seeds. Front Neurol, 2013. 4: p. 93.

122. Avila, J., et al., Role of tau protein in both physiological and pathological conditions. Physiol Rev, 2004. 84(2): p. 361-84.

123. Hernandez, F. and J. Avila, Tauopathies. Cell Mol Life Sci, 2007. 64(17): p. 2219-33.

124. Wang, Y.P., et al., Stepwise proteolysis liberates tau fragments that nucleate the Alzheimer-like aggregation of full-length tau in a neuronal cell model. Proc Natl Acad Sci U S A, 2007. 104(24): p. 10252-7.

125. Alonso, A., et al., Hyperphosphorylation induces self-assembly of tau into tangles of paired helical filaments/straight filaments. Proc Natl Acad Sci U S A, 2001. 98(12): p. 6923-8.

126. Hanger, D.P., B.H. Anderton, and W. Noble, Tau phosphorylation: the therapeutic challenge for neurodegenerative disease. Trends Mol Med, 2009. 15(3): p. 112-9.

127. Schneider, A., et al., Phosphorylation that detaches tau protein from microtubules (Ser262, Ser214) also protects it against aggregation into Alzheimer paired helical filaments. Biochemistry, 1999. 38(12): p. 3549-58.

128. Bullmann, T., et al., Expression of embryonic tau protein isoforms persist during adult neurogenesis in the hippocampus. Hippocampus, 2007. 17(2): p. 98-102.

129. Congdon, E.E. and K.E. Duff, Is tau aggregation toxic or protective? J Alzheimers Dis, 2008. 14(4): p. 453-7.

130. Demuro, A., et al., Calcium dysregulation and membrane disruption as a ubiquitous neurotoxic mechanism of soluble amyloid oligomers. J Biol Chem, 2005. 280(17): p. 17294-300.

131. Gomez-Ramos, A., et al., Extracellular tau is toxic to neuronal cells. FEBS Lett, 2006. 580(20): p. 4842-50.

132. Gomez-Ramos, A., et al., Extracellular tau promotes intracellular calcium increase through M1 and M3 muscarinic receptors in neuronal cells. Mol Cell Neurosci, 2008. 37(4): p. 673-81.

133. Polydoro, M., et al., Age-dependent impairment of cognitive and synaptic function in the htau mouse model of tau pathology. J Neurosci, 2009. 29(34): p. 10741-9.

134. Meraz-Rios, M.A., et al., Tau oligomers and aggregation in Alzheimer's disease. J Neurochem, 2010. 112(6): p. 1353-67.

135. Marx, J., Alzheimer's disease. A new take on tau. Science, 2007. 316(5830): p. 1416-7.

136. Kayed, R., et al., Annular protofibrils are a structurally and functionally distinct type of amyloid oligomer. J Biol Chem, 2009. 284(7): p. 4230-7.

137. Maeda, S., et al., Granular tau oligomers as intermediates of tau filaments. Biochemistry, 2007. 46(12): p. 3856-61.

138. Clavaguera, F., et al., Transmission and spreading of tauopathy in transgenic mouse brain. Nat Cell Biol, 2009. 11(7): p. 909-13.

139. Liu, L., et al., Trans-synaptic spread of tau pathology in vivo. PLoS One, 2012. 7(2): p. e31302.

140. de Calignon, A., et al., Propagation of tau pathology in a model of early Alzheimer's disease. Neuron, 2012. 73(4): p. 685-97.

141. Tian, H., et al., Trimeric tau is toxic to human neuronal cells at low nanomolar concentrations. International Journal of Cell Biology, In press.

142. Kasturirangan, S., et al., Nanobody specific for oligomeric beta-amyloid stabilizes nontoxic form. Neurobiol Aging, 2012. 33(7): p. 1320-8.

143. Kasturirangan, S., et al., Isolation and characterization of antibody fragments selective for specific protein morphologies from nanogram antigen samples. Biotechnol Prog, 2013. 29(2): p. 463-71.

144. Oddo, S., et al., Amyloid deposition precedes tangle formation in a triple transgenic model of Alzheimer's disease. Neurobiol Aging, 2003. 24(8): p. 1063-70.

145. Oddo, S., et al., Triple-transgenic model of Alzheimer's disease with plaques and tangles: intracellular Abeta and synaptic dysfunction. Neuron, 2003. 39(3): p. 409-21.

146. Nacharaju, P., et al., Accelerated filament formation from tau protein with specific FTDP-17 missense mutations. FEBS Lett, 1999. 447(2-3): p. 195-9.

147. Pennanen, L., et al., Accelerated extinction of conditioned taste aversion in P301L tau transgenic mice. Neurobiol Dis, 2004. 15(3): p. 500-9.

148. Brun, A. and E. Englund, Regional pattern of degeneration in Alzheimer's disease: neuronal loss and histopathological grading. Histopathology, 2002. 41(3A): p. 40-55.

149. Braak, H., et al., Staging of Alzheimer disease-associated neurofibrillary pathology using paraffin sections and immunocytochemistry. Acta Neuropathol, 2006. 112(4): p. 389-404.

150. Braak, H. and E. Braak, Staging of Alzheimer's disease-related neurofibrillary changes. Neurobiol Aging, 1995. 16(3): p. 271-8; discussion 278-84.

151. Ballatore, C., V.M. Lee, and J.Q. Trojanowski, Tau-mediated neurodegeneration in Alzheimer's disease and related disorders. Nat Rev Neurosci, 2007. 8(9): p. 663-72.

152. Goedert, M., Tau protein and neurodegeneration. Semin Cell Dev Biol, 2004. 15(1): p. 45-9.

153. Gregersen, N., Protein misfolding disorders: pathogenesis and intervention. J Inherit Metab Dis, 2006. 29(2-3): p. 456-70.

154. Hardy, J. and D. Allsop, Amyloid deposition as the central event in the aetiology of Alzheimer's disease. Trends Pharmacol Sci, 1991. 12(10): p. 383-8.

155. Oddo, S., et al., Temporal profile of amyloid-beta (Abeta) oligomerization in an in vivo model of Alzheimer disease. A link between Abeta and tau pathology. J Biol Chem, 2006. 281(3): p. 1599-604.

156. Small, S.A. and K. Duff, Linking Abeta and tau in late-onset Alzheimer's disease: a dual pathway hypothesis. Neuron, 2008. 60(4): p. 534-42.

157. Harper, J.D., et al., Observation of metastable Abeta amyloid protofibrils by atomic force microscopy. Chem Biol, 1997. 4(2): p. 119-25.

158. Roher, A.E., et al., Morphological and biochemical analyses of amyloid plaque core proteins purified from Alzheimer disease brain tissue. J Neurochem, 1993. 61(5): p. 1916-26.

159. Walsh, D.M. and D.J. Selkoe, A beta oligomers - a decade of discovery. J Neurochem, 2007. 101(5): p. 1172-84.

160. Bretteville, A. and E. Planel, Tau aggregates: toxic, inert, or protective species? J Alzheimers Dis, 2008. 14(4): p. 431-6.

161. Roberson, E.D., et al., Reducing endogenous tau ameliorates amyloid beta-induced deficits in an Alzheimer's disease mouse model. Science, 2007. 316(5825): p. 750-4.

162. Yoshiyama, Y., et al., Synapse Loss and Microglial Activation Precede Tangles in a P301S Tauopathy Mouse Model. Neuron, 2007. 53(3): p. 337-351.

163. Honson, N.S. and J. Kuret, Tau aggregation and toxicity in tauopathic neurodegenerative diseases. J Alzheimers Dis, 2008. 14(4): p. 417-22.

164. Braak, H., et al., Staging of brain pathology related to sporadic Parkinson's disease. Neurobiol Aging, 2003. 24(2): p. 197-211.

165. Arnold, S.E., et al., The topographical and neuroanatomical distribution of neurofibrillary tangles and neuritic plaques in the cerebral cortex of patients with Alzheimer's disease. Cereb Cortex, 1991. 1(1): p. 103-16.

166. McKee, A.C., et al., Chronic traumatic encephalopathy in athletes: progressive tauopathy after repetitive head injury. J Neuropathol Exp Neurol, 2009. 68(7): p. 709-35.

167. Nowinski, C., Head Games: Football's Concussion Crisis From the NFL to Youth Leagues. Drummond Publishing Group, 2006.

168. Geddes, J.F., et al., Neurofibrillary tangles, but not Alzheimer-type pathology, in a young boxer. Neuropathol Appl Neurobiol, 1996. 22(1): p. 12-6.

169. Tokuda, T., et al., Re-examination of ex-boxers' brains using immunohistochemistry with antibodies to amyloid beta-protein and tau protein. Acta Neuropathol, 1991. 82(4): p. 280-5.

170. Ojo, J.O., et al., Repetitive Mild Traumatic Brain Injury Augments Tau Pathology and Glial Activation in Aged hTau Mice. J Neuropathol Exp Neurol, 2013. 72(2): p. 137-51.

171. Loffler, T., et al., Stable mutated tau441 transfected SH-SY5Y cells as screening tool for Alzheimer's disease drug candidates. J Mol Neurosci, 2012. 47(1): p. 192-203.

172. Tian, H., et al., Trimeric tau is toxic to human neuronal cells at low nanomolar concentrations. Int J Cell Biol, 2013. 2013: p. 260787.

173. Mouzon, B.C., et al., Chronic neuropathological and neurobehavioral changes in a repetitive mild traumatic brain injury model. Ann Neurol, 2014. 75(2): p. 241-54.

174. Furst, A.J. and G.A. Kerchner, From Alois to Amyvid: seeing Alzheimer disease. Neurology, 2012. 79(16): p. 1628-9.

175. Ivanovova, N., et al., High-yield purification of fetal tau preserving its structure and phosphorylation pattern. J Immunol Methods, 2008. 339(1): p. 17-22.